OCEANOGRAPHIC OBSERVATIONS ACROSS
THE NORTHERN GULF STREAM
by
Thomas B. Curtin and
Leonard J. Pietrafesa

Oceanographic Observations Across the Northern Gulf Stream

by
THOMAS B. CURTIN
and
LEONARD J. PIETRAFESA

Cover Photo: Satellite photo off the
North Carolina – New Jersey Coastline.
Courtesy of R. Legeckis, NOAA/NESS.

Oceanographic Observations Across the Northern Gulf Stream

by

Thomas B. Curtin

Leonard J. Pietrafesa

Project Report

to

National Aeronautics and Space Administration

Wallops Island, Virginia

for research entitled

Prediction of Major Current Boundary Locations

From Surface Thermal/Topographic Signature

(Contract NAS6-2617)

Department of Marine Sciences & Engineering

Report No. 78-3

July 1978

NORTH CAROLINA STATE UNIVERSITY AT RALEIGH
DEPARTMENT OF MARINE SCIENCE AND ENGINEERING
P. O. BOX 5923
RALEIGH, N. C. 27650

Table of Contents

List of Figures

List of Tables

1. Introduction

The use of satellites offers the opportunity for the synoptic observations necessary to measure the spatial and temporal variability of large scale dynamic systems such as the Gulf Stream. Confidence in the interpretation of various satellite data, however, can only be developed through accumulated correlation of satellite signals with simultaneous surface and subsurface oceanographic measurements. Toward this end, a concurrent satellite and ship experiment across the Gulf Stream in the region north of Cape Hatteras was performed during the period 21 May to 4 June 1976 by personnel from NASA Wallops, NASA Langley, NOAA/NESS, the U.S. Naval Research Laboratory, and North Carolina State University.

The objectives of this study were the determination of the current hydrographic and pressure structure of the Gulf Stream (cf. Figure 1), as a function of the vertical and cross-stream spatial directions; the calculation of the Gulf Stream transport, the correlation of the surface temperature, salinity and velocity of the Gulf Stream with meteorological forcing; the comparison of remotely sensed, satellite imagery with the oceanographic station data; and the development of a first order model which might be used for intercomparison between satellite imagery and ground truth. This model is the subject of a separate report (P., J and B-M). The site chosen for the field effort was the area north of Cape Hatteras, N. C. along several lines from the Chesapeake Bay to Bermuda.

Without a doubt, the most engrossing problem that has concerened the physical oceanographic community is that of the general ocean circulation. The descriptions which have been evolving of major ocean circulations

1
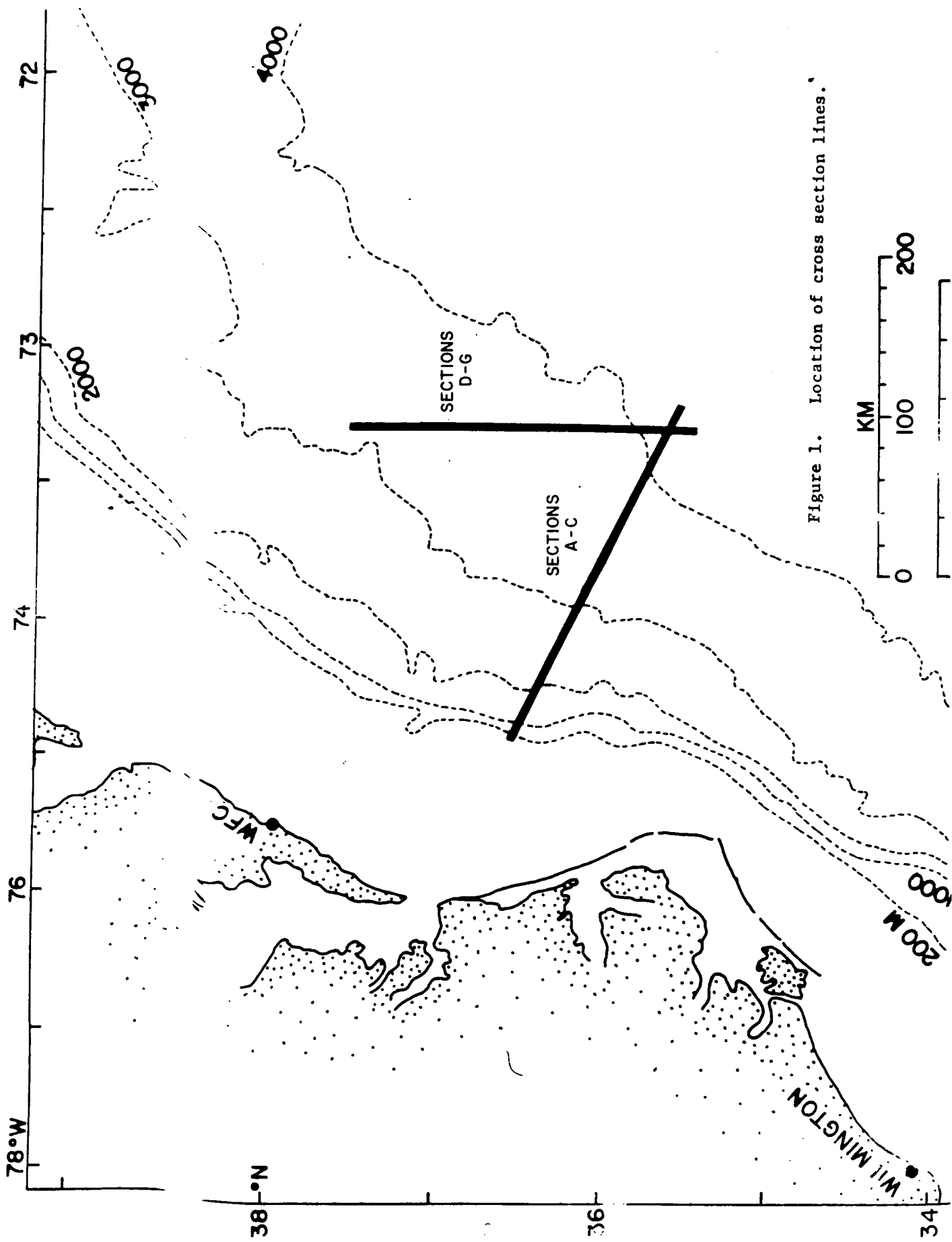
Figure 1. Location of cross section lines.

consistently postulated large gyral type circulations with broad, slow moving surface flows on the northern, southern and eastern extents of the ocean basins and intense, narrow bands of boundary currents on the western margins of the oceanic basins. The data corroborating the existence and character (mostly hydrographic) of these currents, which hug the eastern shores of the subtropical continents of the world, comprise more volumes of scientific testimony than any other oceanic phenomena. Along with these data, theories began to evolve which substantiated the necessary existence of anti-cyclonic (cyclonic) gyres between the equator and approximately 60° North (South) latitude. The time-averaged, theoretical, general circulation picture, which was essentially born in the late 1940's, indicated that mean global winds and thermodynamic forcing were responsible for the observed global circulation patterns. As so often occurs though, when the technology became available to allow the scientific community to make more sophisticated measurements of the oceanic phenomena, the theories and beliefs which were so certain were found inadequate and inaccurate. This is true of both the conceptual models of the general oceanic circulation as well as those of the western boundary currents, including the Gulf Stream and the Kyroshio Current.

Satellites have recently given us some dramatic thermal gradient pictures of the surface signature of the Gulf Stream. These products, available on a daily to weekly basis (NOAA-NESS), have demonstrated the dynamic variability, both spatial and temporal, of the Gulf Stream and have shown us that our basic understanding of western boundary current dynamics if fairly crude. Moreover, it is apparent that the only rational way to approach the western boundary current dynamics problem is through

the combined use of ocean research vessel, airplanes and satellites. Satellite capabilities are expecially well suited to detect and monitor these intense, poleward flowing bands of continental margin hugging currents. While the measurement of oceanic temperature fields, such as those associated with western boundary currents, with remote sensing devices has been successfully performed since the 1960's, few investigators have ventured to infer from the wealth of thermal data any but most general features of current boundaries and circulation patterns.

Western boundary currents can usually be identified, at the ocean's surface, as prominently and persistently strong density (derived from temperature, mainly) gradient features. They, in fact, have enormously high temperatures across their surface widths and appear as northwestern fronts of warm lenses of subtropical water in the Northern Hemisphere. They usually flow poleward, along the continental margin, meander laterally and occasionally shed large filaments or eddies along either lateral extreme. These patches of water may or may not detach themselves from the main boundary current, have been called shingles, sausages, filaments and more typically spin off eddies and can rotate either cyclonically or anti-cyclonically; typically the events on the landward side tend to be warm core and cyclonically rotating. When these events occur, there is typically an entrainment of nearby water masses into the western boundary current. The western boundary currents typically turn toward the east, leaving the coastal margin, approximately at latitudes where the curl of the mean zonal wind is zero. The Gulf Stream also deflects and meanders offshore possibly due to topographically induced vorticity constraints (eg. Pietrafesa, 1978) and moreover the mean path of the Stream and the envelope of the

4

meanders can be explained by topographic control of the Stream path (Warren, 1963; Hansen, 1970; Robinson, 1971; Pietrafesa, 1978).

In April 1971 the NOAA I scanning radiometer observed a cold body of water moving southwest from the Gulf Stream off Cape Hatteras (Richardson, et. al.; 1973). Ground-truth studies made with XBT's confirmed the existence of a cyclonic eddy traveling at one mile a day. DeRycke and Rao (1973) reported a similar sighting in 1973 based on NOAA II VHRR (Very High Resolution Radiometer) pictures. The same instrument, measuring sunglint, noted the effectiveness of the Lesser Antilles in protecting their lee waters from wind-generated waves (Strong, et. al., 1973). Rough waters show up darker than calm waters on such photographs. Sunglint variability also provided an outline of the Gulf Stream and the Gulf of Mexico's Loop Current, both of which have opposing (and therefore steeper) waves superimposed on them by prevailing winds (Strong and DeRycke, 1973). This characteristic provides an alternative to purely thermal boundary signatures, which are seasonal in some major current systems. Another alternative, suggested by Maul (1973), relies on optical properties influenced by chlorophyll and other substances present in bodies of water. An analysis of ERTS-1 photographs of the Gulf Loop Current produced mixed results related to seasonality of color signals.

Szekielda (1972) has reported the location of upwelling regions off the northwest coast of Africa by studying color enhanced prints of infrared radiometer photographs. Multispectral analysis of photographs taken during May and June of 1966 also revealed the characteristic features of the Benguela and Agulhas currents around southern Africa. Three studies of the Somali Current (in 1966, 1969, and 1970) with Nimbus satellites documented upwelling and translation of the upwelled water. Warneke et. al.

5

(1971) used Nimbus II to investigate the demarcation line between the Falkland and Brazil currents. In addition, they found that satellite and aircraft radiometers produced very similar estimates of the position of the Gulf Stream western boundary. In 1973, ERTS-1 photography of the New York Bight (Charnell, et. al., 1974) opened up the possibility of limited three-dimensional analysis of near surface phenomena. Recognizing that lower bands of the Multispectral Scanner penetrated deeper into the sea, researchers were able to deduce some sub-surface spreading of warm river water, and even picked up internal wave patterns.

As mentioned previously, the Gulf Stream varies dramatically in intensity, width and seasonal persistence. In addition, the "short"-scale spatial and "short"-term temporal variabilities are poorly characterized and understood. The Stream is characterized by seaward meanders of the length scale orders of 10's to 100's of kilometers (km). For the past several decades, the role of the Gulf Stream in the general recirculation of the North Atlantic was thought to be understood but, even though the Stream may be the world's most intensely probed and studied oceanic phenomenon, it's role is now being reevaluated both theoretically and experimentally. The current field of the Gulf Stream has been measured from aircraft and research vessels (W.S. Richardson and Schmitz, 1965; Barret and Schmitz, 1971; P.L. Richardson, 1972; Niiler and W.S. Richardson, 1973) and its surface signature is now presented quasi-weekly by both NOAA-NESS when the cloud cover permits and weekly by the Naval Oceanographic Office. Still, we are now only certain of the variability of the Gulf Stream.

6

The fate of the eddy energy is not at all certain. Whether or not they are directly coupled to the mean circulation or are dissipated in the possible generation of heat of internal waves is unknown. The origins of these eddies is also unknown. Theoretical concepts exist which cover many possible eddy origins, and one can count an abundance of possible eddy sources, including agents which concentrate energy in western boundary currents but the reason and role for eddies remains unknown. One thing is certain though, given their generation and persistence, the western boundary current undergoes a change. Whether the change is cause or effect is not known.

From the extensive ocean station data base and from the satellite images one can see that 4 day to 2 week temporal and spatial fluctuations in the local Stream hydrography are present and furthermore the fluctuation energetics seem to be such that energy can be transferred either to or from the mean flow (Webster, 1961). The contention herein is that over the entire length of the Gulf Stream, the kinetic energy can be locally doubled and is balanced by an opposite potential energy transfer, so that a persistent current is maintained (Schmitz and Niiler, 1969). Unfortunately, the presently existing data is not sufficient for estimates of energy transfer since in order to determine fluctuation energetics, one must measure both the mass and velocity fields in three dimensions (at many points in the horizontal and vertical) all at the "approximate" same time. This has certainly not been done.

The problem of the meanders and eddies is, of course, of interest of themselves but they may play a role in the overall general circulation and in that sense, the dynamics of these intermediate scale instabilities

7

must be understood. One can see from the literature that a considerable amount of observational information on the location of the Gulf Stream is presently available and is being collected on a weekly basis. Still, velocity data is scant so that the bulk of new data are surface observables. The actual location of the Gulf Stream from data sets is probably best given by hydrographic data indicating the location of the "axis" ($\tilde{A}$) of the Gulf Stream by the intersection of the $15^\circ C$ isotherm with the 200 meter subsurface depth.

The $15^\circ C$ isotherm at 200 m depth $\tilde{A}$ is a "typical" indicator of the location of the thermal front which is evident in vertical and horizontal ocean station data and from the satellite and airbourne radiometer data. The $\tilde{A}$ location is often cited as the best indicator of the landward extreme of the Gulf Stream frontal feature, within the cyclonic shear zone. The surface thermal feature, so prominent in infrared thermometry has been found to migrate laterally from the Gulf Stream axis, i.e., the horizontal distance, $\tilde{L}$, along the surface from the thermal front surface intersection point to the point at the surface, directly above (along the vertical axis from) $\tilde{A}$. The reasons that this distance changes are many in possibility, but reliable estimates of $\tilde{A}$ and $\tilde{L}$ will require simultaneous measurements of: low level winds, sea state, Lagrangian currents, sea surface temperature, meanders of the Gulf Stream and eddy formation and time history, all of which are in the realm of remote sensing possibility. Given these products, the hope is that eventually with sufficient insight and understanding we may need to detect only the position of the surface thermal front, the cross-stream surface temperature

8

gradient and perhaps something about the local atmospheric conditions and be able to accurately predict $\tilde{L}$ and $\tilde{A}$. This would give us an instantaneous Gulf Stream path picture along the whole of the stream.

Sturges (1972) addressed the use of altimetry to measure geostrophic currents. Although incapable of resolving the problem of levels of no motion, altimeter readings accurate to 10 cm can identify western boundary currents, detached eddies, and possibly eastern boundary currents.

The change of the surface height across any part of the Gulf Stream may be of the order of one to several meters resulting in a cross-stream slope of approximately $5 (10^{-4}) - 10^{-6}$. This gradient is too small to be realized by conventional oceanographic methods. Consequently, previous to the introduction of remote sensing, the only sea surface work was done with tide gauges and hydrography. The data from the tide gauges is direct but of itself yields only longshore slope. The hydrography data, though difficult to obtain can be used, with appropriate reservation, to indirectly compute sea currents and sea surface slope. This method was generated by Helland-Hansen (1903) on the basis of the Bjerknes circulation theorem (Bjerknes, 1900) and makes it possible to imply surface topography without direct measurement.

In a baroclinic ocean, i.e., an ocean in which constant pressure surfaces and surfaces of constant density are allowed to intersect, the horizontal pressure gradient and current velocity may become zero at some depth at and below which the baroclinic and barotropic pressure gradients become equal and opposite in magnitude and direction. This level of no motion may extend below the bottom so that the pressure gradients due to

9

inhomogeneities in the field of mass are not in mutual compensation with the free surface slope pressure gradient. Though this assumption may be grossly invalid, it can be assumed that the Gulf Stream is in "local" geostrophic equilibrium, i.e., that the Gulf Stream is locally friction-less and non-accelerated. It is thus implicitly suggested that forces due to the rotation of the earth and horizontal pressure gradients are in balance. This means that the horizontal current direction will be parallel to the lines of constant pressure. The current will thus be in a direction perpendicular to the pressure gradient such that the higher pressure will be to the right of an observer facing the direction of flow or "downstream".

A method for calculating the magnitude and direction of oceanic currents using only salinity and temperature data was proposed by L. Sand-strom and B. Helland-Hansen (1903) and is based on the assumption that the balance of forces is geostrophic. This approach is referred to as the "dynamic" method and is explained and interpreted by Fomin (196-). The method is a melding of the geostrophic and hydrostatic balances, i.e, the combining of the geostrophic and hydrostatic balances, i.e., the combining of the geostrophic, horizontal plane balance with the rate change of pressure in the vertical, which is assumed equal to the density variable times the gravitational acceleration constant. In a stratified ocean, the horizontal pressure gradient in a direction is composed of two components: the slope of the sea surface in that direction and the vertical integral of the horizontal density gradient, i.e., the difference in density from point to point, along the co-ordinate direction. The former component is known as the barotropic-geostrophic pressure gradient while the latter is referred

to as the baroclinic-geostrophic pressure gradient. It is further assumed that at some depth, baroclinic and barotropic effects will be equal and opposite and therefore the absolute geostrophic current will equal zero. Of course, if one knows the surface slope and/or the surface current and/or bottom pressures across the Stream, then one has the problem addressed in its entirety.

There are pitfalls in these simple assumptions, but the dynamic method does allow for the computation of current velocities and sea surface topography from the observed field of mass, i.e., from ocean station data consisting of temperature, salinity and depth/pressure and any complementary sources such as surface or interior currents or surface slopes across the Stream.

It is clear from the discussion that infrared imagery indicates the surface temperature signature and is readily available from satellites, but unfortunately such data, i.e., temperature gradient signature, may not be a very good indicator of the position of the Gulf Stream since winds can blow the surface layer of the Gulf Stream away, though leaving the main body of the Stream intact. There would be poor correlation between infrared imagery and surface topography data in such a case. Such an occurrence is probably the rule rather than the exception since wind forcing is rather active in the region of the Gulf Stream. Thus it is of great value to have additional satellite data such as the altimeter offers. With the use of the RA and the VHRR, it is conceivable that one could indicate the time and space history of the surface waters and indicate where the actual core or main axis of the Gulf Stream is located. In an attempt to address such problems, one of the most extensively co-ordinated surveys of the Gulf Stream

was conducted during a several week period during May - June, 1976 by personnel from North Carolina State University, contemporaneously with NRL (National Aeronautics and Space Administration and Naval Research Laboratory) NASA/Wallops and NASA/Langley. This survey included seven transects of the Gulf Stream from Cape Henry, Virginia, to Bermuda and includes 1.5 (10^6) hydrographic data points, down to 3000 meters depth. Current meter, ship's drift and meteorological data were also obtained. This report describes the experiment scenario, presents the data results and indicates that an objective to be able to routinely determine the dynamical/physical character of the Gulf Stream from satellite imagery is not without future feasability. A report entitled "Concurrent Satellite and Ship Observations Across the Gulf Stream North of Cape Hatteras" by Curtin, Pietrafesa and Huang (1978) describes an intercomparison of the various data sets and conclusions which can be derived therein.

The results of the co-ordinated study are that the surface topography of the Gulf Stream has been determined and the current structure of the Gulf Stream has been calculated as a function of the spatial variables, for different times, from oceanographic station data. Gulf Stream transport has also been calculated based on the station data. A correlation between the distribution of temperature, salinity, velocity fields and pressure gradients at the surface and the vertical cross-sectional structure of these variables using actual observations of salinity, temperature and velocity and calculated velocities and surface topography and remotely sensed imagery, including radar altimetric (RA), infrared radiometric (IR) and very high resolution radiometric (VHRR) was accomplished. The results of this study were so encouraging that it is not too ambitious to state

12

that field observations from aircraft and satellite and ground truth, ship, observations are an obvious extension of any future large scale satellite application programs.

13

2. Methods

The primary instrument used for conductivity, temperature, depth measurements was a Guildline CTD system. Specifications for the Guildline Model 8705 are given in Table 1. For rapid surveying and between some CTD stations, a Sippican expendable bathythermograph (XBT) was used. Specifications for the XBT system are given in Table 2. Continuous near surface temperature, salinity measurements were generated between stations using a Plessey Model 6600T Thermosalinograph (TS) coupled to the ship's cooling water intake port (about 3 m below the surface). Specifications for the TS system are given in Table 3. The XBT and TS data output was in analog (strip chart) format and the recorded signals were manually digitized later onshore. CTD output was directly through digital magnetic tape, as well as analog plots and panel display. CTD and TS accuracy was monitored in situ using water sampling (Nisken) bottles equipped with reversing thermometers ($\pm 0.03°C$). Water samples were obtained at the surface (0 m) and near cast bottom just above the probe. The bottles were tripped at each cast's extremity after a five minute equilibration time. Salinity samples were analyzed on a laboratory bench salinometer standardized with normal sea-water ($\pm 0.003°/_{\circ\circ}$). A Barnes PRT-5 radiometer was also used to compare with the TS near surface temperature measurements. This unit was hand-held, and readings taken from bridge height aimed at the sea surface about 10° away from the ship's vertical hull line.

Conductivity (actually conductivity ratio) to salinity conversion was performed as indicated schematically in Figure 2. Compression and editing of the raw CTD data files were performed as described in Curtin and Britton (1978). Sigma-t, specific volume, dynamic depth anomaly, sound speed, and

Table 1. Specifications for Guildline Model 8705 CTD System.

RANGE	ACCURACY	RESOLUTION
Conductivity(1) 28 to 40 PPT 40 PPM to 40 PPT	±0.01 PPT ±2 PPM to ±0.05 PPT	±0.002 PPT ±1 PPM to ±0.02 PPT
Temperatures -2°C to +38°C	±0.01°C	±0.001°C
Depth FSP = 3000 decibars	±0.25% FSP	±0.05% FSP

NOTE 1:   The conductivity accuracy statement is given in equivalent salinity, and is based on the work of Dr. A. S. Bennett, Atlantic Oceanographic Laboratory, Bedford Institute, Canada.

RESPONSE TIME CONSTANT:

Less than 50 milliseconds all channels, including sensors and associated electronics.

DATA FORMAT:

Code: Multiplexed analog outputs converted to offset binary, in turn converted to 3 level (+1, 0, -1) return-to-zero for cable transmission.

Bit rate: 4800 Hz

Cycle time: 80 milliseconds.

SENSORS:

Conductivity - four electrode conductivity cell, spatial resolution in vertical plane approximately 5 cm. Nominal conductance 10 mmhos at 35 PPT, 15°C.

Temperature - Resistance thermometer consisting of fine copper wire sensing element encase in oil-filled stainless steel capillary tube, terminated in a four terminal configuration. Nominal ice point resistance 46 ohms.

Pressure - Strain gage type transducer having an output of 2mV/V. Available in ranges up to 6000 decibars, overrange capability 50%.

Table 2. Specifications for Sippican Expendable Bathythermograph (XBT) System

Temperature sensing range	28° to 96°F (-1. 7°C to +35. 5°C)
Temperature accuracy	± 0. 4°F (± 0. 2°C)
Depth accuracy	±2% or 15 feet, whichever is greater
Cycle time	36 seconds for 660 foot drop
	90 seconds for 1500 foot drop
	180 seconds for 2500 foot drop
	360 seconds for 6000 foot drop

(2)   PROBE

Thermal response	63% of a step change in temperature in 3 feet; 95% of a step change in temperature in 9 feet

(3)   RECORDER

Minimum slew rate	45°F/Second (2°F/foot of depth)
Operating modes	(a) Reload
	(b) Check/Run
	(c) Launch
	(d) Measure
Power Requirement	117 ± 12 VAC, 57 to 63 Hz, 1-phase, 35 watts
Ambient Temperature Range	0°C to 50°C (32°F to 122°F)

16

Table 3. Specifications for Plessey Model 6600T Thermosalinograph

SALINITY

Salinity Ranges:

(1) 20.0 – 30.0 ppt
(2) 28.0 – 38.0 ppt
(3) 28.0 – 30.0 ppt
(4) 29.5 – 31.5 ppt
(5) 31.0 – 33.0 ppt
(6) 32.5 – 34.5 ppt
(7) 34.0 – 36.0 ppt
(8) 35.5 – 37.5 ppt

Accuracy:

±0.03 ppt on ranges (3) through (8) including recorder errors and the effects of temperature variations from –2° to +35 C. Ranges (1) and (2), the accuracy is ±0.15 ppt.

Repeatability:

Normally limited only by the recorder; that is, approximately ±0.01 ppt.

TEMPERATURE

Temperature Ranges:

(1) – 2 to + 8°C
(2) + 5 to + 15°C
(3) +12 to + 22°C
(4) +19 to + 29°C
(5) +26 to + 36°C

Accuracy:

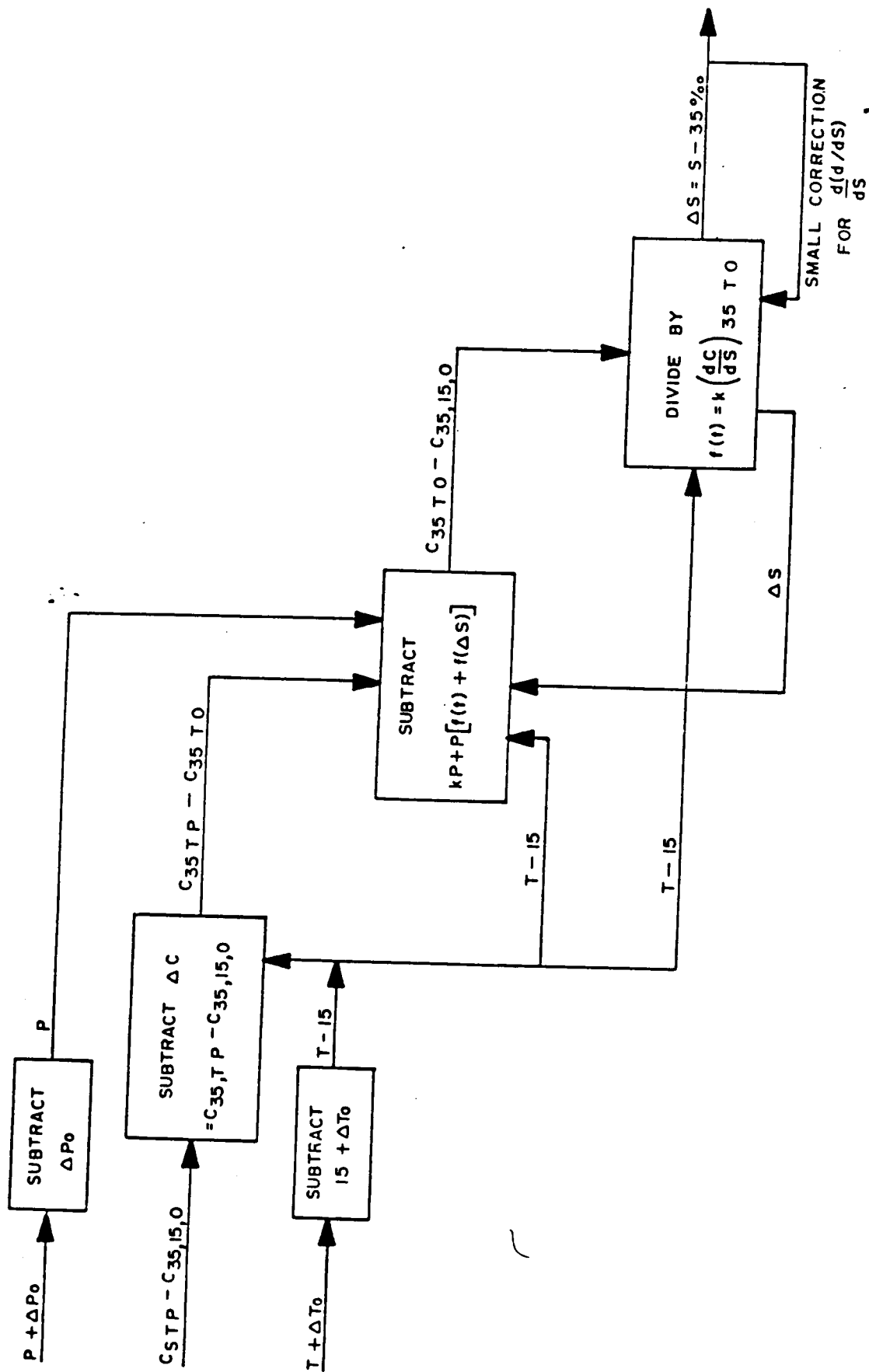Error less than ±0.1°C on all ranges are read on the recorder.

Figure 2. Conductivity ratio to salinity conversion schematic.

the Vaisala-Brunt frequency squared (N^2) were computed at each depth. Sigma-t was calculated using the empirical formula developed by Knudsen (1901) and rewritten for programming by Fofonoff and Tabata (1958). N^2 was derived from the difference of buoyancy of two fluid elements transferred isentropically to the mean pressure between the two levels considered. The Ekman (1908) equation of state was used to calculate the specific volume. The adiabatic lapse rate was computed by an empirical formula given by Fofonoff (1962). Corrections to Fofonoff's formula, as pointed out by Wang and Millero (1973), were not applied.

Direct surface current estimates were based on observed ship's drift during hydrographic stations, typically of 2 to 3 hour duration. Positions were fixed via loran C, and empirical corrections applied for vessel windage effects. The overall precision of the directly calculated surface currents is estimated to be ±20%. The surface currents derived from ship's drift were used to convert relative geostrophic velocity values calculated from cross-stream dynamic depth gradients to absolute velocity component estimates.

Salinity profiles were generated for stations with only subsurface temperature observations (XBT) using surface salinity measurements (TS) and the North Atlantic Central Water mass curve at depth.

3. Results

Tables 4 and 5 delineate the section and cruise particulars: The data from each transect are presented sequentially in the sections following. Within each section, the following format is adhered to:

station positions and wind, swell vectors

atmospheric and sea surface observations at stations

surface temperature, salinity, and sigma-t along transect

profiles of observed and derived variables

temperature, salinity, sigma-t cross sections

observed surface velocity along transect

absolute geostrophic velocity cross section

Profiles of observed and derived variables are presented in sequential format, and ordered within each group nearshore to offshore (left to right). The profiles are staggered uniformly along the reference axes; plot distance between profiles is not scaled to actual station spacing. The numerical data, corresponding to these profiles, are given by station in Appendix A.

Table 4. Section Designations, Station Coordinates, and Primary Data Types

Section Designation	Station Number	Latitude (° ´N)	Longitude (° ´W)	Mo./Day (1976)	Time (GMT)	Data (Type)
A	01	36 30.0	74 41.0	5/21	0530	XBT
A	02	36 25.0	74 30.0	5/21	0705	XBT
A	03	36 20.0	74 19.0	5/21	0834	XBT
A	05	36 15.0	74 08.0	5/21	1000	XBT
A	07	36 11.0	73 57.0	5/21	1136	XBT
A	09	36 05.0	73 46.5	5/21	1315	XBT
A	10	36 00.0	73 35.0	5/21	1415	XBT
A	11	35 55.2	73 25.1	5/21	1605	XBT
A	12	35 50.5	73 16.0	5/21	1740	XBT
A	13	35 45.5	73 03.3	5/21	1910	XBT
A	14	35 40.4	72 52.5	5/21	2134	XBT
A	15	35 36.0	72 41.5	5/22	0000	XBT
A	16	35 31.0	72 31.0	5/22	0145	XBT
A	17	35 26.0	72 21.5	5/22	0315	XBT
A	18	35 21.5	72 11.0	5/22	0430	XBT
B	18	35 21.5	72 11.0	5/22	0430	CTD
B	16	35 32.0	72 31.5	5/22	0905	CTD
B	14	35 40.5	72 52.5	5/22	1330	CTD
B	12	35 50.5	73 15.5	5/22	1720	CTD
B	10	36 00.0	73 34.5	5/22	2105	CTD
B	09	36 05.2	73 46.0	5/23	0000	CTD
B	08	36 08.0	73 53.0	5/23	0300	CTD
B	07	36 11.0	73 57.0	5/23	0640	CTD
B	06	36 12.5	74 02.6	5/23	1330	CTD
B	05	36 13.0	74 10.5	5/23	1600	CTD
B	04	36 16.5	74 15.0	5/23	1830	CTD,XBT
B	03	36 20.0	74 19.0	5/23	2039	CTD
B	02	36 25.0	74 30.0	5/23	2315	CTD
B	01	36 30.0	74 40.0	5/24	0150	CTD
C	01	36 30.0	74 40.0	5/24	0150	XBT
C	02	36 24.5	74 30.5	5/24	0104	XBT
C	03	36 20.0	74 19.5	5/24	0520	XBT
C	04	36 17.5	74 15.5	5/24	0620	XBT
C	05	36 14.0	74 08.0	5/24	0740	XBT
C	06	36 12.5	74 03.0	5/24	0805	XBT
C	07	36 10.0	73 53.0	5/24	0835	XBT
C	08	36 07.5	73 52.5	5/24	0910	XBT
C	09	36 05.0	73 41.5	5/24	1035	XBT
C	10	36 00.0	73 35.0	5/24	1340	XBT
C	11	35 55.0	73 25.0	5/24	1515	XBT
C	12	35 50.8	73 14.0	5/24	1618	XBT
C	14	35 40.5	72 52.5	5/24	1828	XBT
C	16	35 31.5	72 31.0	5/24	2135	XBT

Table 4.   Continued.

Section Designation	Station Number	Latitude (°´N)	Longitude (°´W)	Mo./Day (1976)	Time (GMT)	Data (Type)
D	19	35 28.5	72 30.0	5/24	2220	XBT
D	20	35 48.8	72 30.0	5/25	0250	XBT
D	21	36 09.0	72 29.0	5/25	0720	XBT
D	22	36 28.0	72 30.0	5/25	1030	XBT
D	23	36 39.0	72 30.0	5/25	1305	XBT
D	24	36 43.5	72 30.0	5/25	1350	XBT
D	25	36 49.0	72 30.0	5/25	1430	XBT
D	26	36 54.0	72 30.0	5/25	1500	XBT
D	27	36 59.0	72 30.0	5/25	1530	XBT
D	28	37 04.0	72 30.0	5/25	1615	XBT
E	31	37 28.5	72 30.0	5/27	1035	CTD
E	30	37 18.5	72 30.0	5/27	1352	CTD
E	29	37 09.0	72 30.0	5/27	1555	XBT
E	28	37 03.5	72 30.0	5/27	1640	CTD
E	27	36 58.8	72 30.0	5/27	1904	XBT
E	26	36 54.0	72 30.0	5/27	1936	CTD
E	25	36 49.0	72 30.0	5/27	2158	XBT
E	24	36 43.5	72 30.0	5/27	2238	XBT
E	23	36 38.5	72 30.0	5/27	2327	XBT
E	22	36 28.0	72 30.0	5/28	0130	CTD
F	19	35 28.5	72 30.0	6/2	1230	CTD
F	20	35 48.7	72 30.0	6/2	1650	XBT
F	21	36 08.0	72 30.0	6/2	1940	CTD,CM
F	22	36 28.0	72 30.0	6/2	2310	XBT
F	23	36 38.8	72 30.0	6/3	0020	CTD
F	24	36 43.5	72 30.0	6/3	0230	XBT
F	25	36 49.0	72 30.0	6/3	0315	CTD,CM
F	26	36 53.8	72 30.0	6/3	0553	XBT
F	27	36 59.0	72 30.0	6/3	0634	CTD
F	28	37 03.5	72 30.0	6/3	0927	XBT
F	29	37 08.5	72 30.0	6/3	1023	CTD,CM
F	30	37 18.7	72 30.0	6/3	1320	XBT
F	31	37 28.5	72 30.0	6/3	1445	CTD
G	31	37 28.5	72 30.0	6/3	1445	CTD
G	30	37 18.5	72 30.0	6/3	1810	XBT
G	29	37 09.0	72 30.0	6/3	2013	XBT
G	28	37 04.0	72 30.0	6/3	2113	CTD
G	27	36 59.0	72 30.0	6/4	0008	XBT
G	26	36 54.0	72 30.0	6/4	0055	CTD
G	25	36 49.0	72 30.0	6/4	0340	XBT
G	24	36 43.7	72 30.0	6/4	0445	XBT
G	23	36 39.0	72 30.0	6/4	0459	XBT
G	22	36 28.5	72 30.0	6/4	0620	CTD
G	21	36 09.0	72 30.0	6/4	1025	XBT
G	20	35 48.7	72 30.0	6/4	1240	XBT
G	19	35 28.5	72 30.0	6/4	1445	CTD,XBT,CM

Table 5. Cruise Chronology and Participants

LEG 1: 1800, 19 May 1976
        0700, 29 May 1976

LEG 2: 0030, 1 June 1976
        0700, 6 June 1976

PARTICIPANTS (LEGS)

T. CURTIN (1 & 2)

D. BROOKS (1)

D. LEECH (1 & 2)

R. D'AMATO (1)

C. NEELASRI (1)

J. PAULLING (1)

H. PAULLING (1 & 2)

M. BANNAZADEH (1)

D. ROONEY (2)

K. PARKER (2)

P. BLANKINSHIP (2)

FAN (2)

CHAO (2)

3.1

Section A
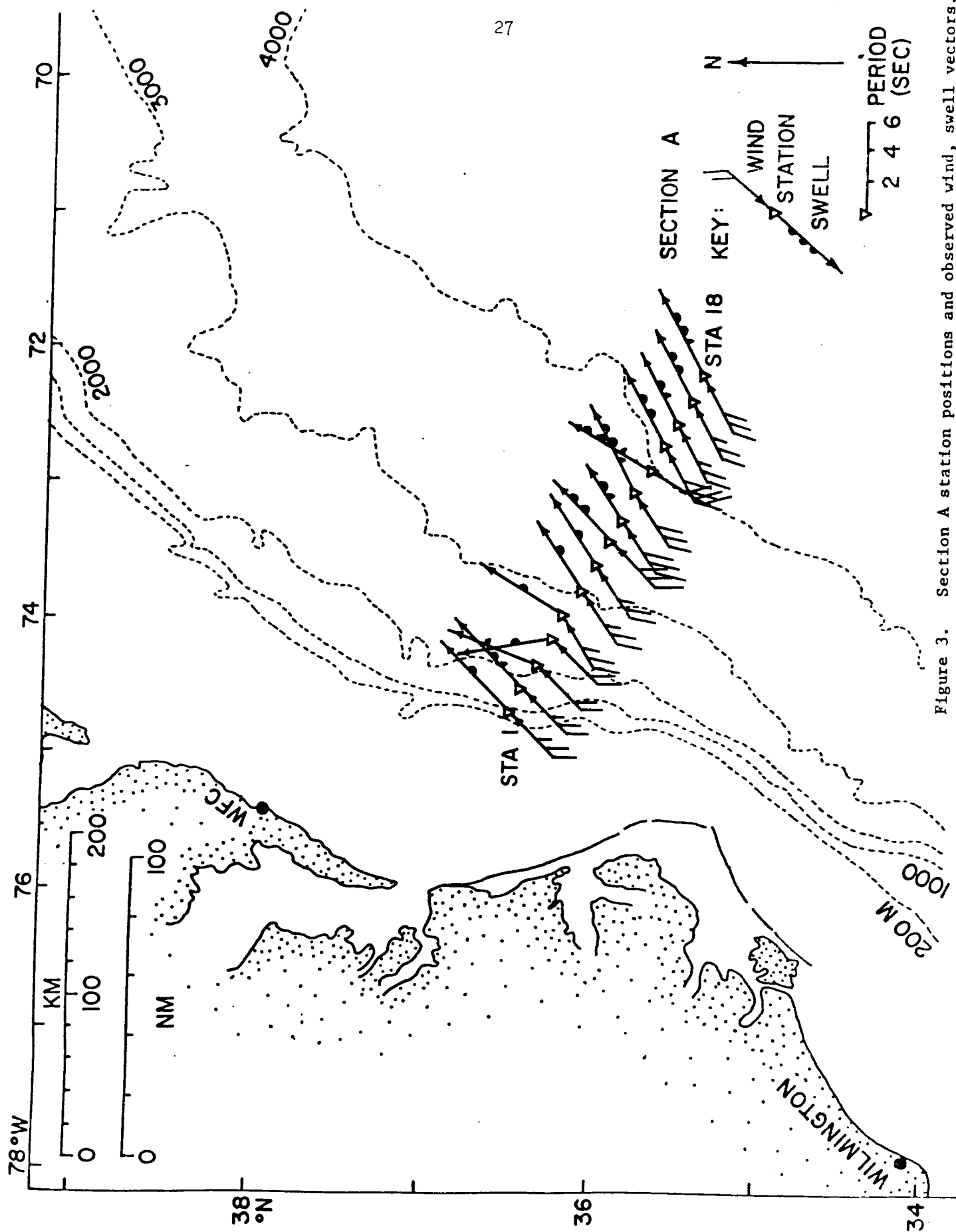
Figure 3. Section A station positions and observed wind, swell vectors.

GENERAL SYMBOL KEY FOR WIND/SWELL FIGURES
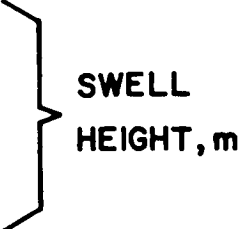
MAP SYMBOL	VELOCITY, MPH
▽	< 1
	1 - 3
	4 - 7
	8 - 12
	13 - 18
	19 - 24
	25 - 31
	32 - 38
	39 - 46
	47 - 54
	55 - 63
	64 - 75
	> 75
•	2
••	4
•••	6

SWELL HEIGHT, m

Figure 4. General symbol key for wind, swell figures.

Table 6. Atmospheric and Sea Surface Observations at Section A Stations

STATION NUMBER	WIND		SWELL			ATM PRESSURE	AIR TEMPERATURE		HUMIDITY
	DIR FROM (°T)	SPEED (M/S)	DIR TO (°T)	HT (M)	PER (S)	SURFACE (MB)	DRY (°C)	WET (°C)	RELATIVE (%)
1	225	9.3	045	1.2	6	1013.2	20.3	16.7	70
2	225	10.3	045	1.5	6	1012.9	18.9	16.1	76
3	225	8.2	020	0.6	6	1012.5	19.0	16.1	75
5	225	8.2	350	0.9	6	1013.2	19.4	16.9	78
7	238	9.3	030	0.9	6	1012.5	22.8	18.3	65
9	235	10.3	055	1.2	5	1012.5	23.3	20.6	78
10	235	9.8	055	1.2	5	1012.2	23.4	20.7	78
11	225	12.9	045	1.8	6	1012.2	22.2	20.3	84
12	235	12.9	055	1.5	4	1011.5	25.3	21.6	72
13	235	13.9	060	2.7	6	1010.8	24.0	20.6	74
14	235	13.9	030	2.4	6	1010.8	22.5	20.7	85
15	210	12.9	060	2.1	5	1009.8	22.3	19.6	78
16	240	10.3	060	1.5	5	1010.5	22.2	20.3	84
17	240	10.3	060	2.1	5	1011.2	21.1	20.0	90
18	240	12.9	060	2.4	6	1010.8	21.4	20.0	88
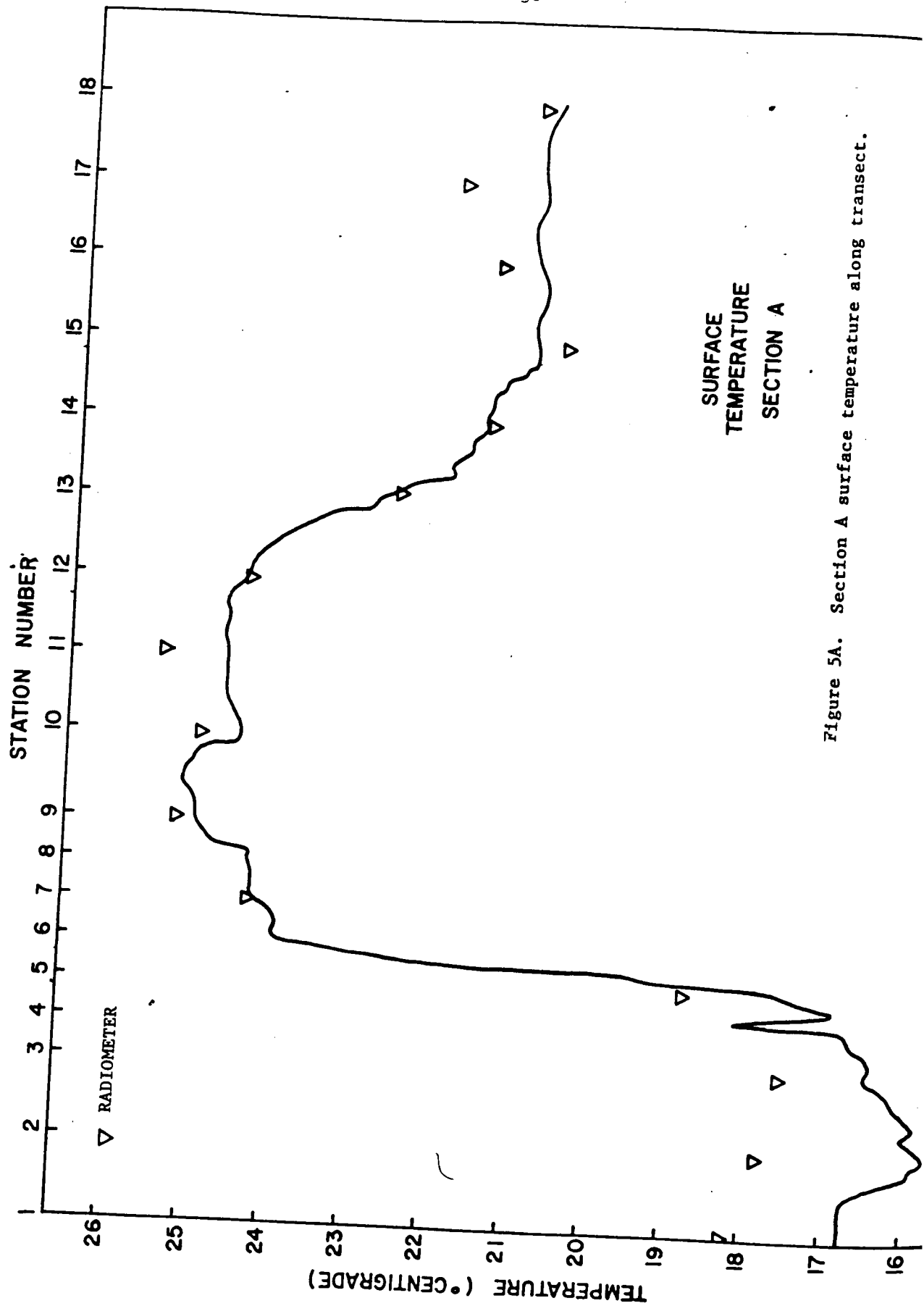
Figure 5A. Section A surface temperature along transect.
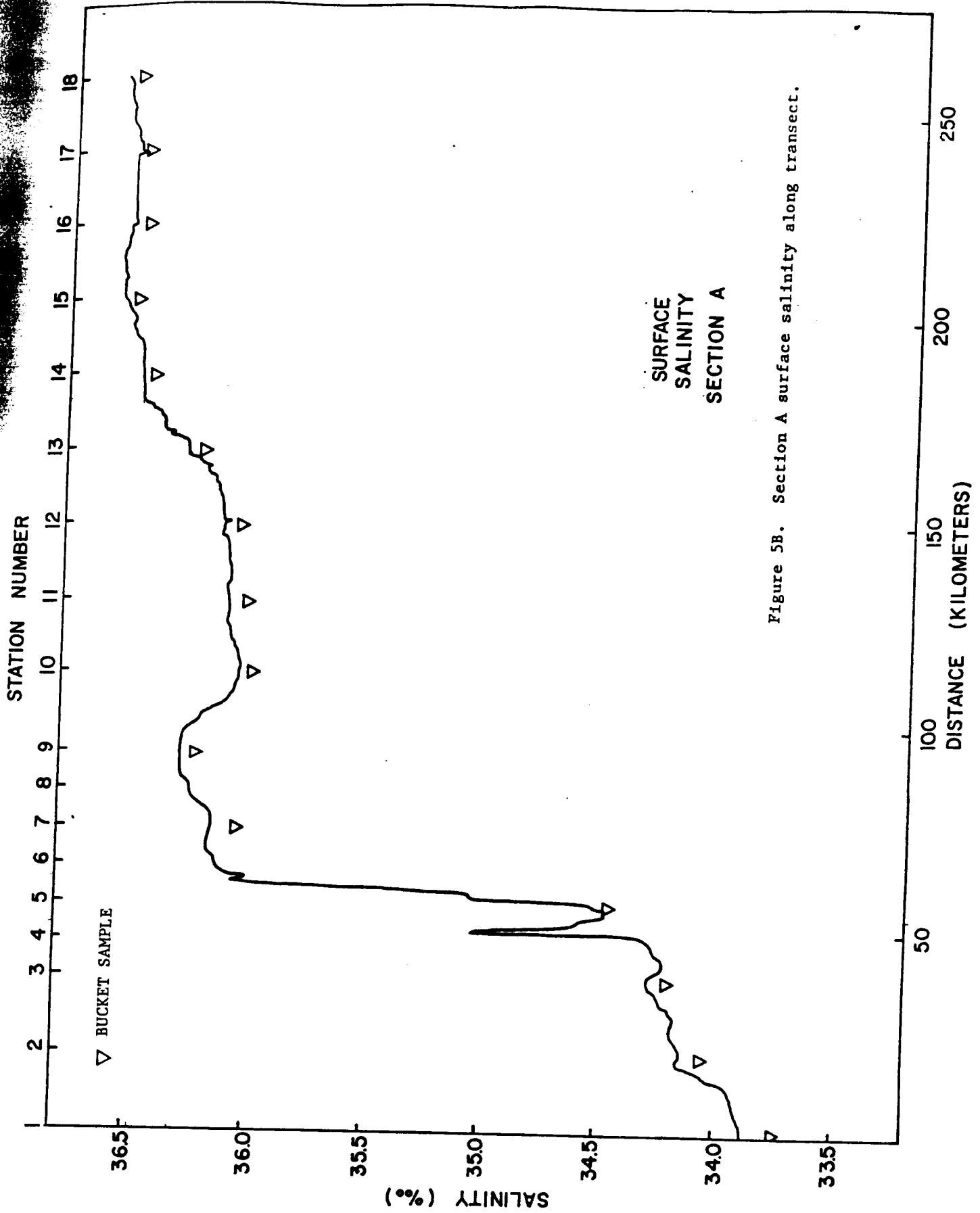
Figure 5B. Section A surface salinity along transect.

Figure 5C. Section A surface sigma-t along transect.
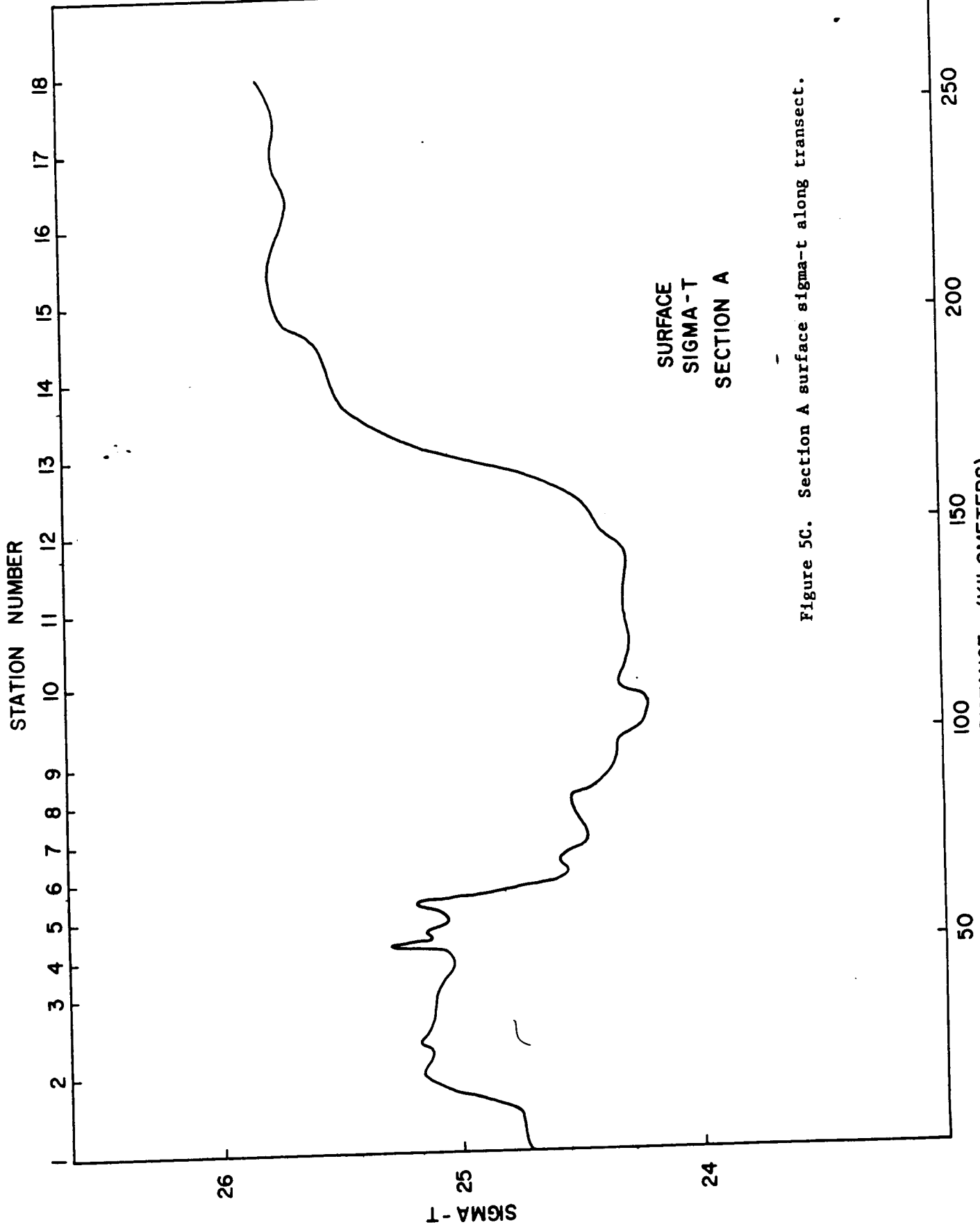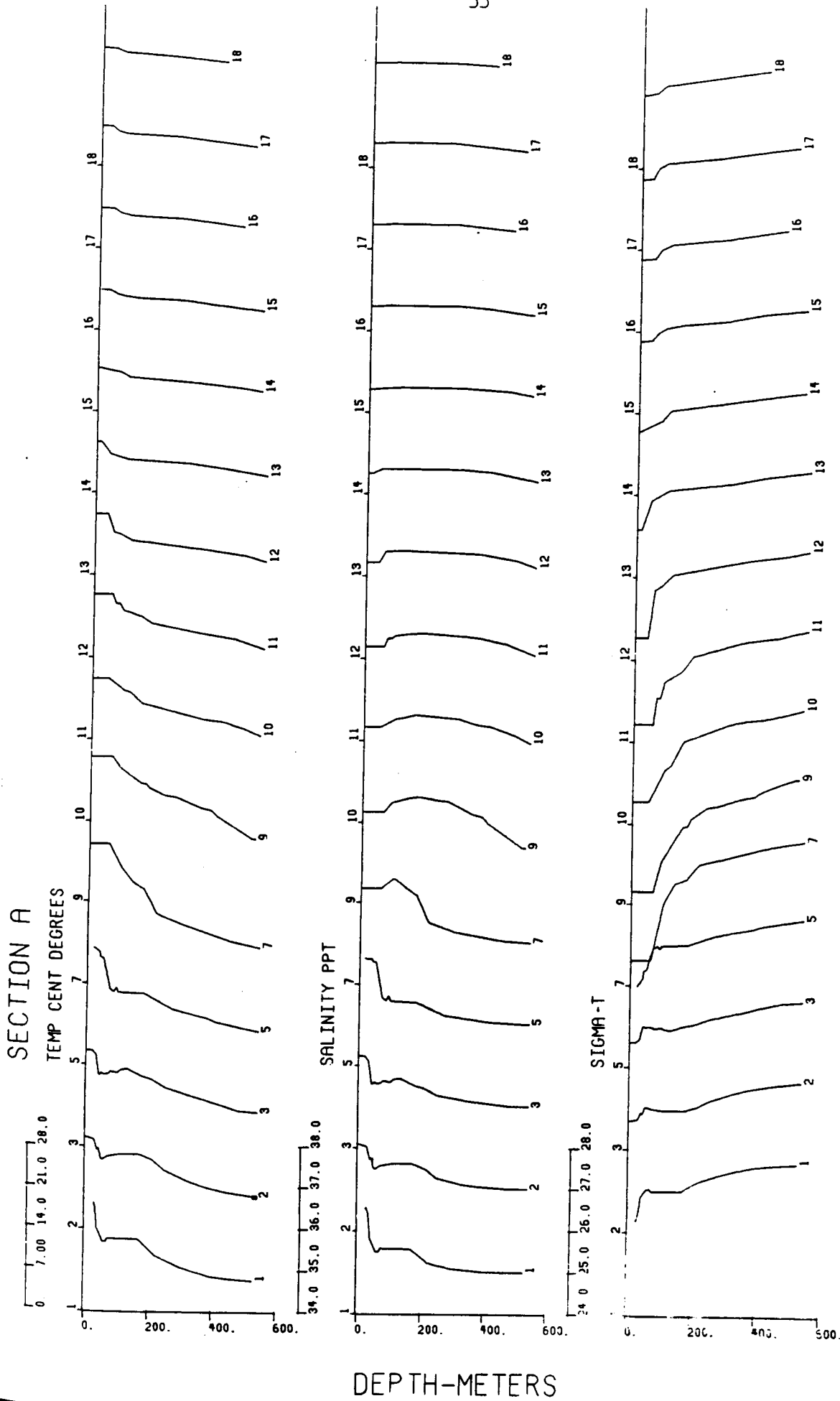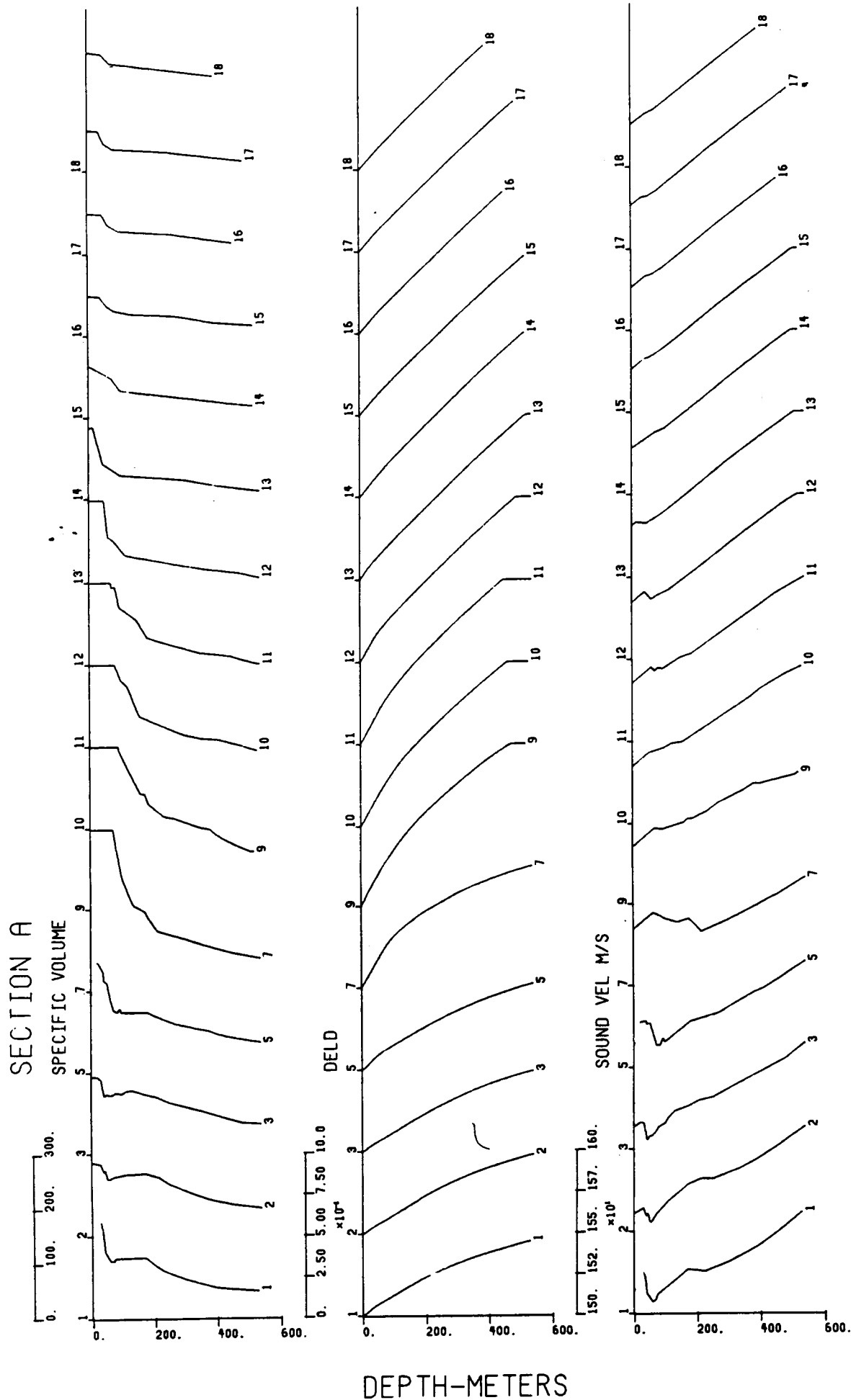
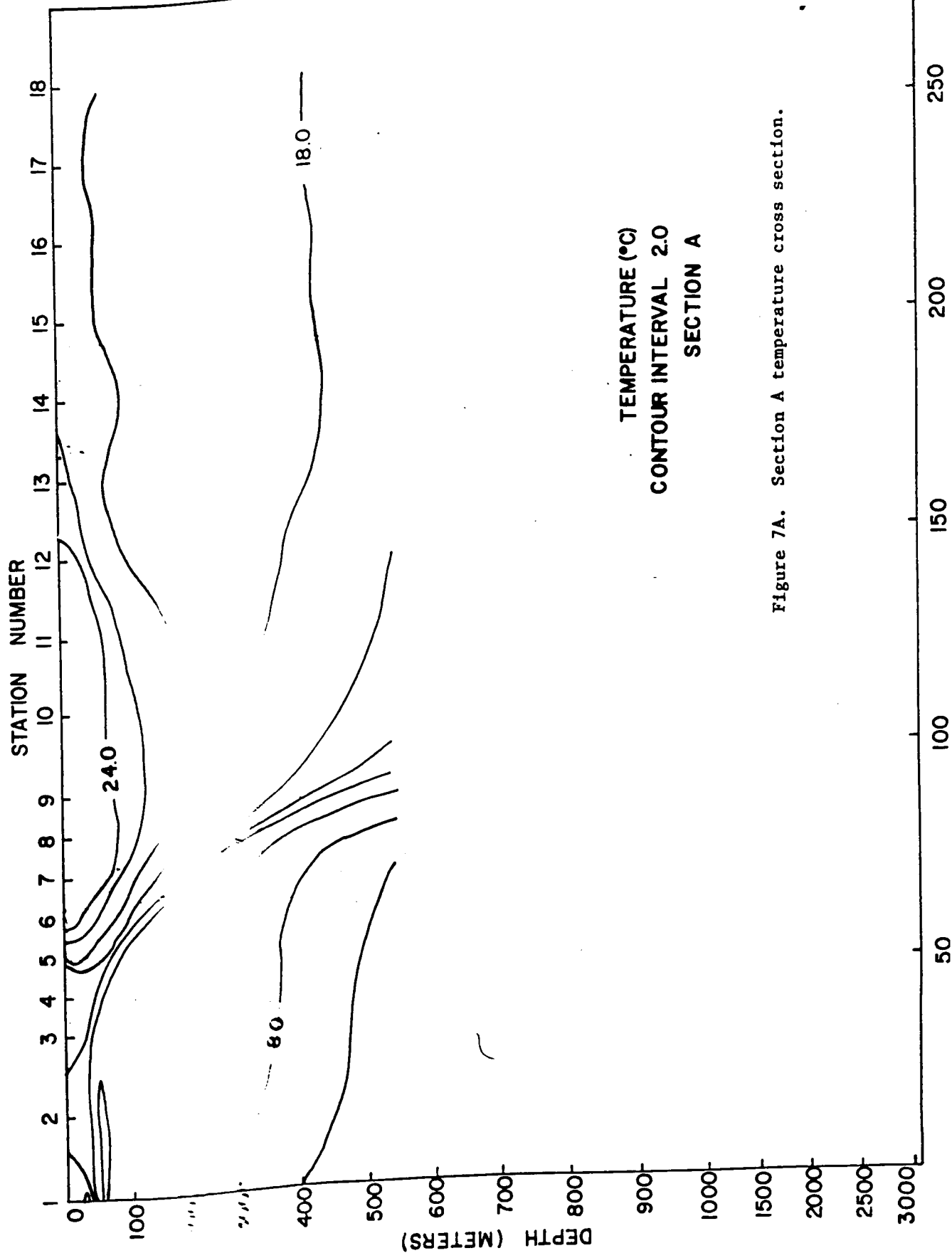Figure 6. Section A observed and derived station profiles.

SECTION A
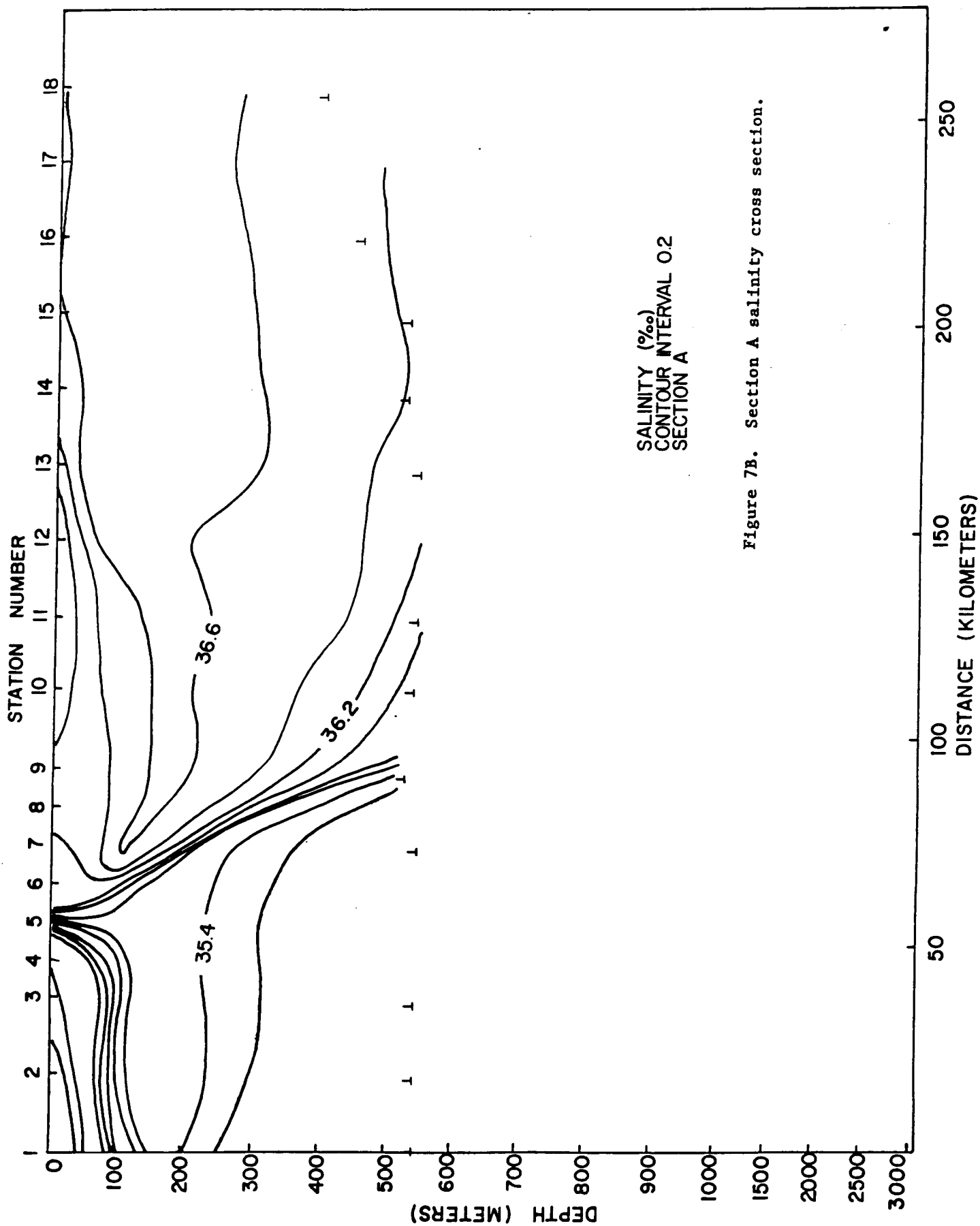SPECIFIC VOLUME

DELD

SOUND VEL M/S

DEPTH-METERS

Figure 6. Continued.

SECTION A

N SQRD

DEPTH—METERS

Figure 6. Continued.

TEMPERATURE (°C)
CONTOUR INTERVAL 2.0
SECTION A
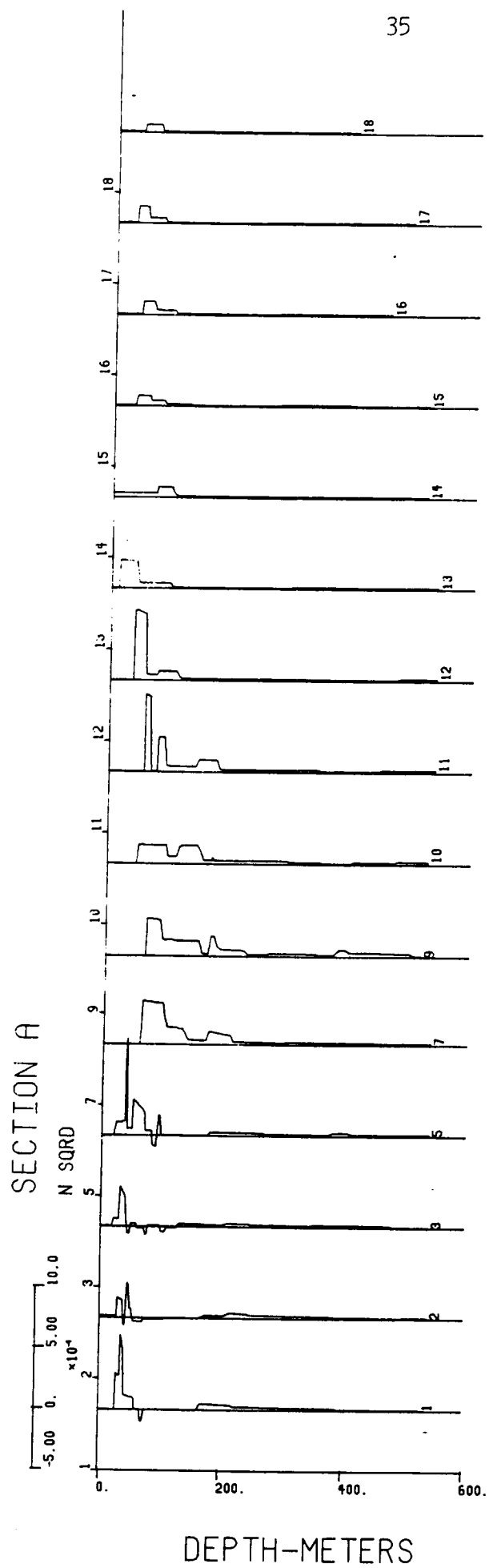
Figure 7A. Section A temperature cross section.

37

SALINITY (‰)
CONTOUR INTERVAL O.2
SECTION A

Figure 7B. Section A salinity cross section.

SIGMA-T
CONTOUR INTERVAL 0.2
SECTION A
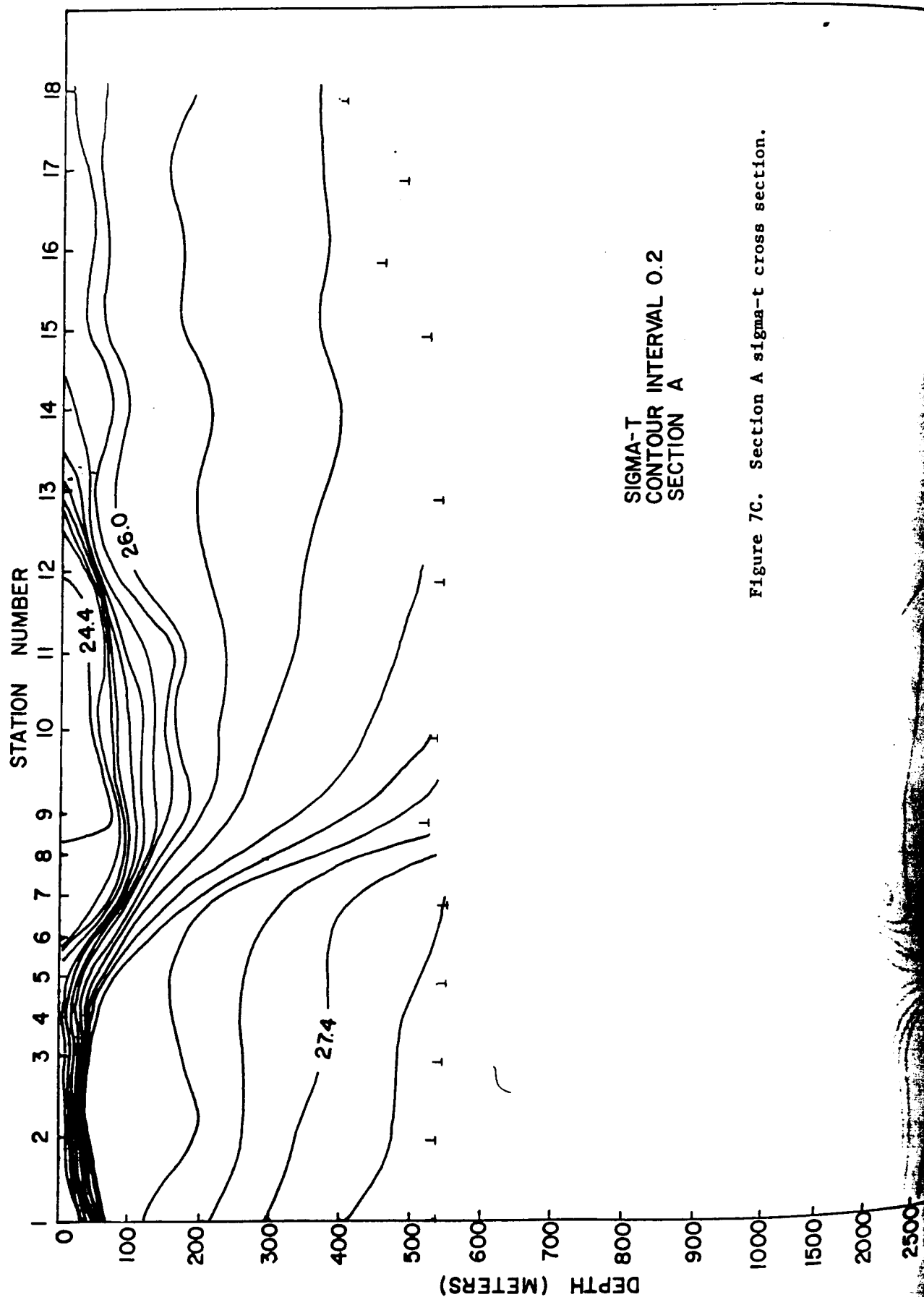
Figure 7C. Section A sigma-t cross section.
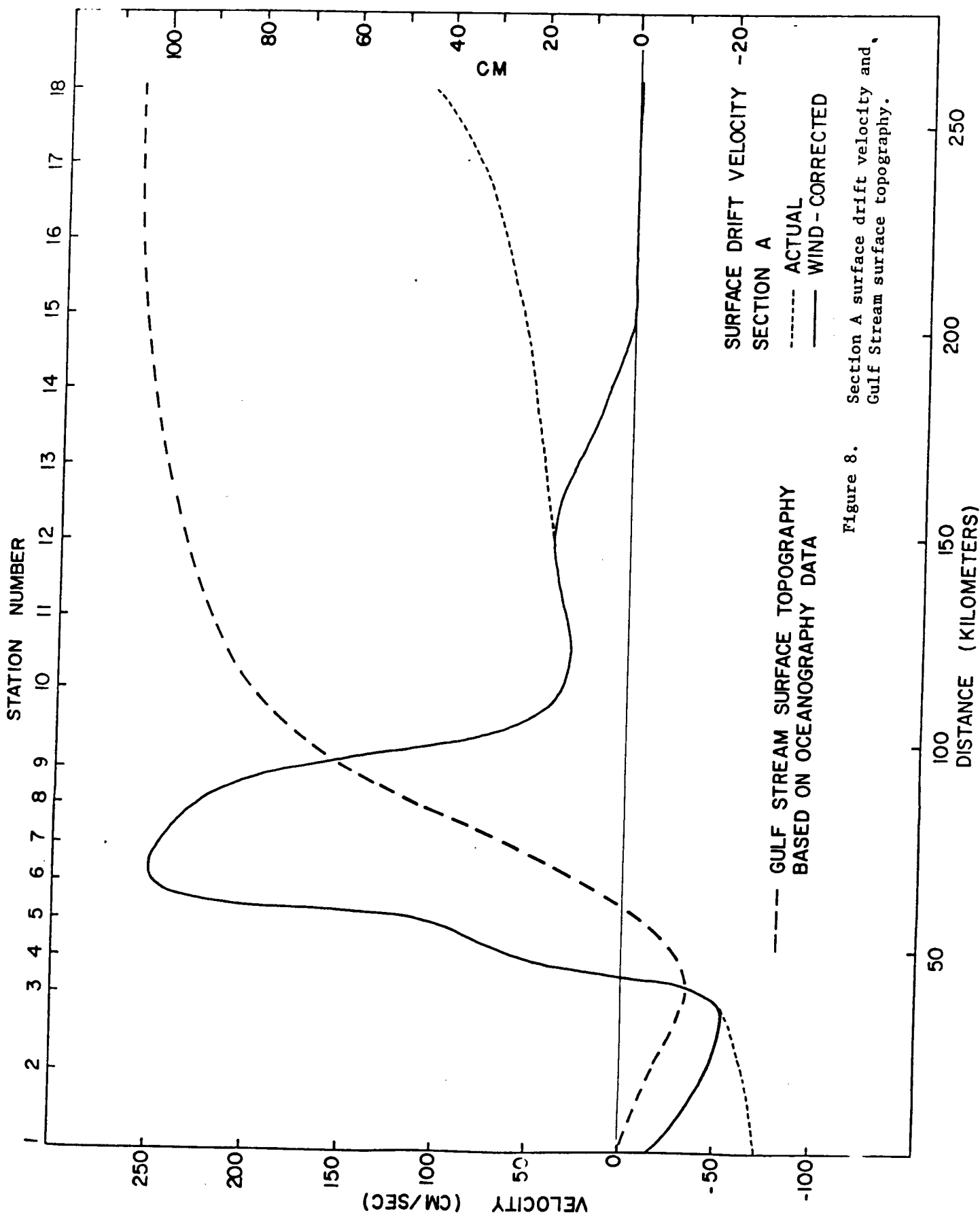
Figure 8. Section A surface drift velocity and Gulf Stream surface topography.
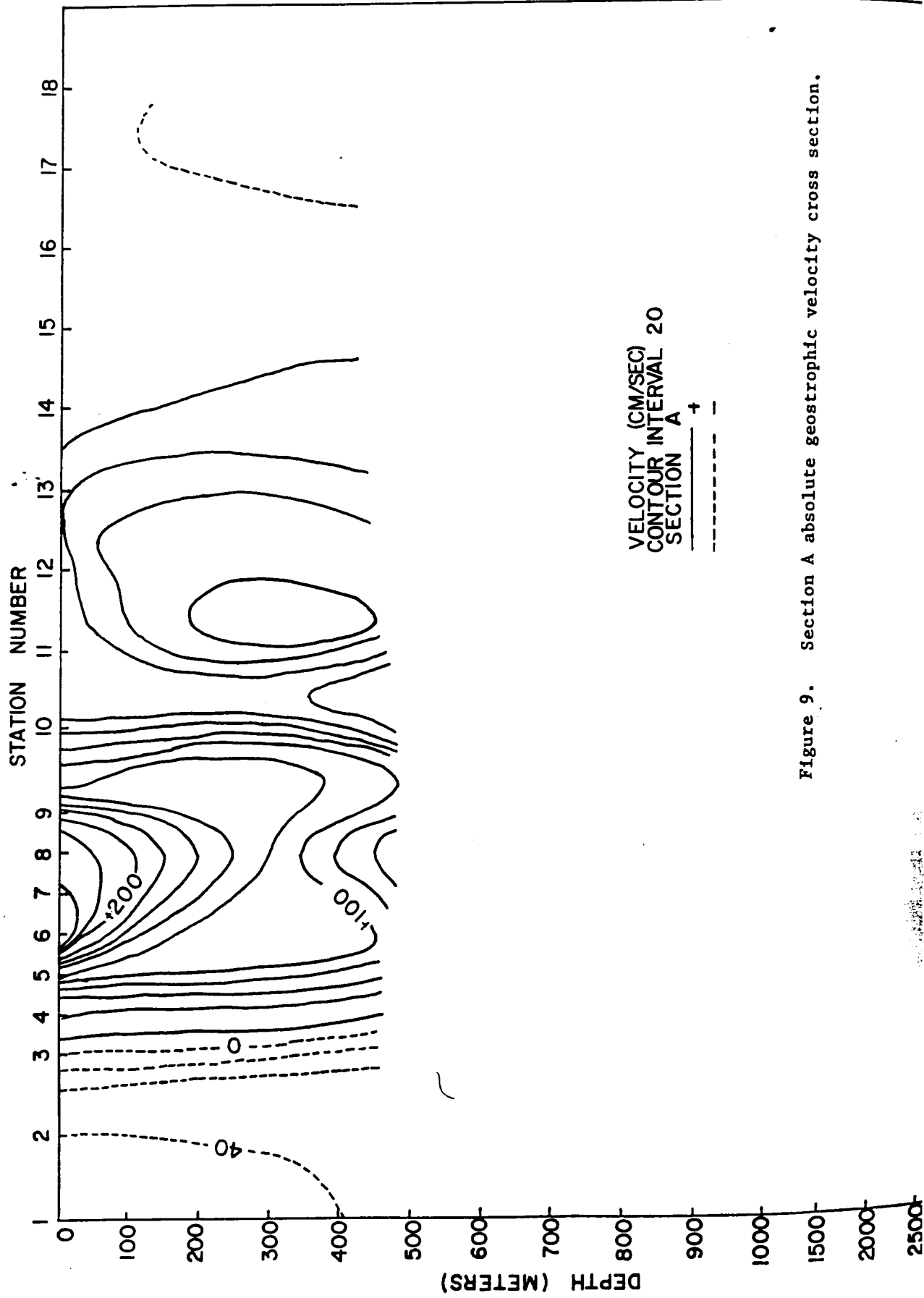
Figure 9.   Section A absolute geostrophic velocity cross section.

3.2

Section B
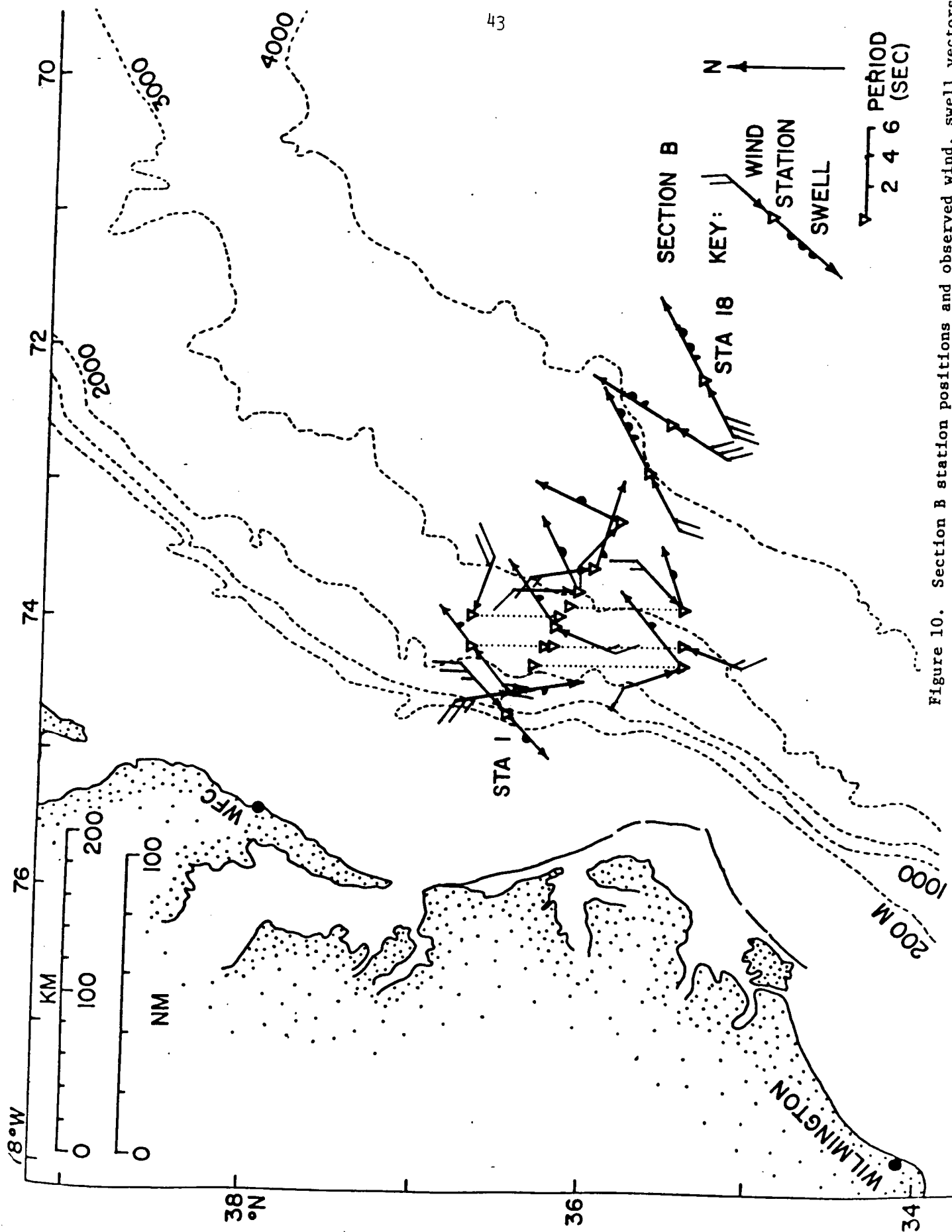
Figure 10. Section B station positions and observed wind, swell vectors.

Table 7. Atmospheric and Sea Surface Observations at Section B Stations

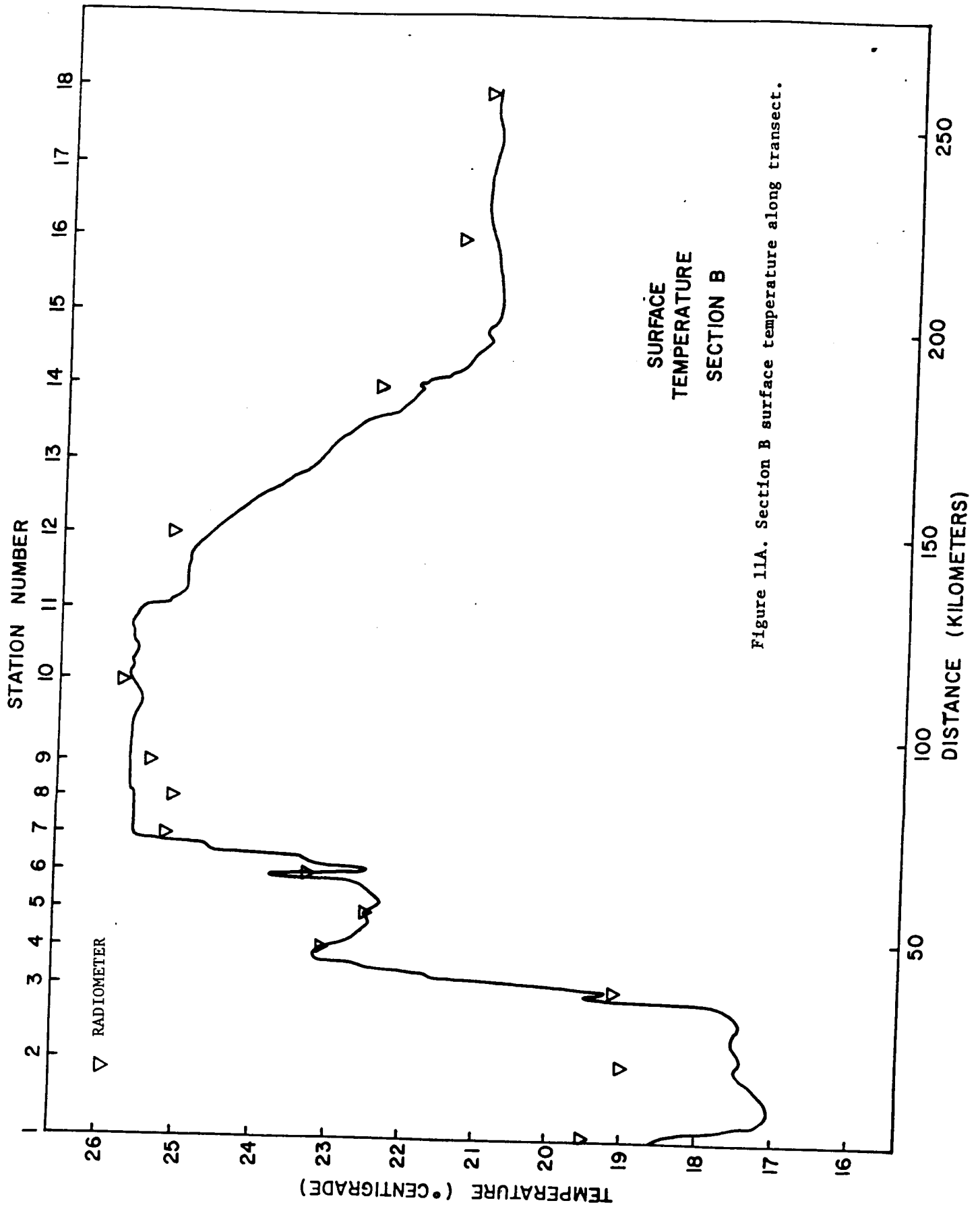| STATION NUMBER	WIND		SWELL			ATM PRESSURE	AIR TEMPERATURE		HUMIDITY
	DIR FROM (°T)	SPEED (M/S)	DIR TO (°T)	HT (M)	PER (S)	SURFACE (MB)	DRY (°C)	WET (°C)	RELATIVE (%)
1	045	9.3	225	1.2	4	1006.8	17.2	15.6	85
2	350	9.3	170	0.6	4	1006.4	16.9	15.8	89
3	340	3.1	160	0.3	6	1006.4	21.6	19.3	81
4	230	7.7	050	0.6	3	1007.8	23.5	20.8	78
5	200	5.1	020			1009.8	23.6	20.7	77
6	200	5.1	020	0.6	5	1009.8	24.9	21.2	72
7	110	6.2	290			1009.8	22.5	17.5	62
8	045	5.1	225	0.9	4	1010.8	23.3	18.3	62
9	000	2.6	180	0.9	5	1010.8	23.3	18.3	62
10	350	4.1	170	0.6	6	1011.2	24.7	18.9	59
12	315	2.1	135	1.2	6	1011.2	26.7	19.4	50
14	240	6.2	060	2.4	6	1011.2	25.6	21.7	71
16	210	12.9	030	1.5	6	1009.8	22.2	20.6	87
18	240	12.9	060	2.4	6	1010.8	21.4	20.0	88

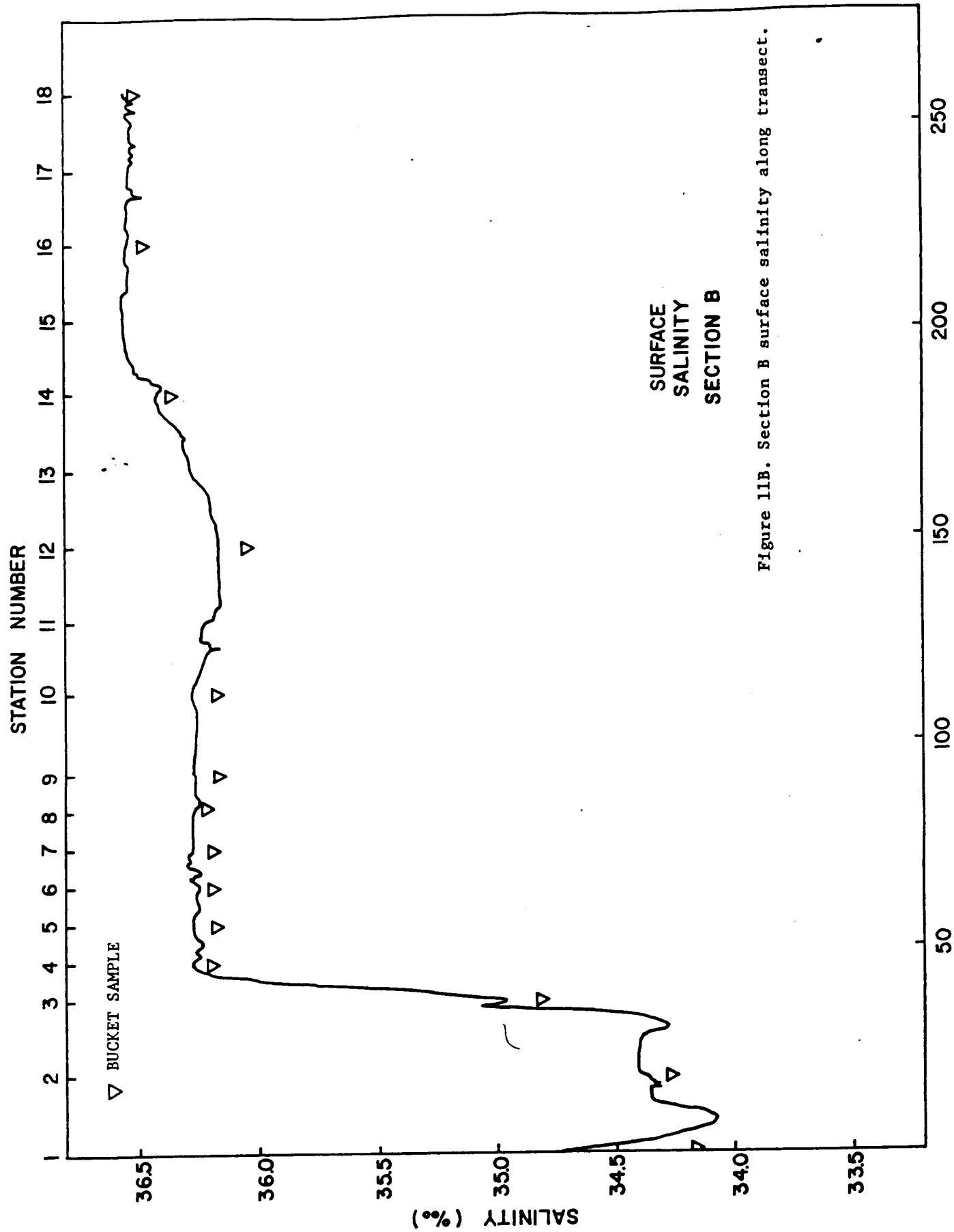Figure 11A. Section B surface temperature along transect.
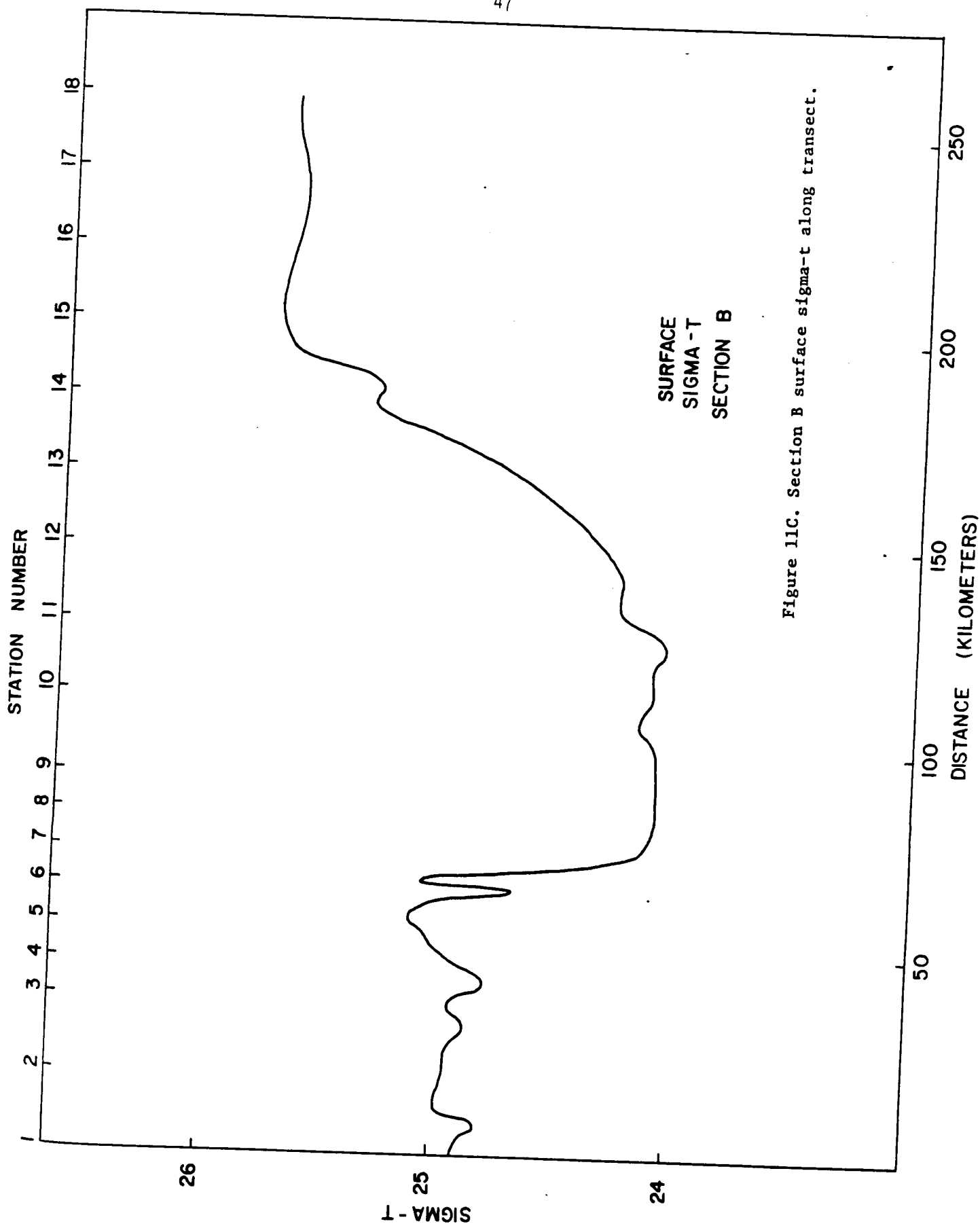
Figure 11B. Section B surface salinity along transect.

Figure 11c. Section B surface sigma-t along transect.

48
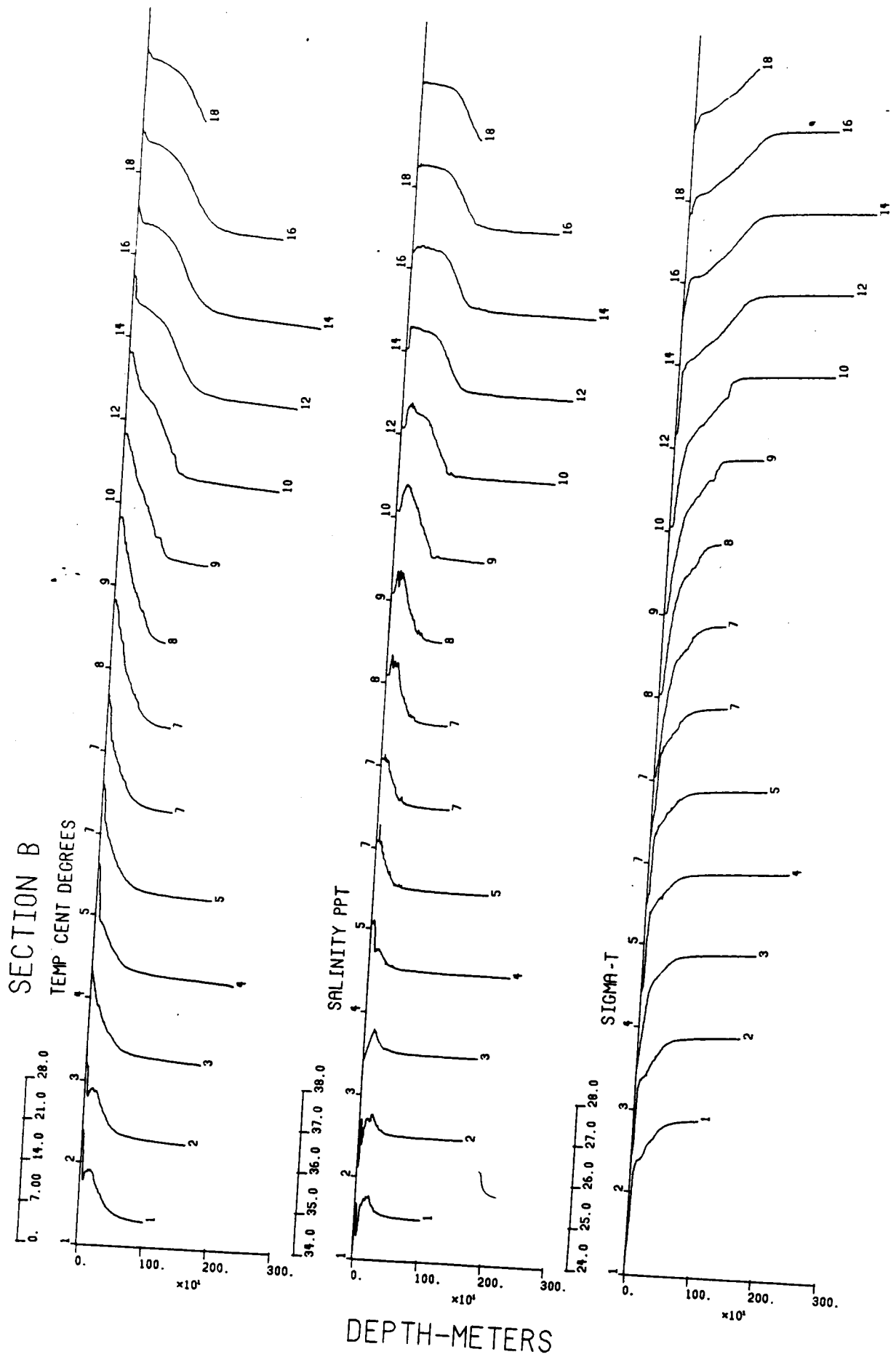
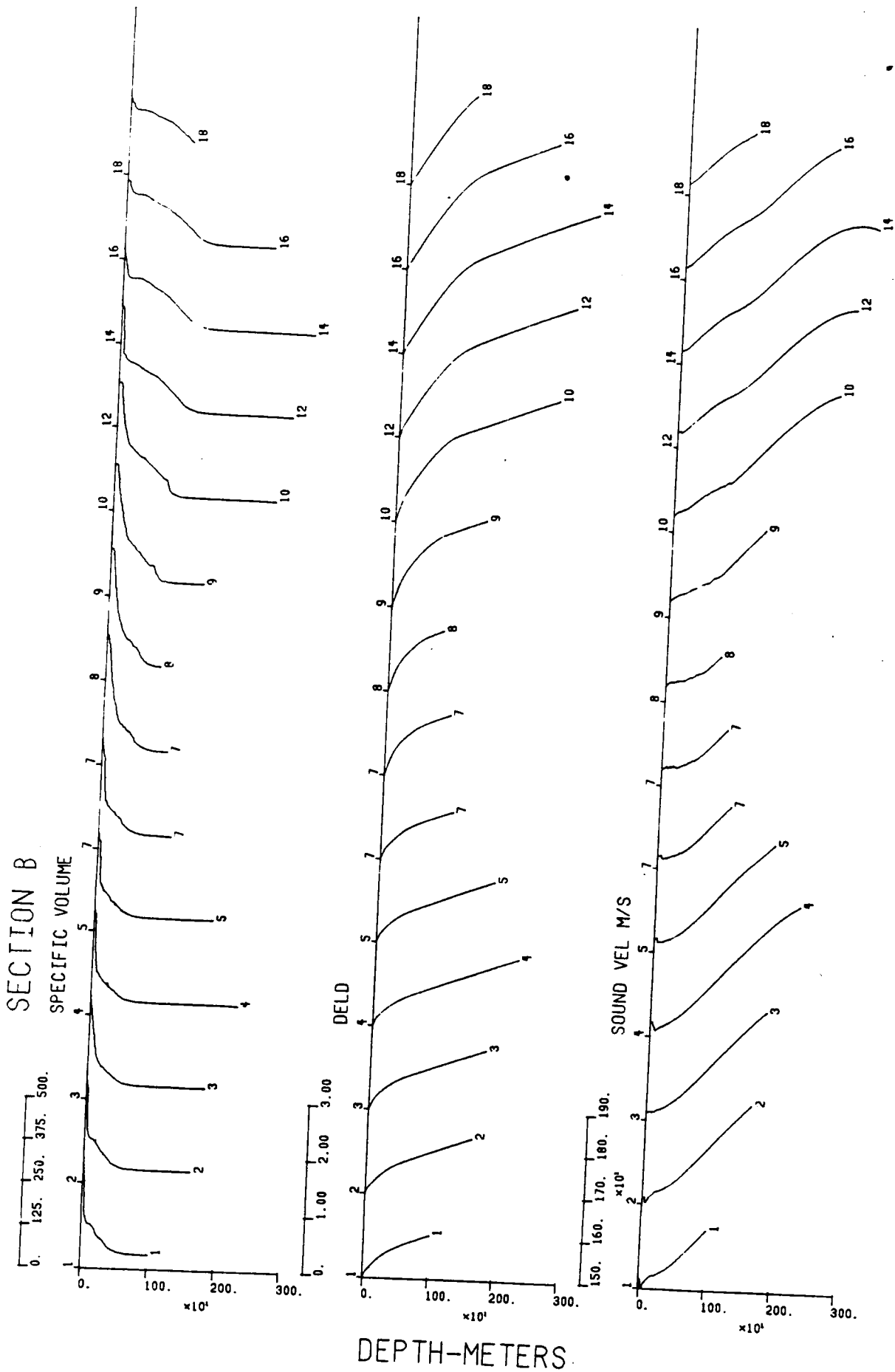Figure 12. Section B observed and derived station profiles.

SECTION B

SPECIFIC VOLUME

DELD

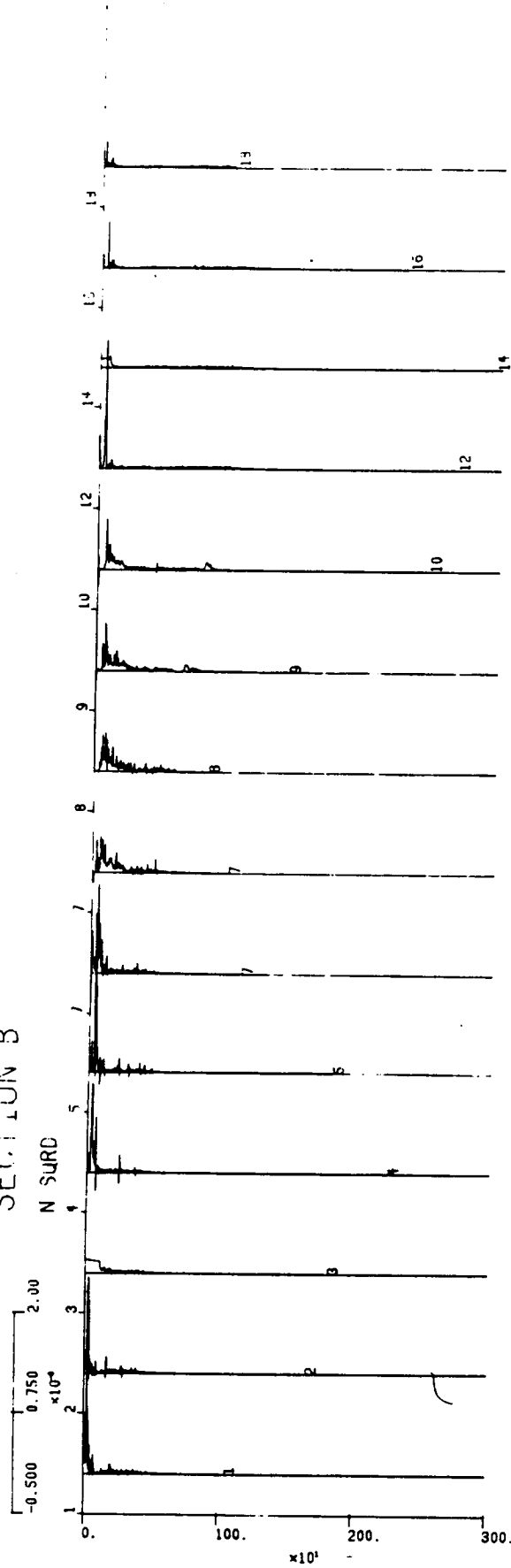SOUND VEL M/S

DEPTH-METERS

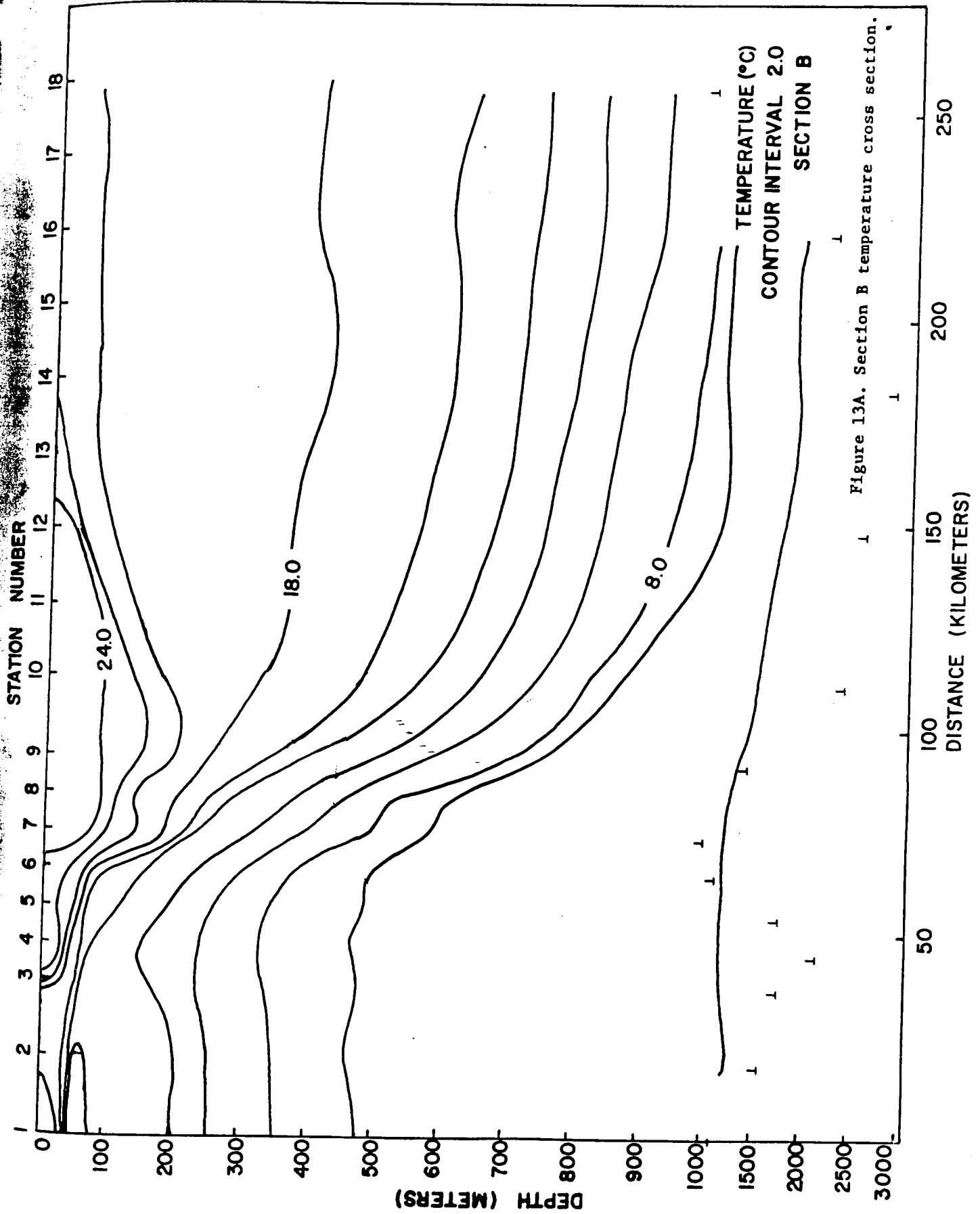Figure 12. Continued.

Figure 12. Continued.
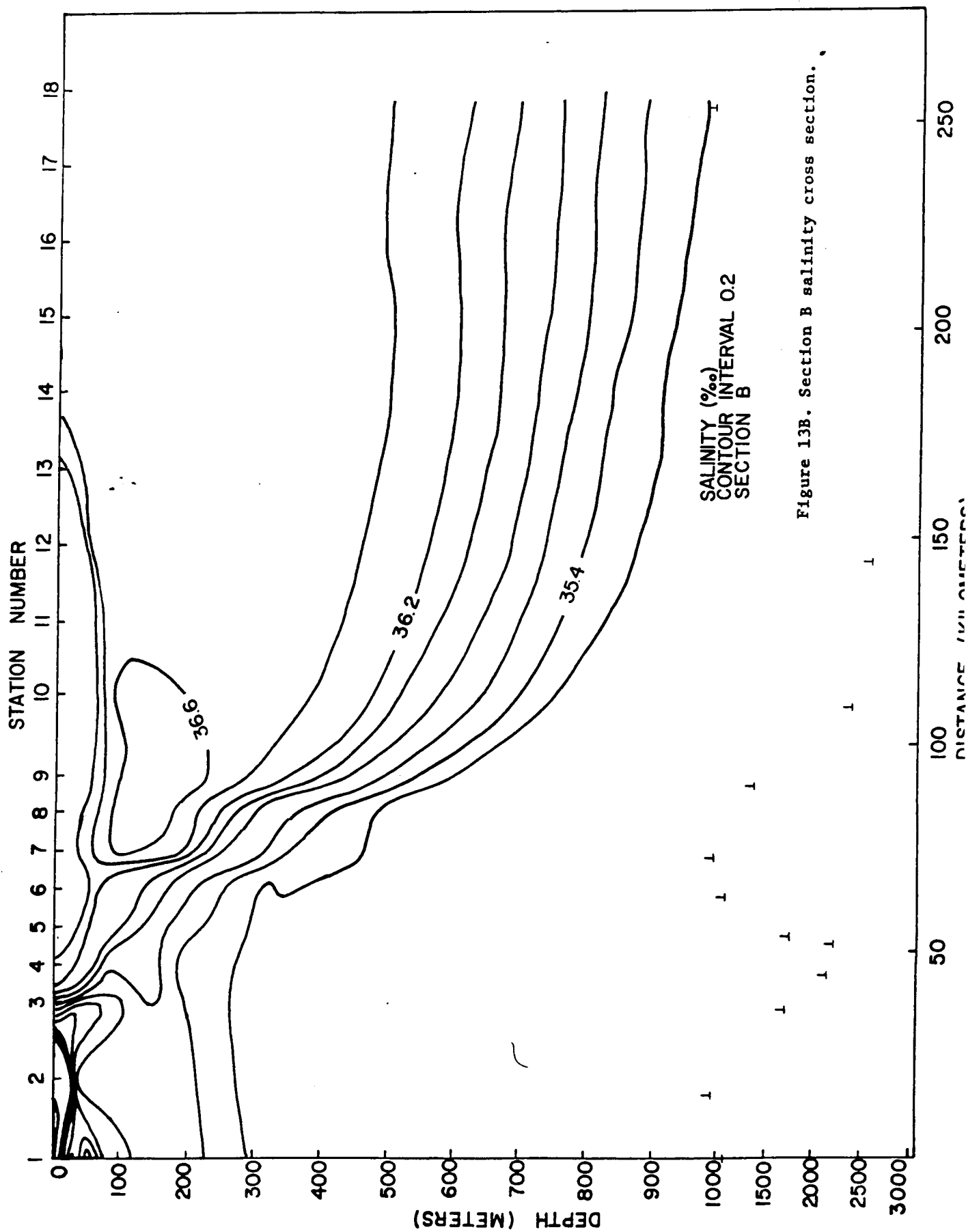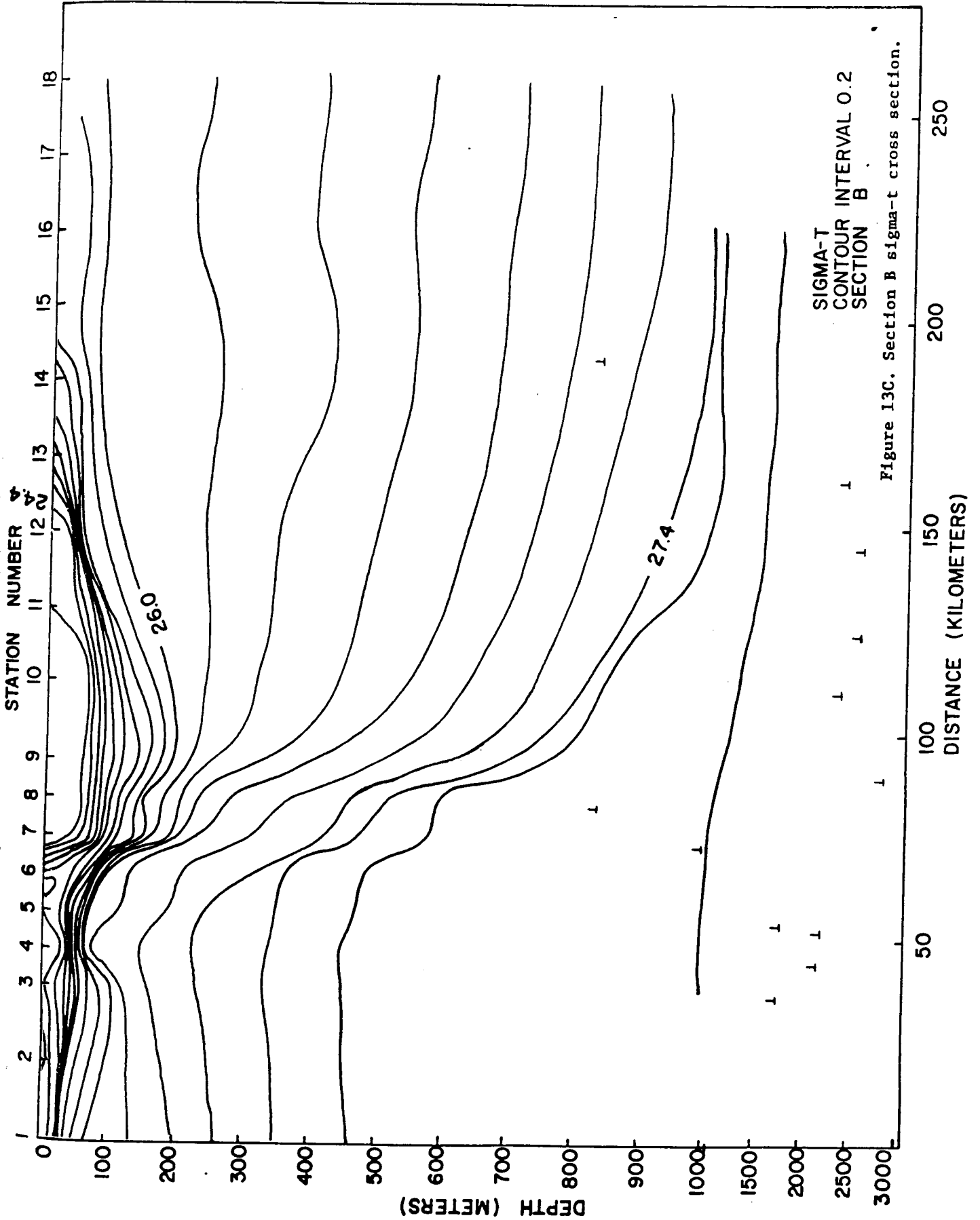
Figure 13A. Section B temperature cross section.

Figure 13B. Section B salinity cross section.

SALINITY (‰)
CONTOUR INTERVAL 0.2
SECTION B

SIGMA-T
CONTOUR INTERVAL 0.2
SECTION B

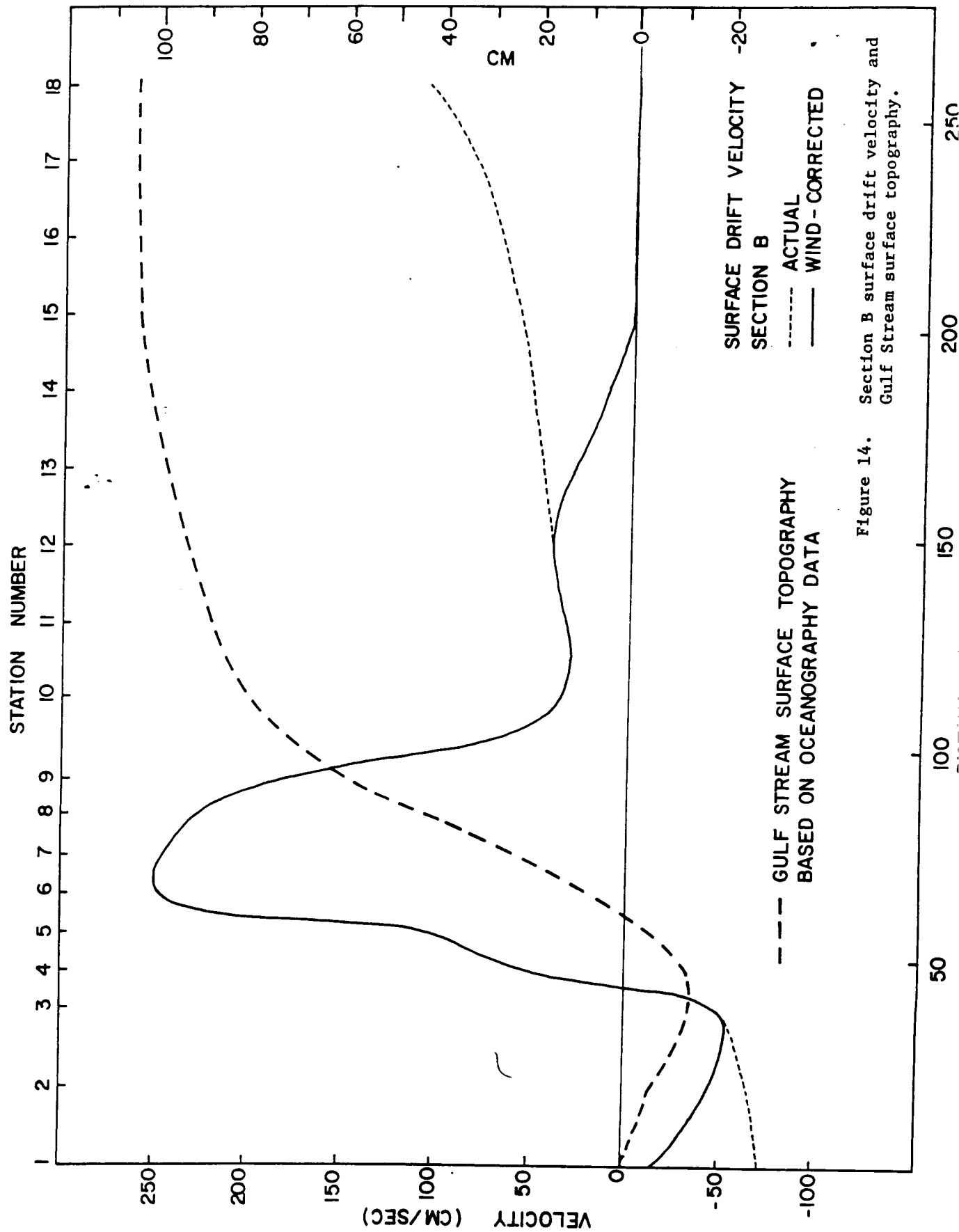Figure 13C. Section B sigma-t cross section.

54

Figure 14. Section B surface drift velocity and Gulf Stream surface topography.
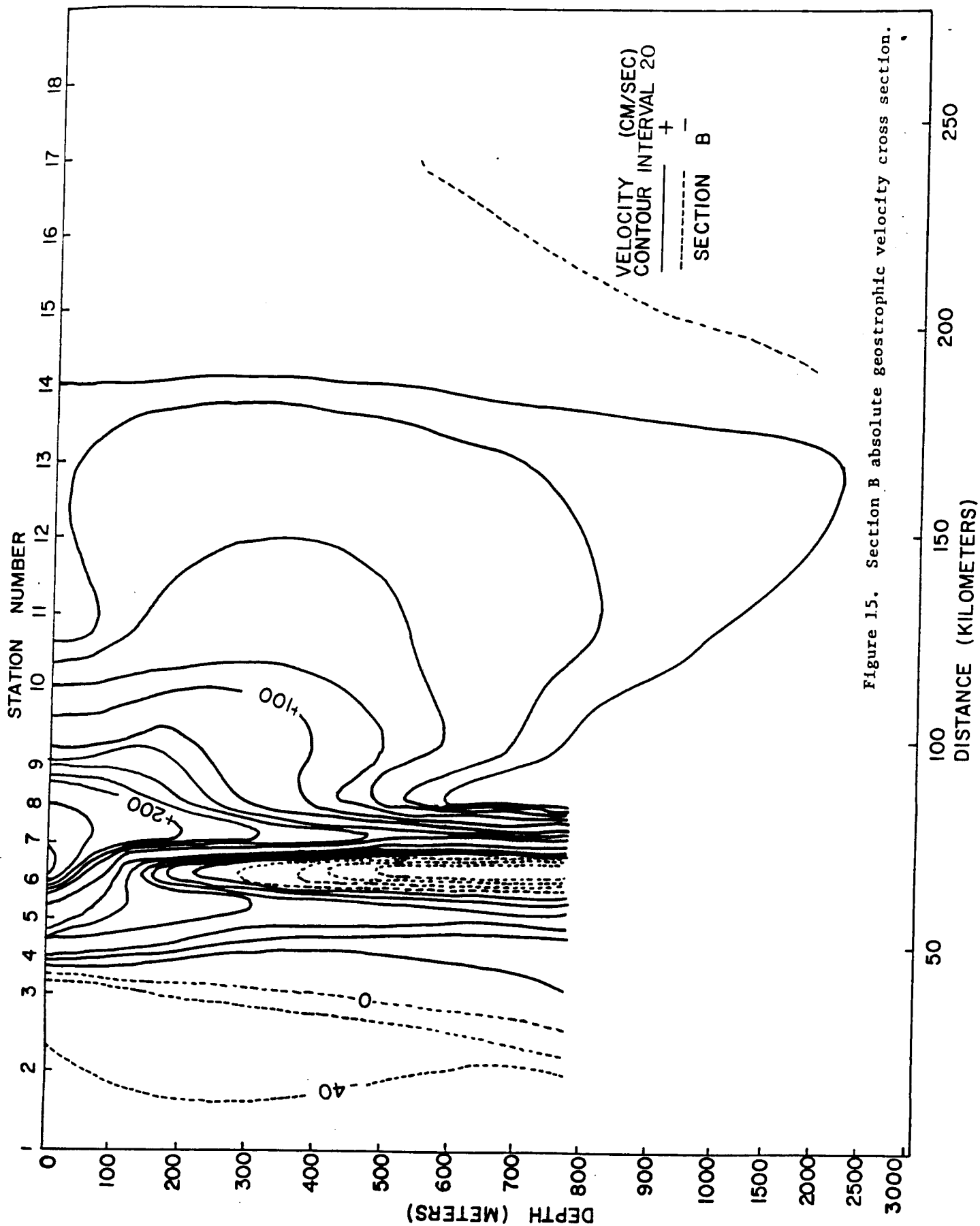
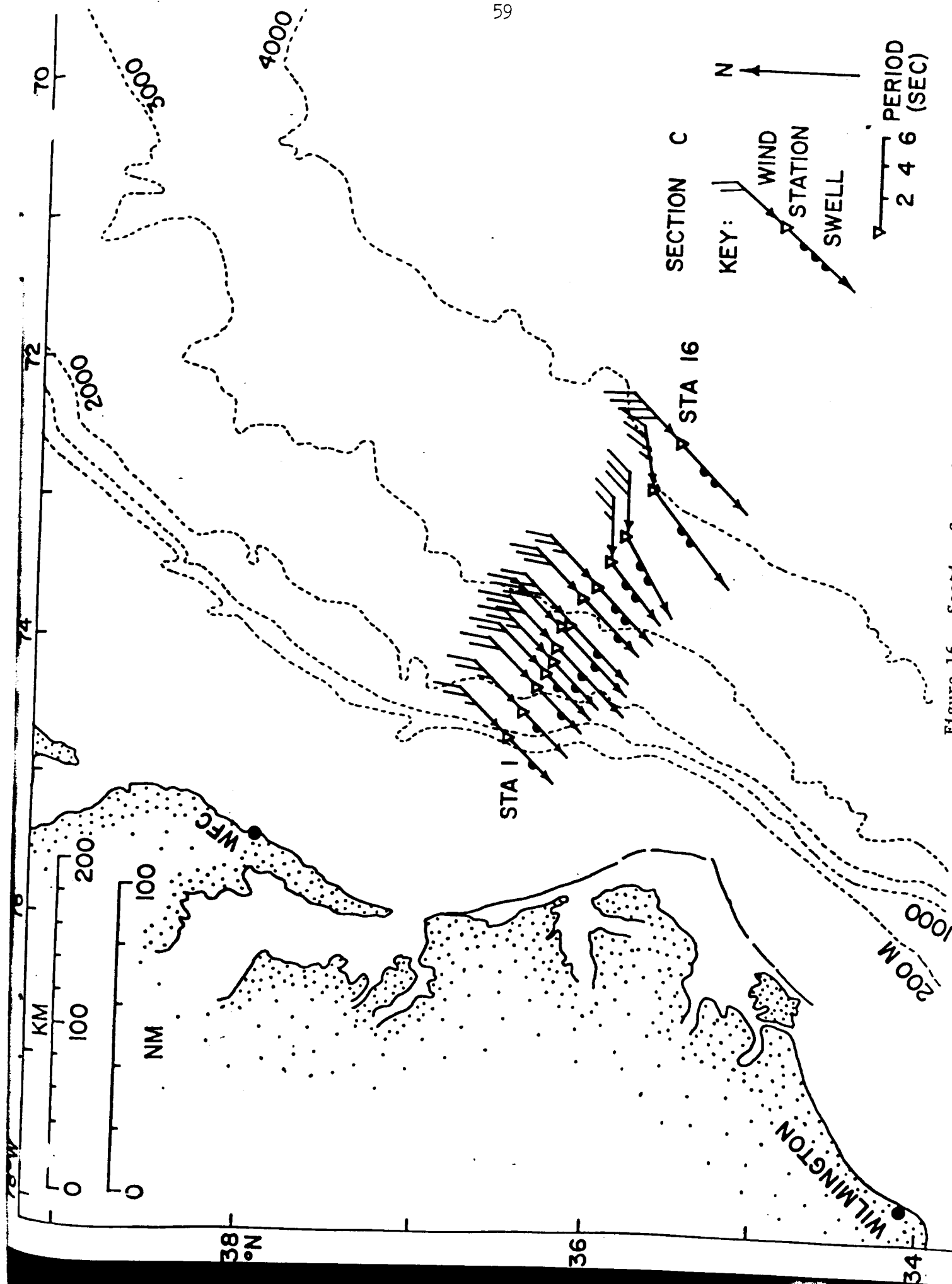Figure 15. Section B absolute geostrophic velocity cross section.

3.3

Section C

Figure 16. Section C station positions and observed wind, swell vector

Table 8. Atmospheric and Sea Surface Observations at Section C Stations

| STATION NUMBER	WIND		SWELL			ATM PRESSURE	AIR TEMPERATURE		HUMIDITY
	DIR FROM (°T)	SPEED (M/S)	DIR TO (°T)	HT (M)	PER (S)	SURFACE (MB)	DRY (°C)	WET (°C)	RELATIVE (%)
1	045	9.3	225	1.2	4	1006.8	17.2	15.6	85
2	045	9.3	225	1.2	4	1006.8	20.6	16.1	64
3	045	7.7	225	1.2	4	1006.8	19.4	17.8	86
4	045	6.2	225	1.2	4	1006.4	20.4	18.3	82
5	045	10.3	225	1.2	4	1003.7	19.5	17.3	81
6	045	12.9	225	0.9	6	1003.1	19.1	17.2	83
7	045	12.9	225	1.2	6	1002.7	19.0	17.4	86
8	045	12.9	225	0.9	5	1003.4	19.4	17.8	86
9	045	13.9	225	0.9	5	1003.1	19.9	18.9	91
10	045	9.3	225	1.8	5	1002.0	20.6	20.3	98
11	090	9.3	230	1.8	5	1001.7	19.4	18.9	95
12	090	19.9	240	2.1	6	1000.0	21.1	19.2	84
14	080	15.4	230	2.1	6	998.7	20.4	18.8	86
16	045	18.0	225	2.1	6	997.3	19.6	18.8	93
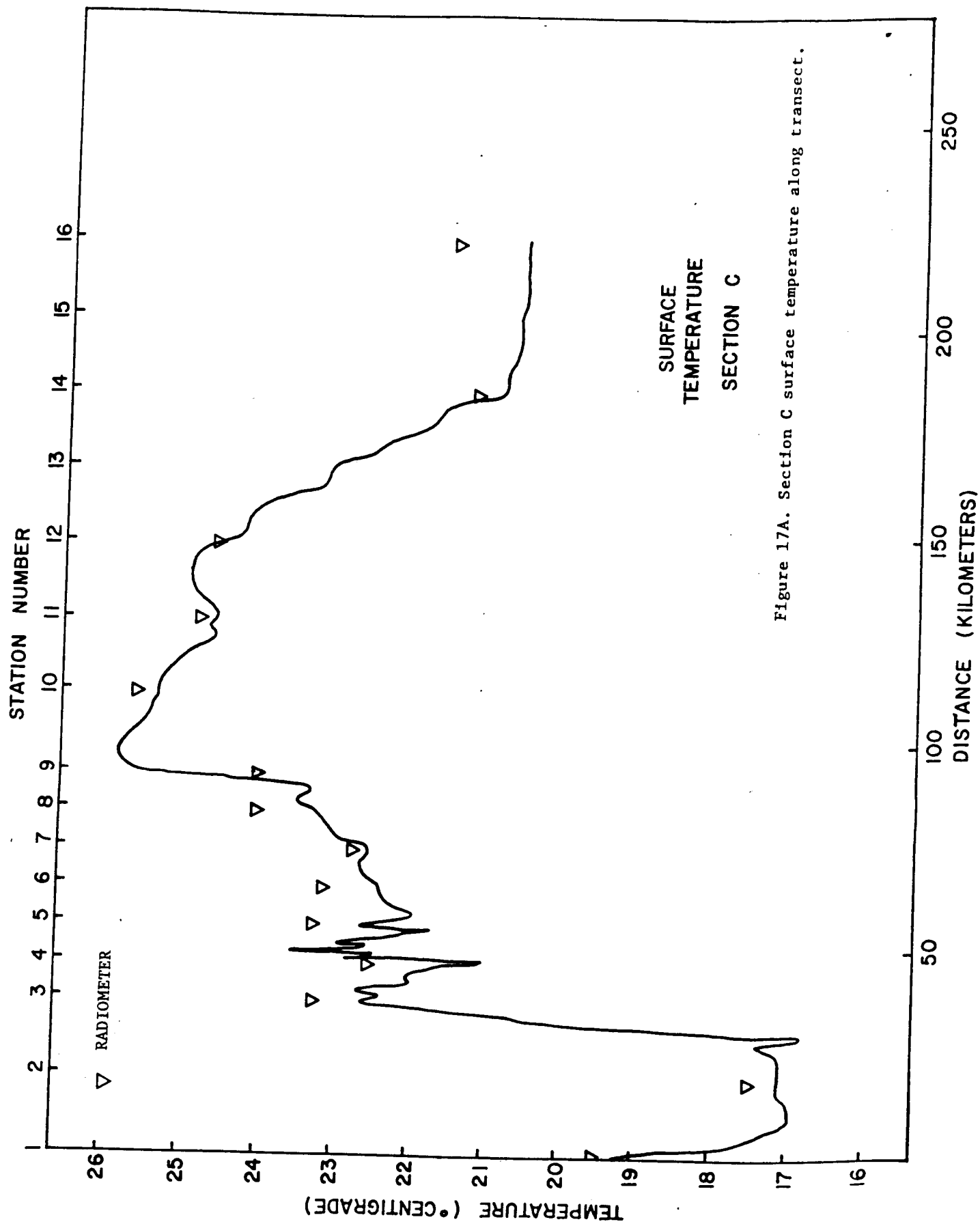
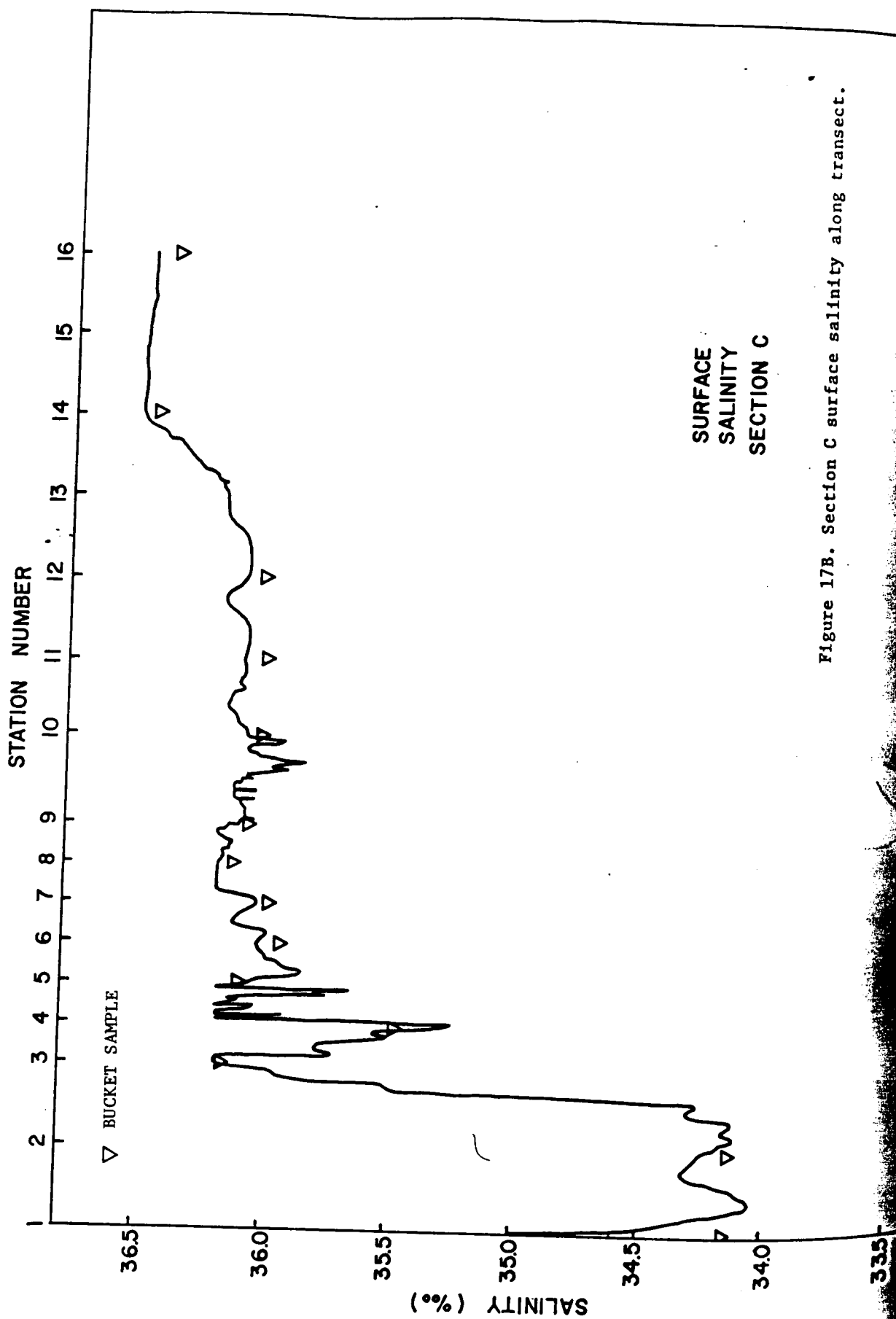Figure 17A. Section C surface temperature along transect.
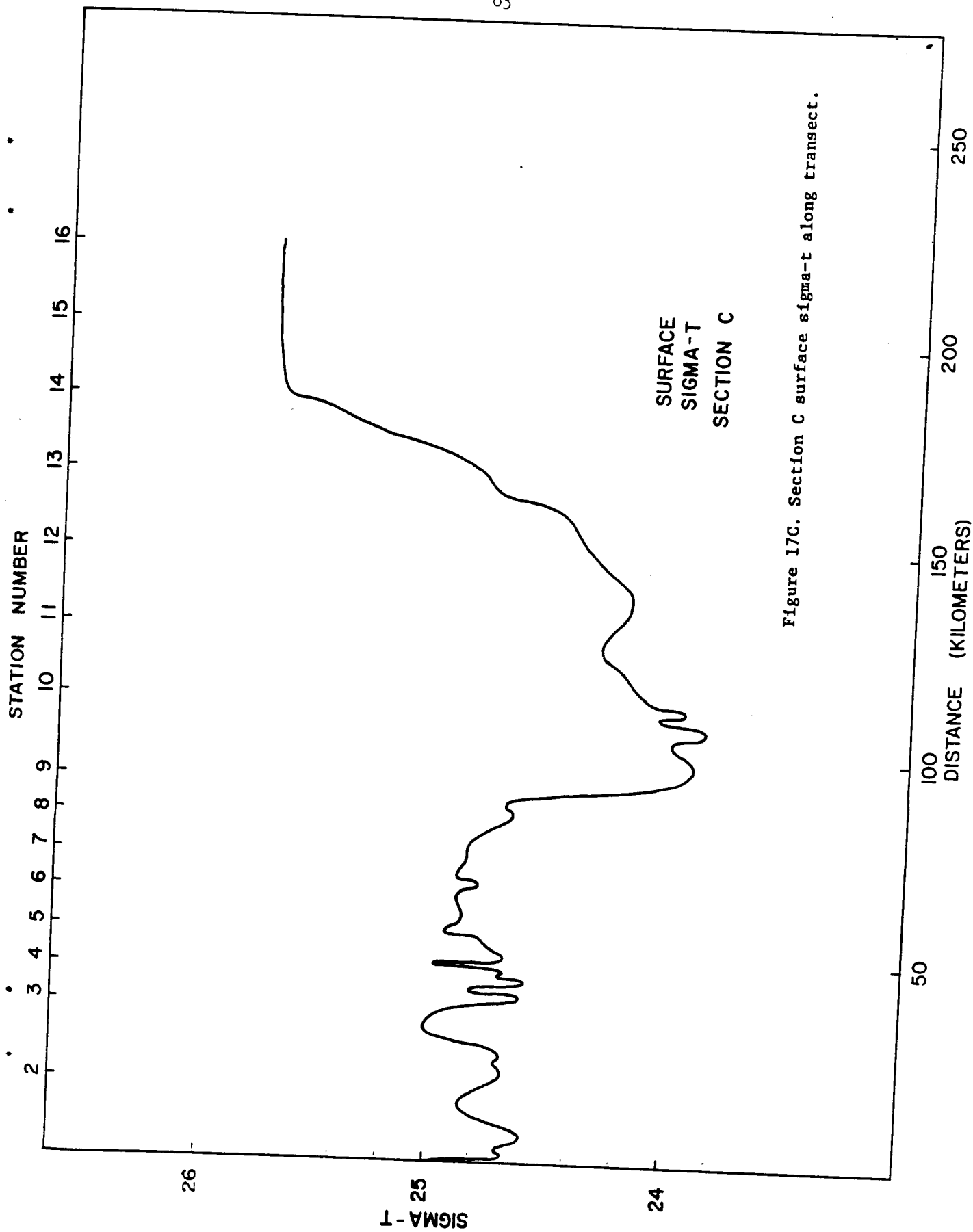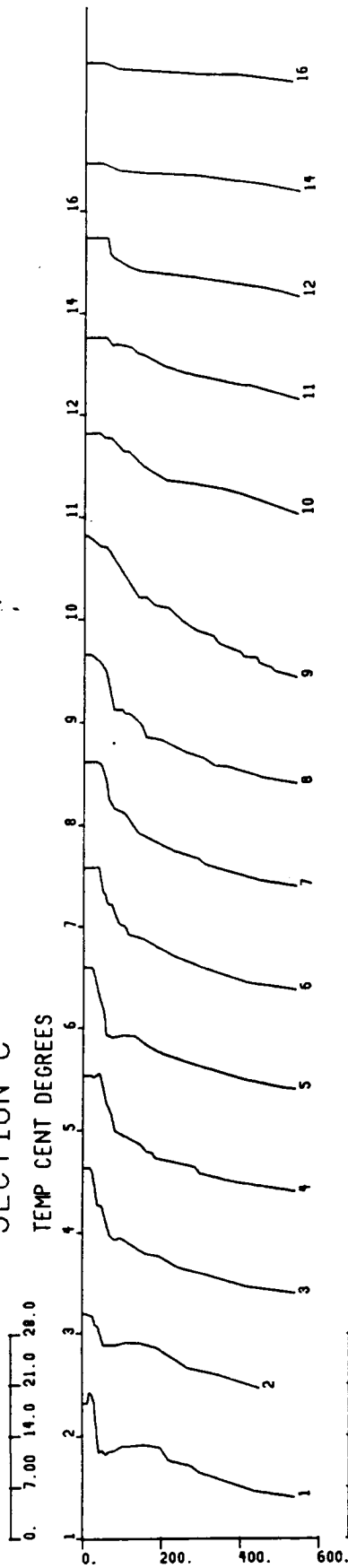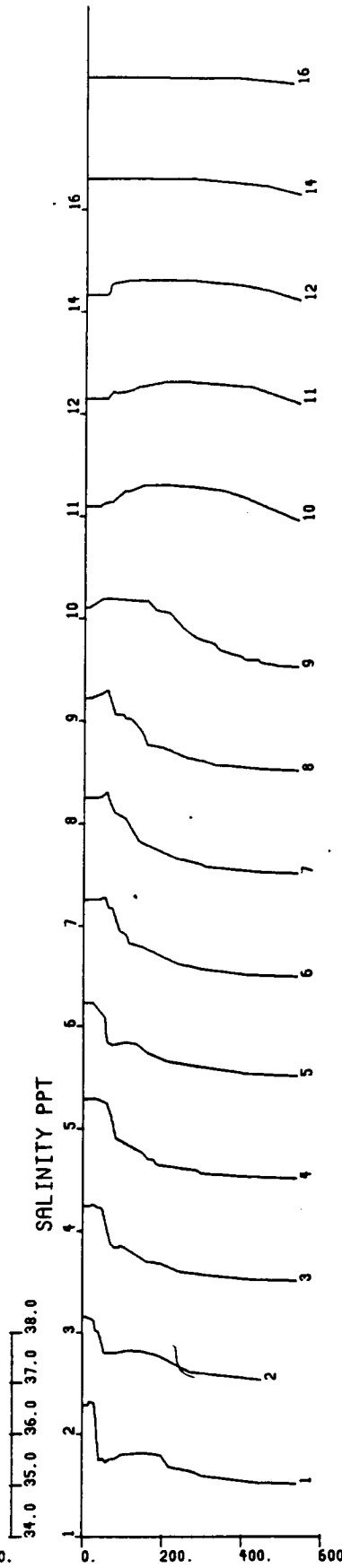
Figure 17B. Section C surface salinity along transect.

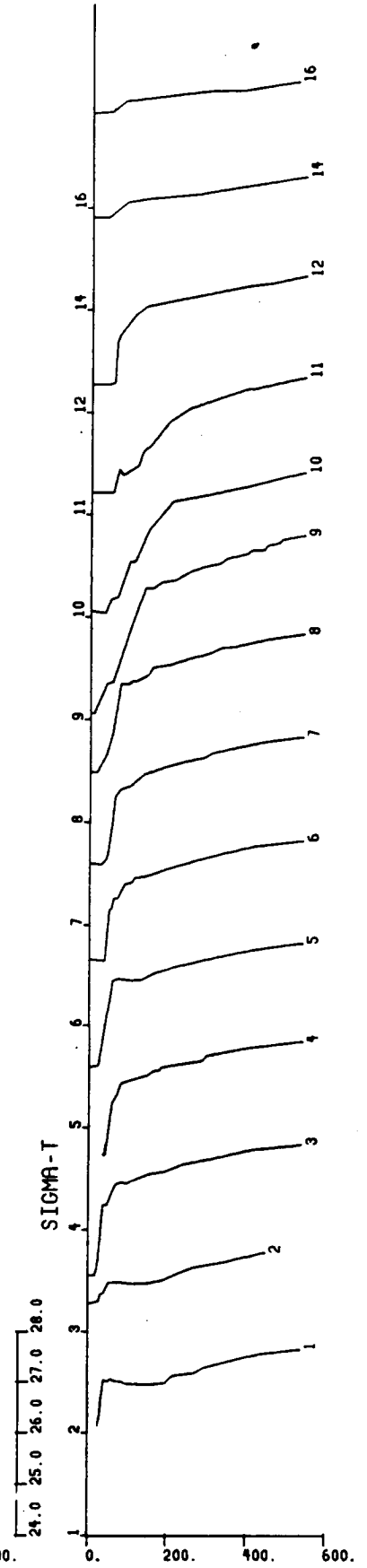Figure 17C. Section C surface sigma-t along transect.

SECTION C

TEMP CENT DEGREES

SALINITY PPT

SIGMA-T

DEPTH-METERS

SECTION C

SPECIFIC VOLUME
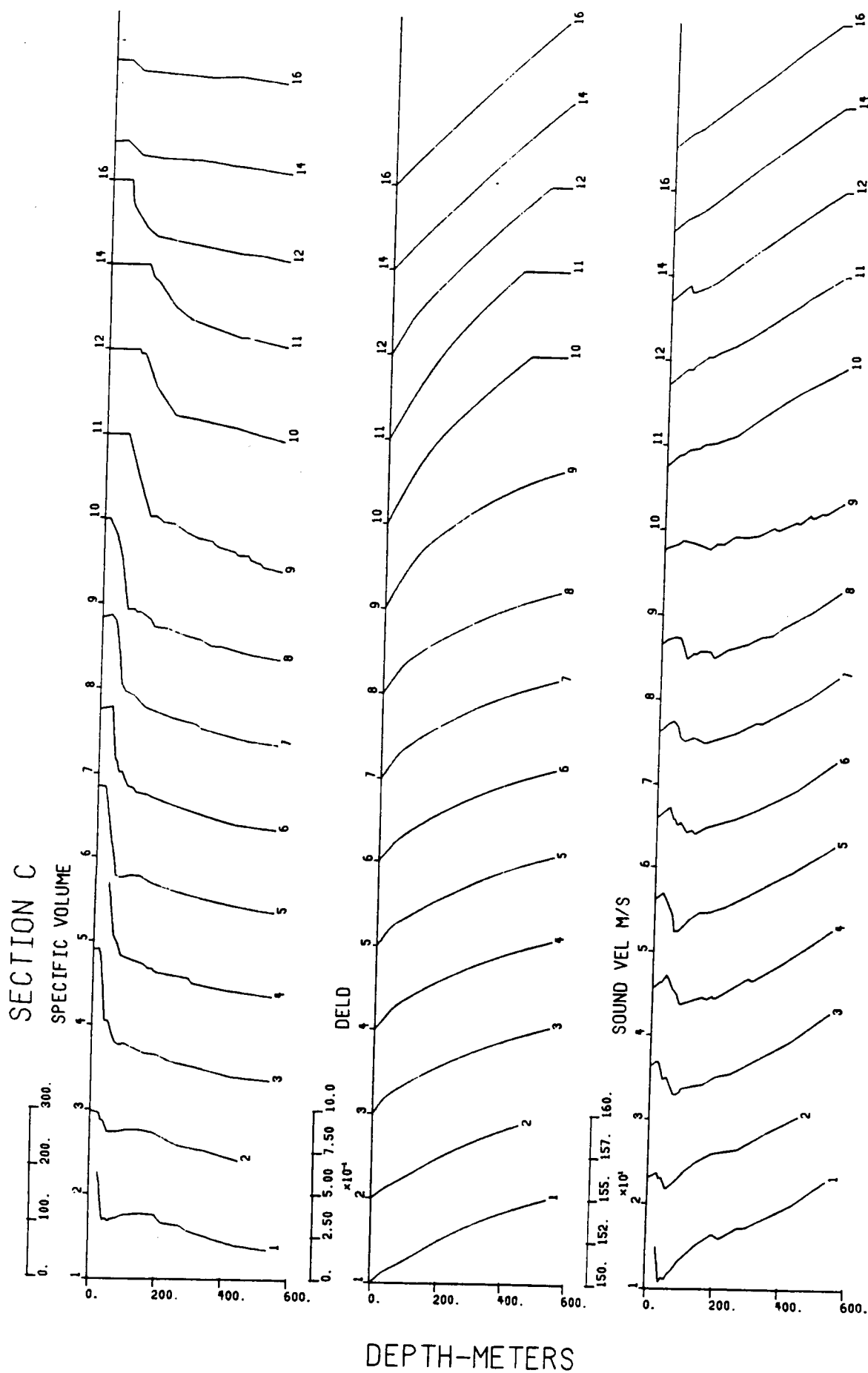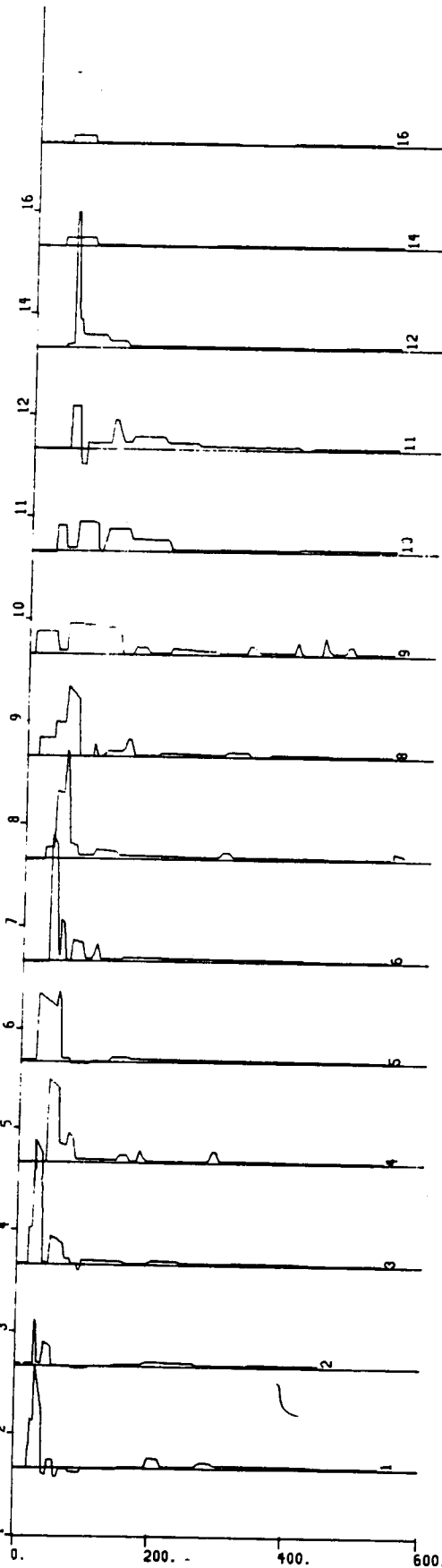
DELD

SOUND VEL M/S

DEPTH-METERS

Figure 18. Continued.

SECTION C

N SQRD

DEPTH—METERS

67

TEMPERATURE (°C)
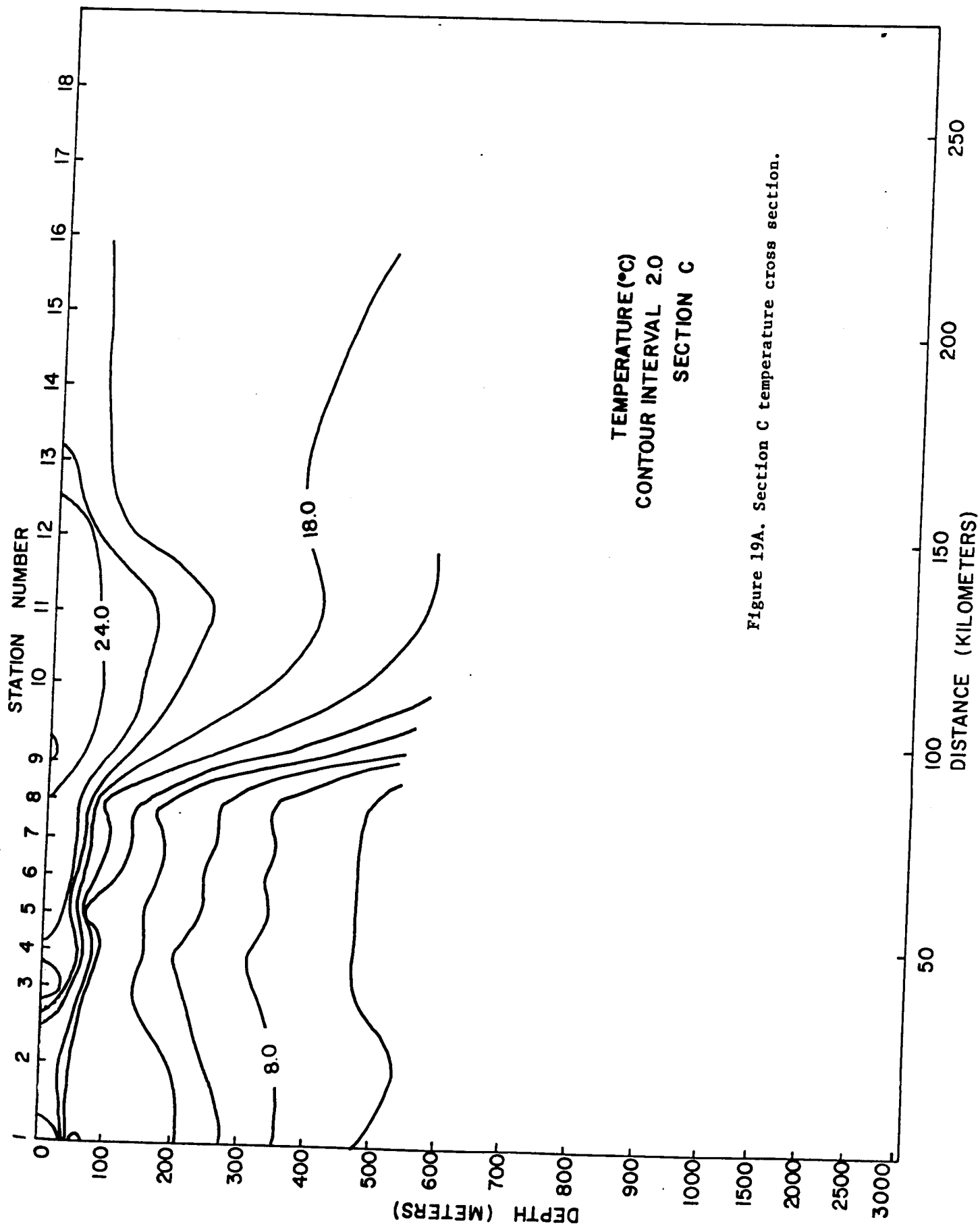CONTOUR INTERVAL 2.0
SECTION C
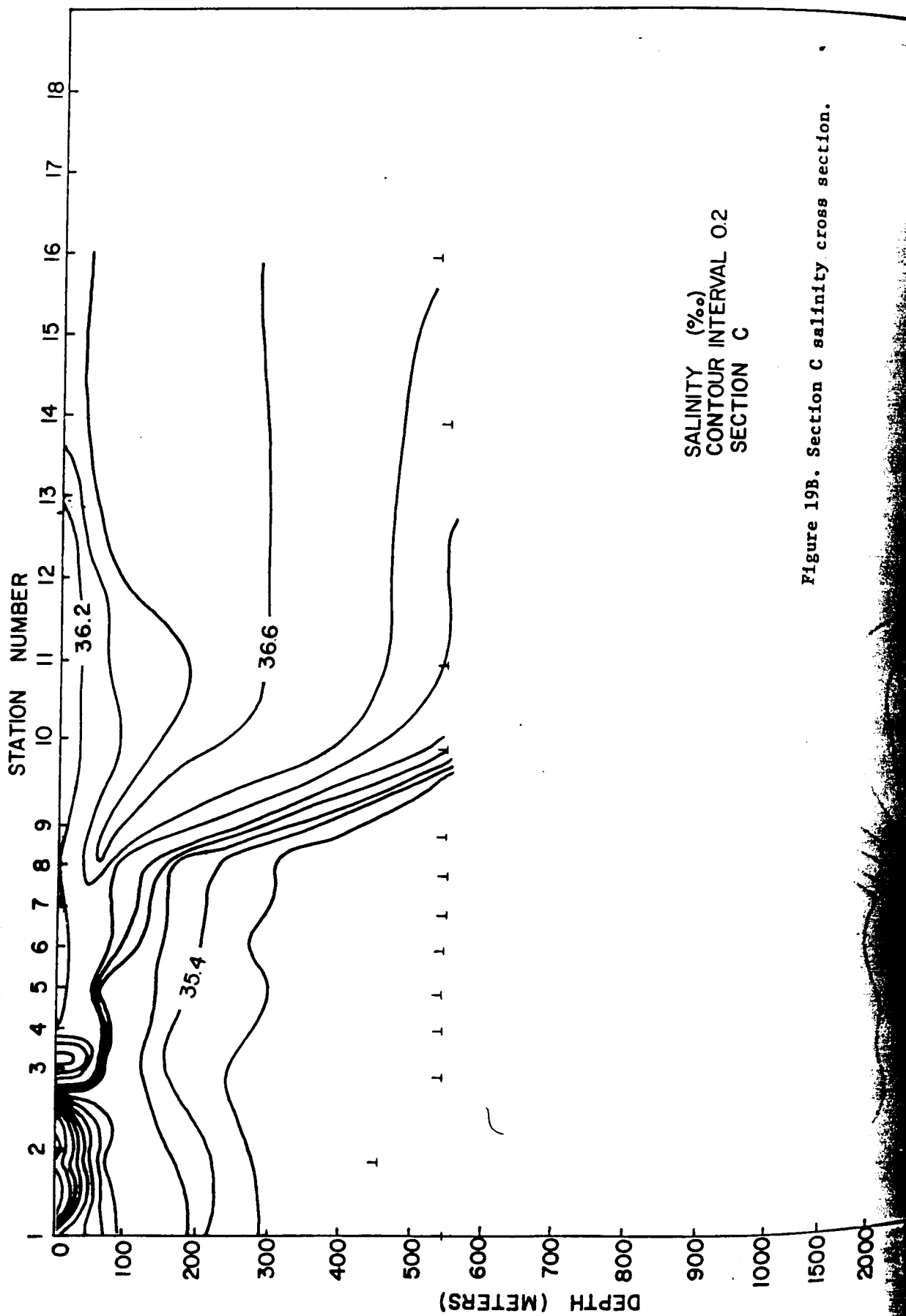
Figure 19A. Section C temperature cross section.

SALINITY (‰)
CONTOUR INTERVAL 0.2
SECTION C

Figure 19B. Section C salinity cross section.

SIGMA-T
CONTOUR INTERVAL 0.2
SECTION C
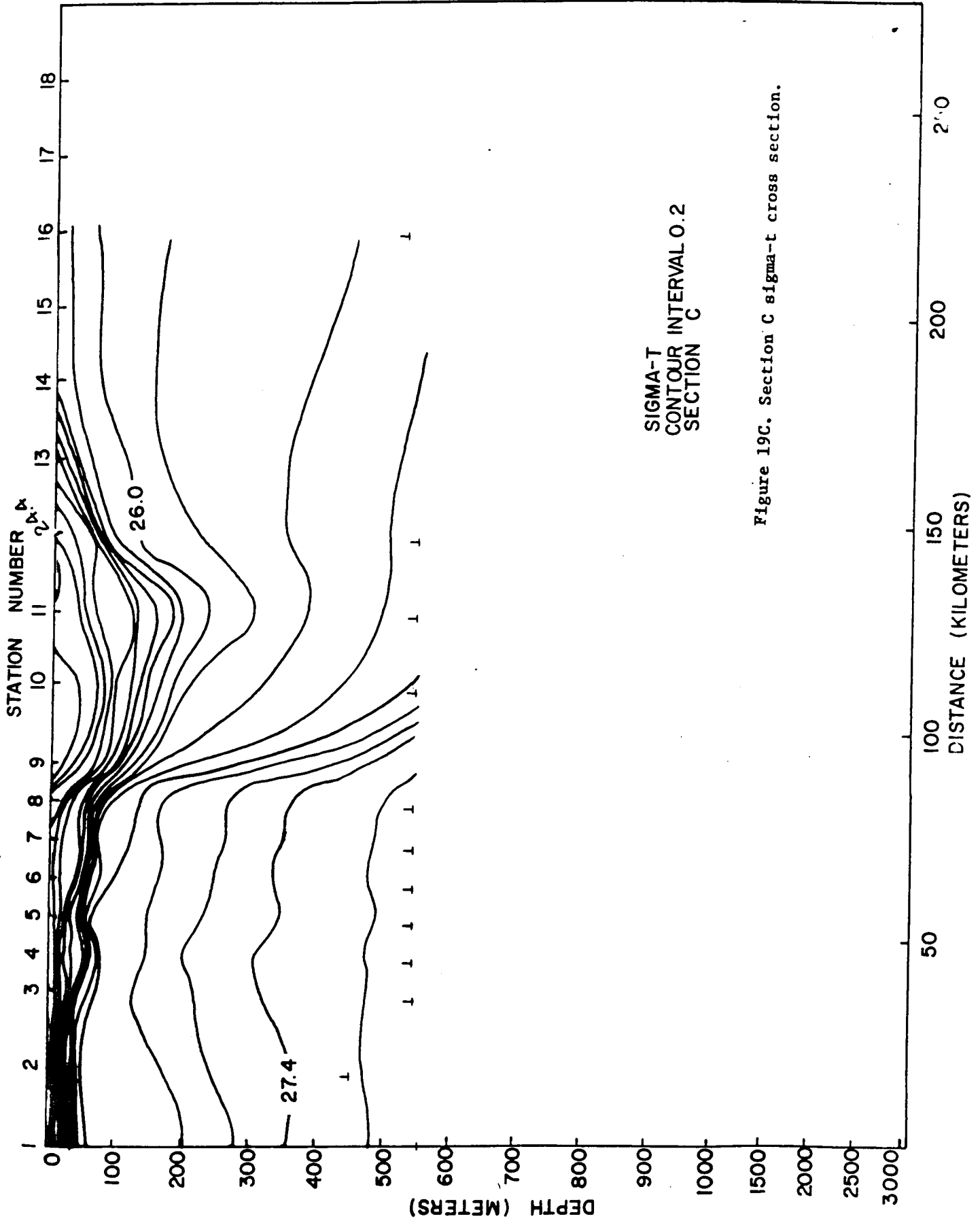
Figure 19C. Section C sigma-t cross section.

Figure 20. Section C surface drift velocity and Gulf Stream surface topography.
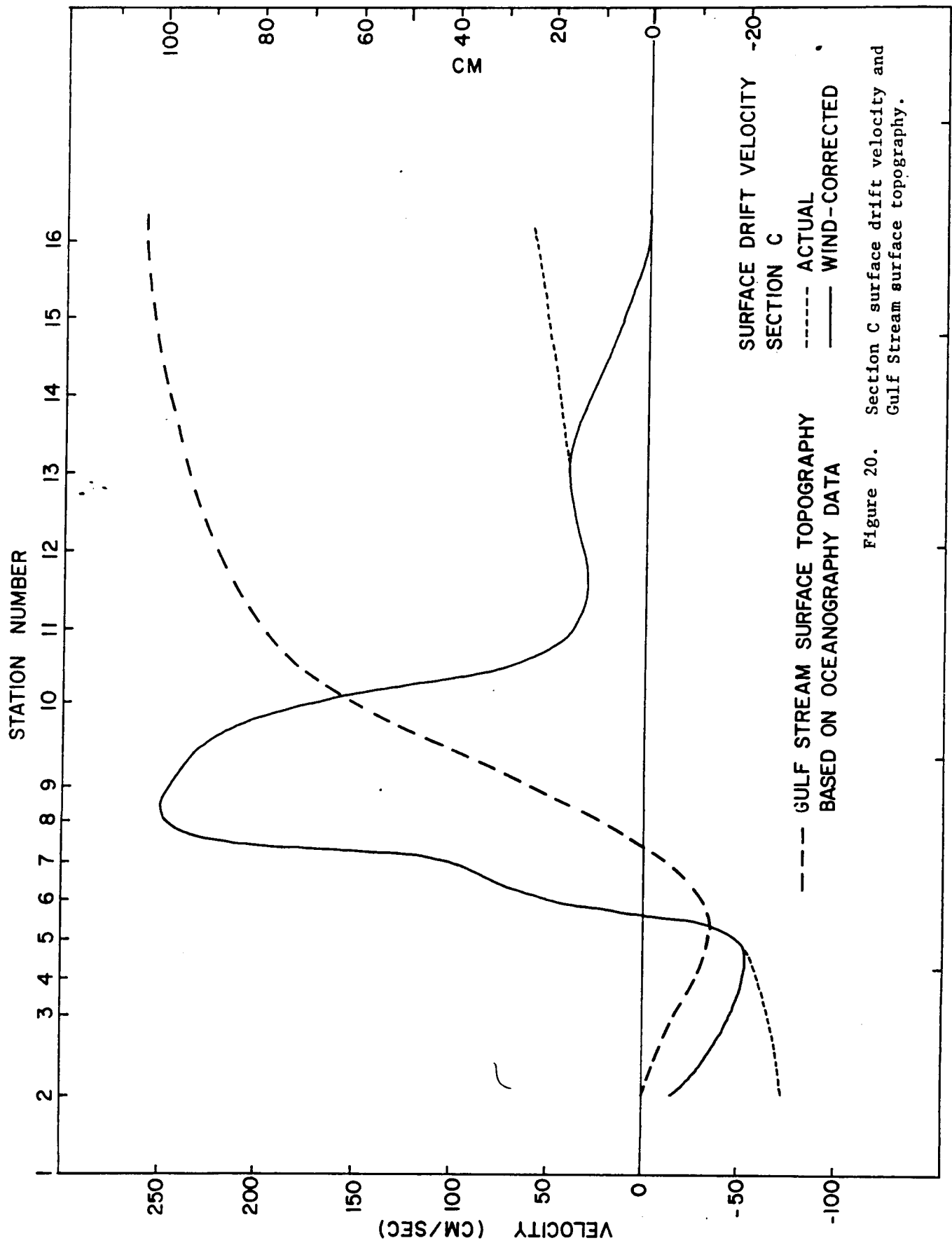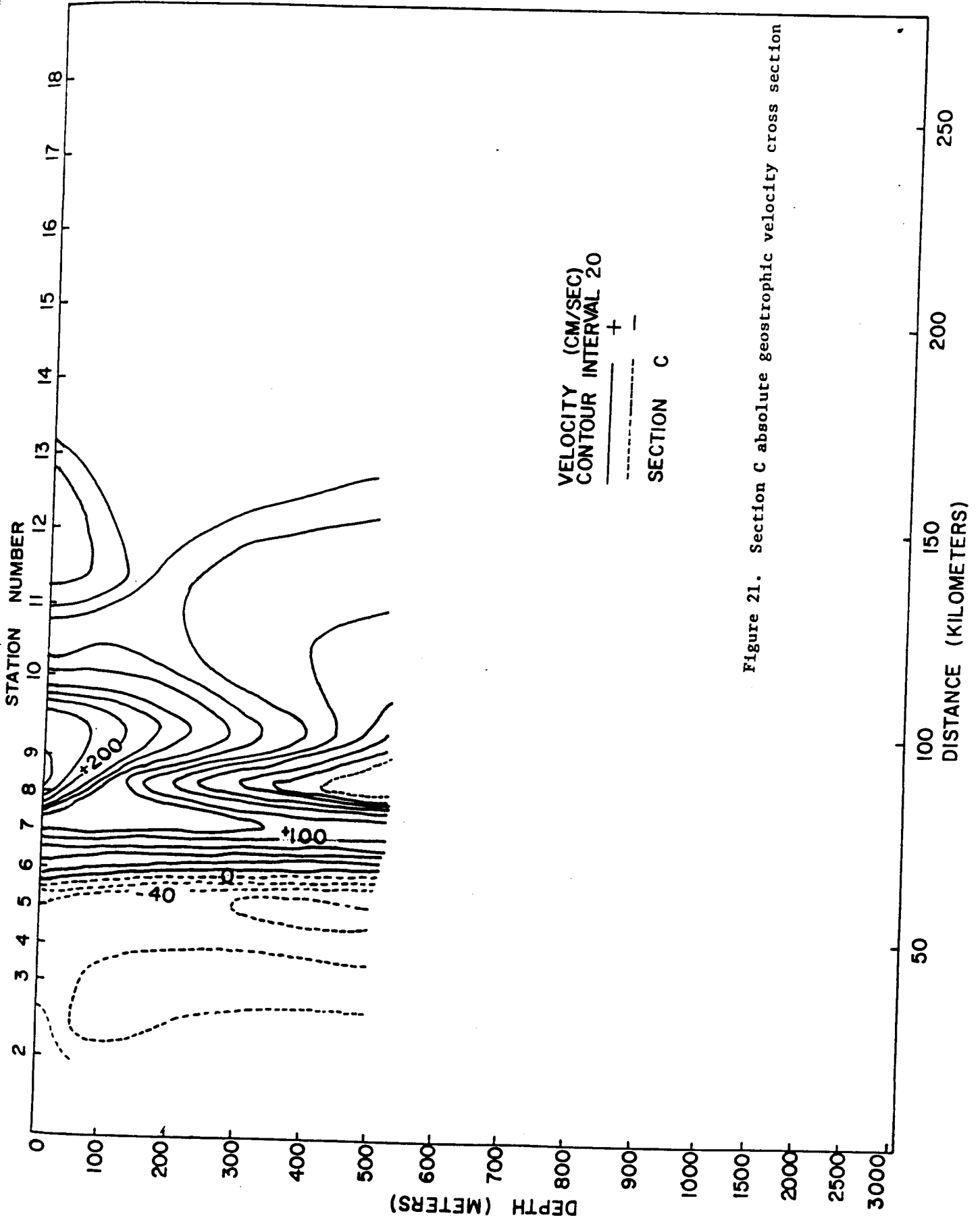
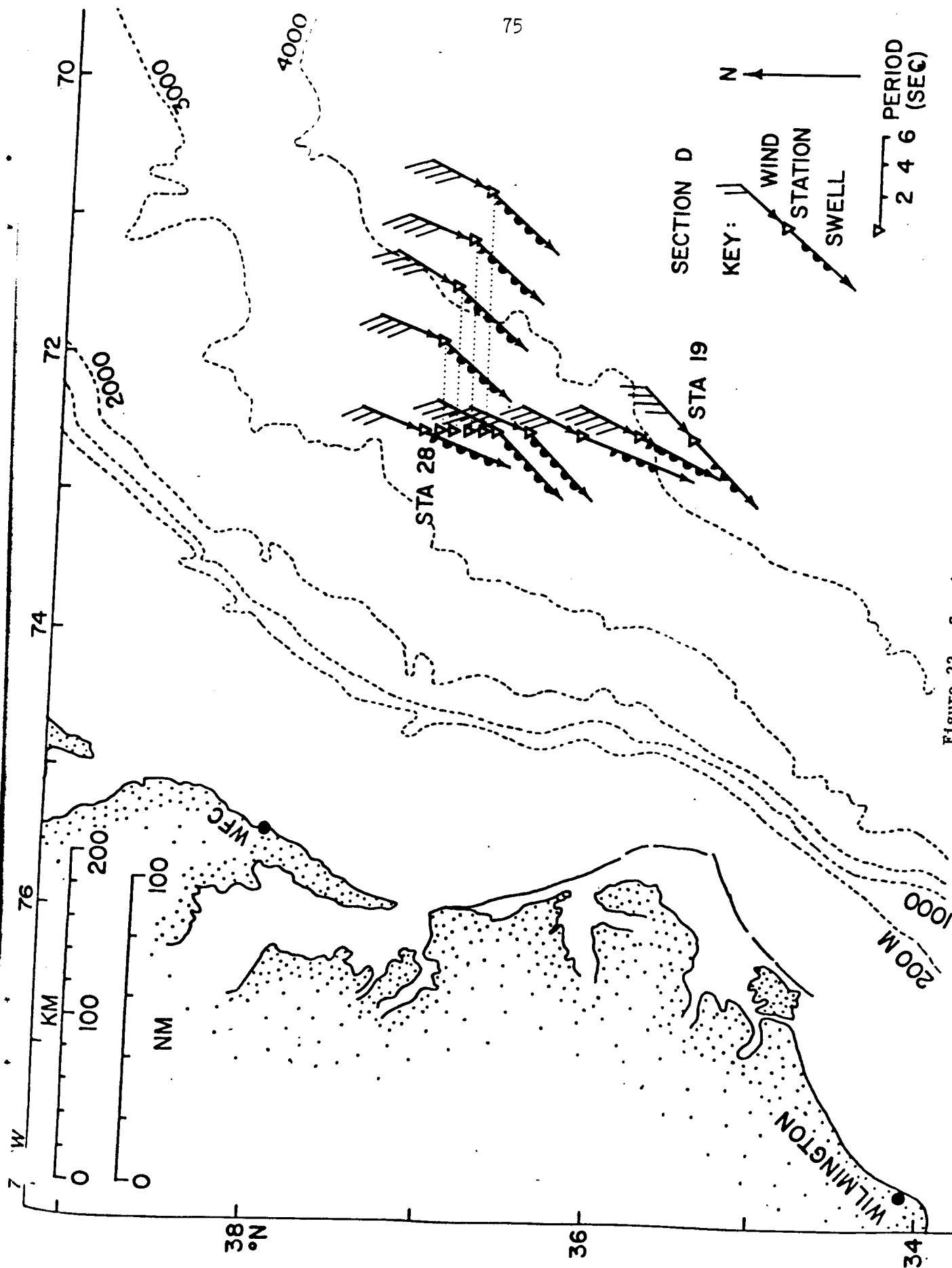Figure 21. Section C absolute geostrophic velocity cross section

3.4

Section D

Figure 22.   Section D station positions and observed wind, swell vectors.

Table 9. Atmospheric and Sea Surface Observations at Section D Stations

STATION NUMBER	WIND		SWELL			ATM PRESSURE	AIR TEMPERATURE		HUMIDITY
	DIR FROM (°T)	SPEED (M/S)	DIR TO (°T)	HT (M)	PER (S)	SURFACE (MB)	DRY (°C)	WET (°C)	RELATIVE (%)
28	020	13.9	200	4.5	6	1007.8	17.5	15.4	81
27	020	18.0	220	4.5	6	1007.8	17.8	16.1	84
26	030	18.0	220	4.5	6	1007.1	18.6	16.7	83
25	020	18.0	220	4.5	6	1006.8	18.3	15.6	76
24	025	18.0	220	4.5	6	1005.8	18.9	16.8	81
23	025	18.0	225	4.8	6	1004.7	17.8	15.6	80
22	020	18.5	225	4.8	6		18.7	16.3	79
21	025	18.0	200	3.6	8	999.0	18.4	17.1	88
20	025	25.7	205	4.5	6	999.7	19.3	16.9	79
19	045	18.0	225	2.7	6	997.3	19.0	18.6	96
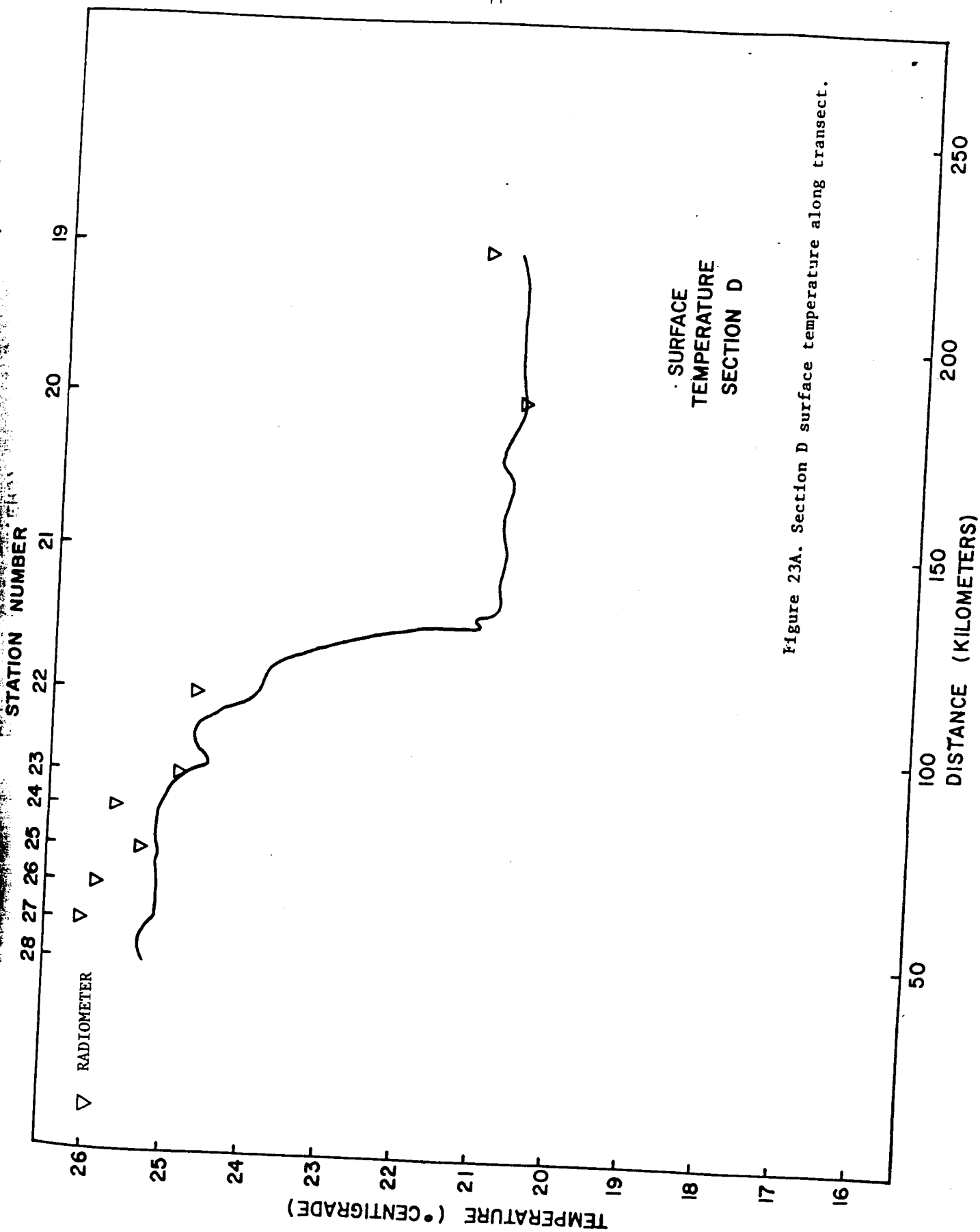
Figure 23A. Section D surface temperature along transect.
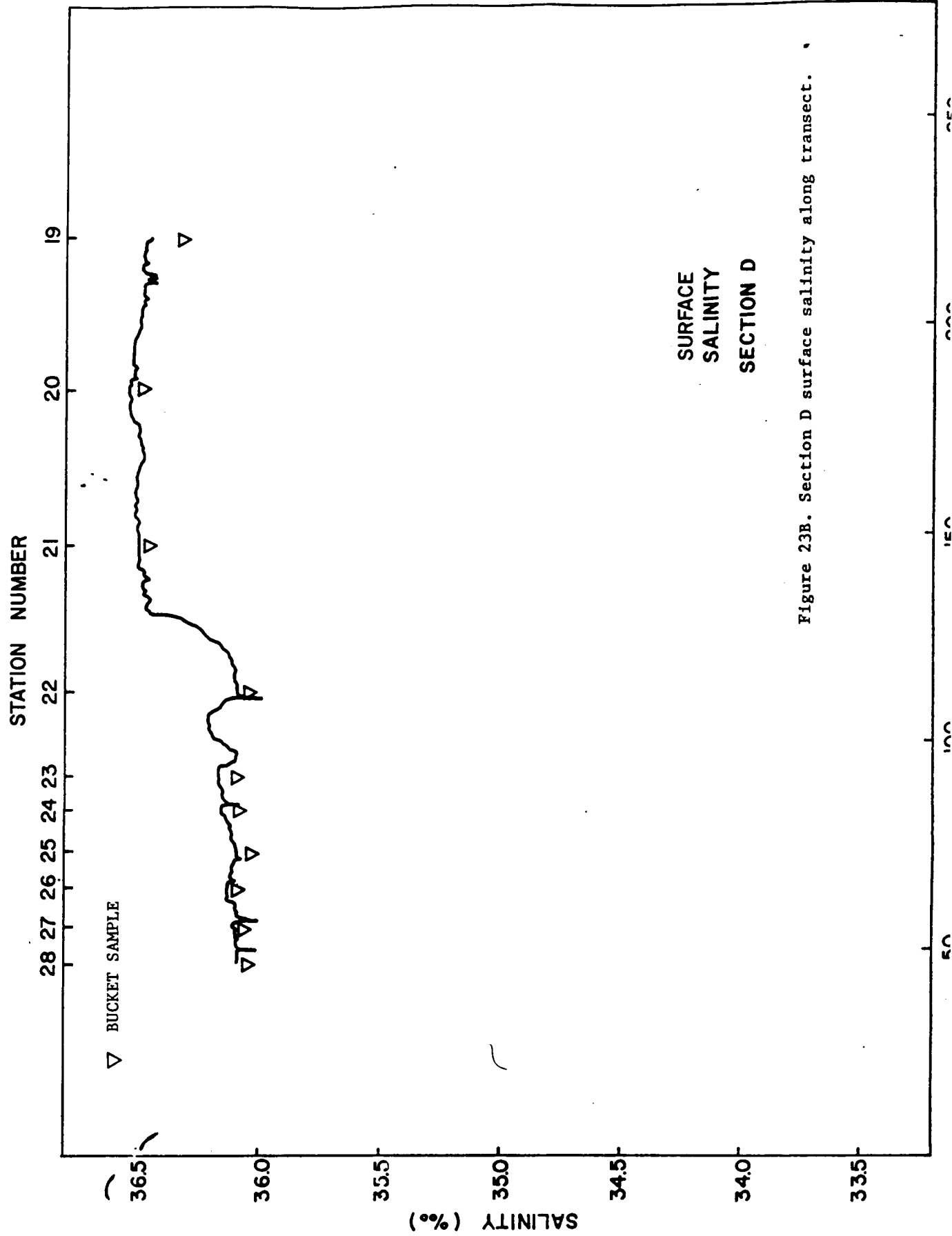
Figure 23B. Section D surface salinity along transect.

Figure 23C. Section D surface sigma-t along transect.

SECTION D

TEMP CENT DEGREES

SALINITY PPT

SIGMA-T

DEPTH-METERS

81
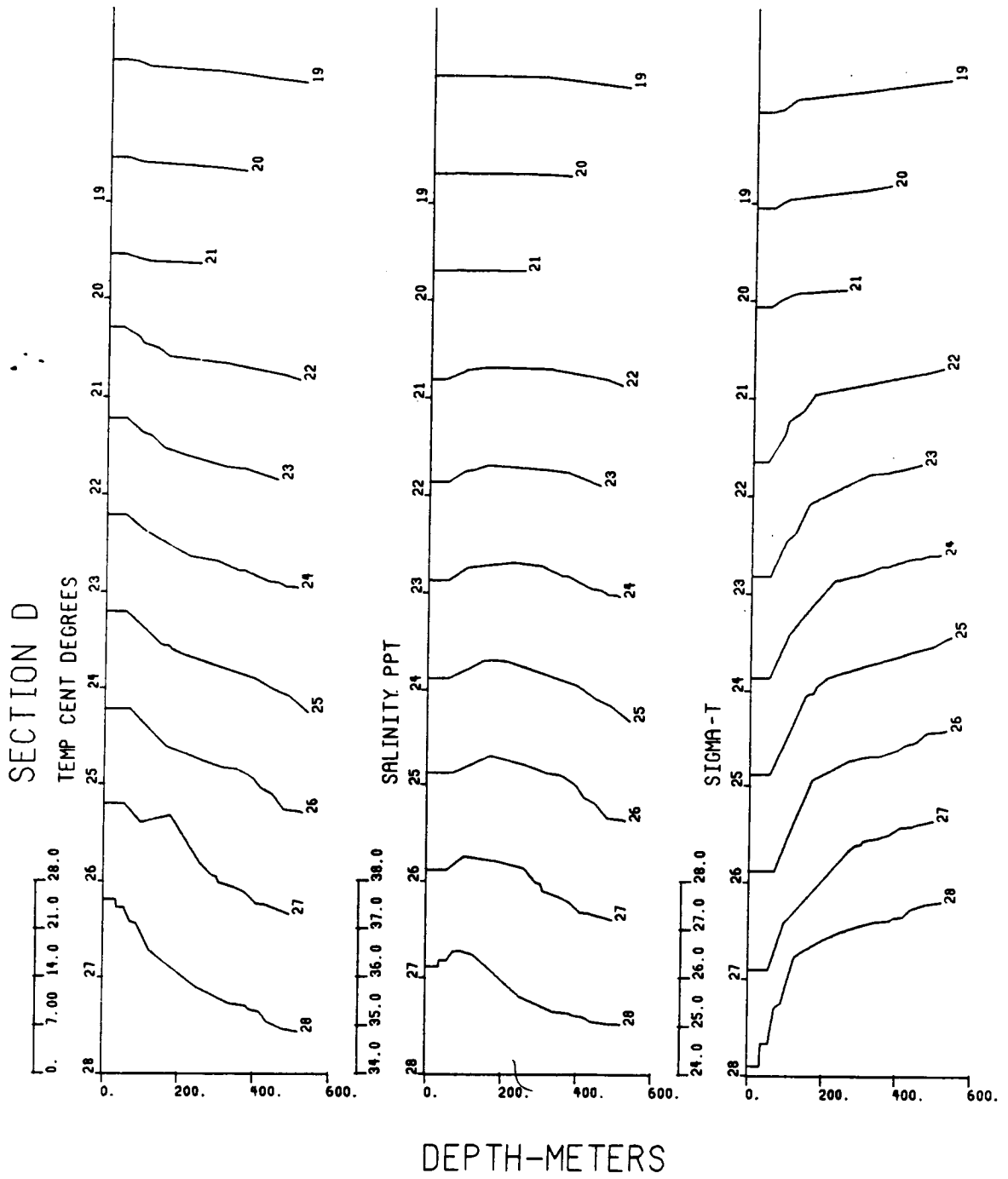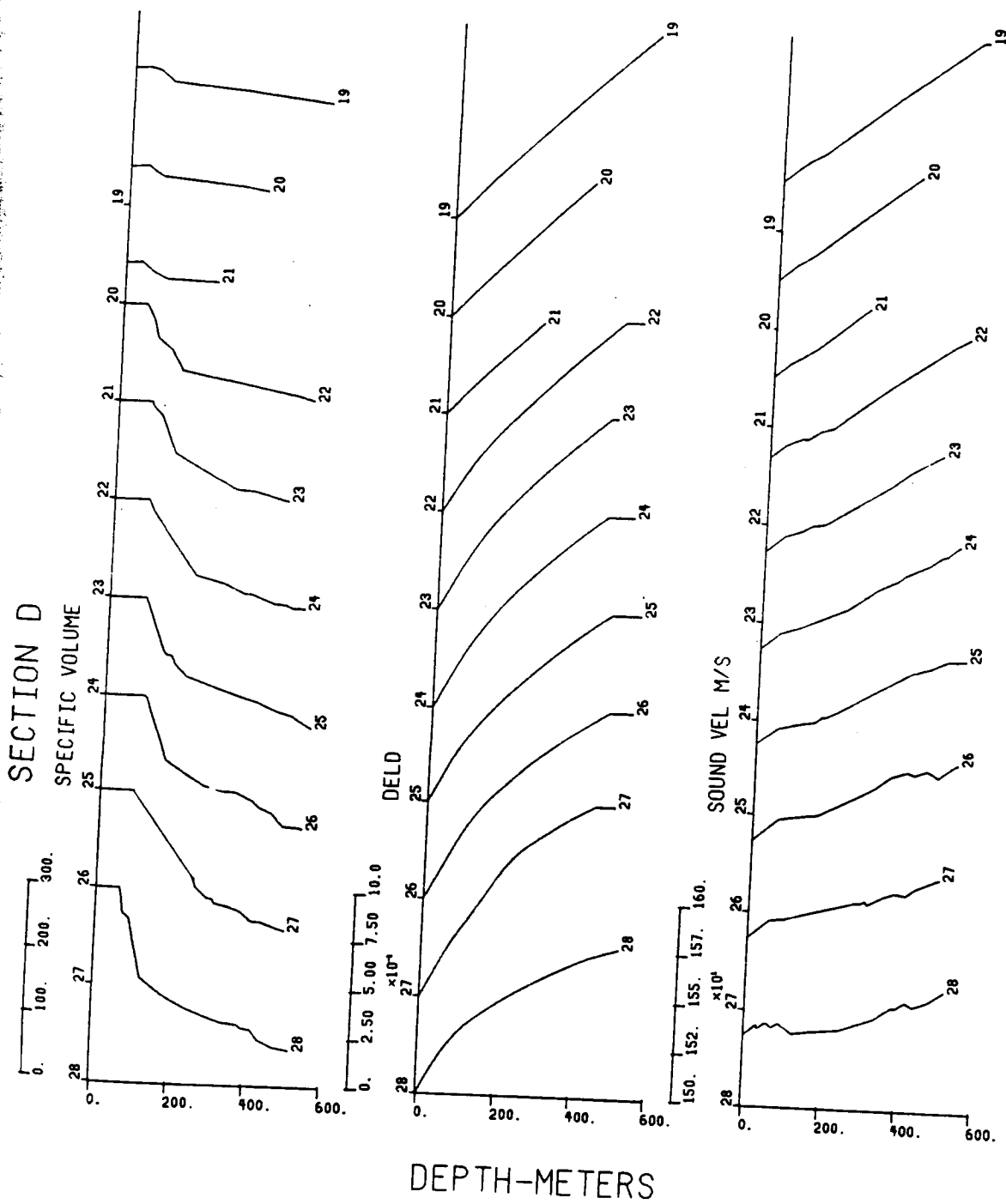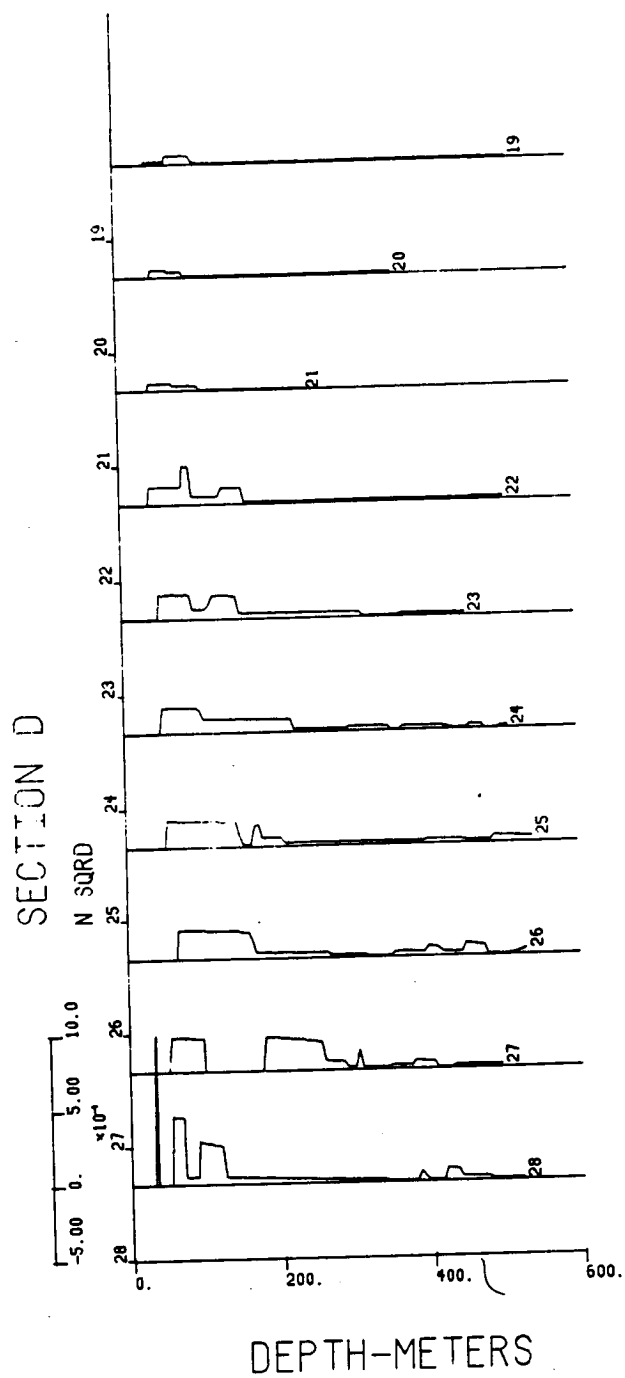
Figure 24. Continued.

Figure 24. Continued.

TEMPERATURE (°C)
CONTOUR INTERVAL 2.0
SECTION D
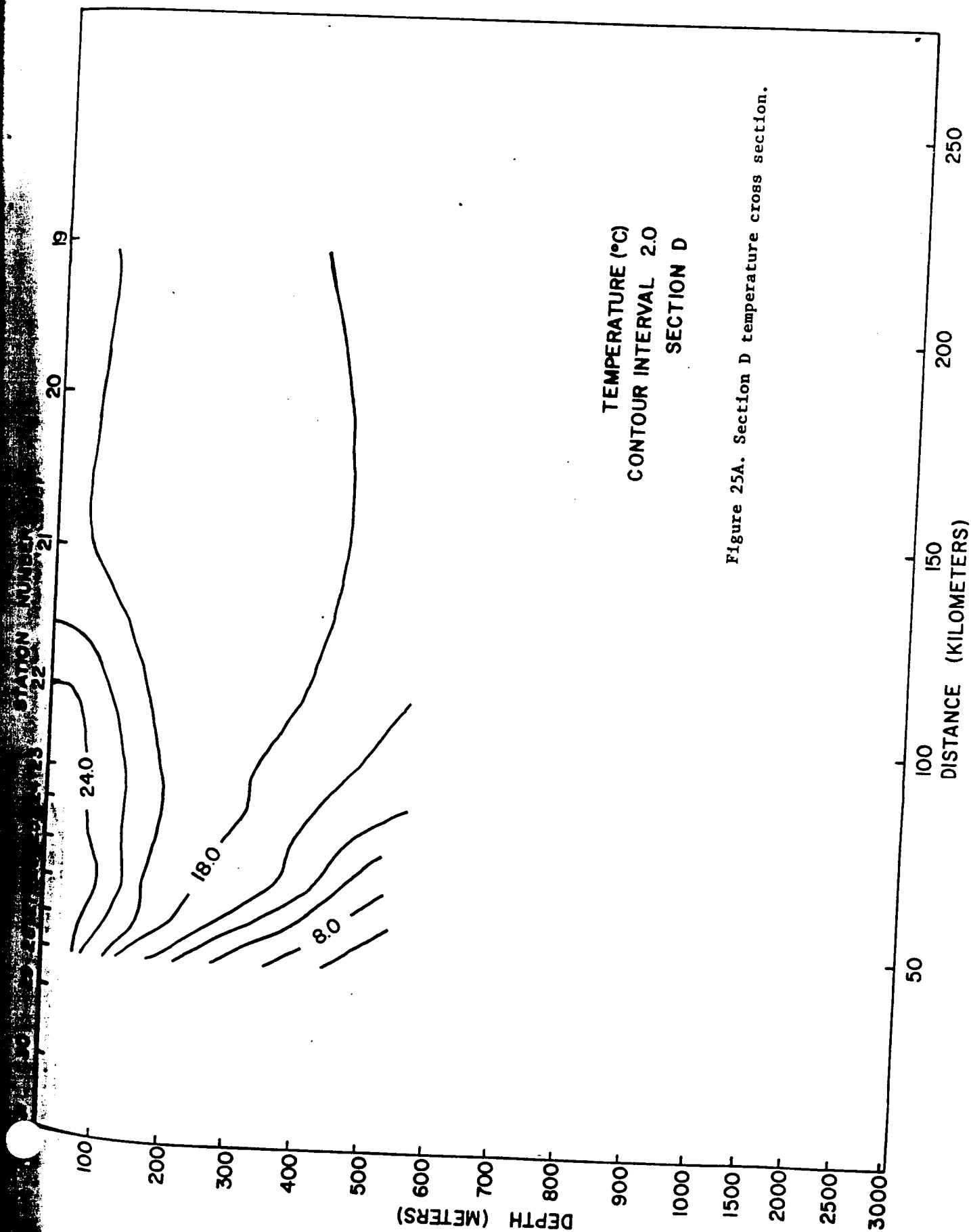
Figure 25A. Section D temperature cross section.

SALINITY (‰)
CONTOUR INTERVAL 0.2
SECTION D
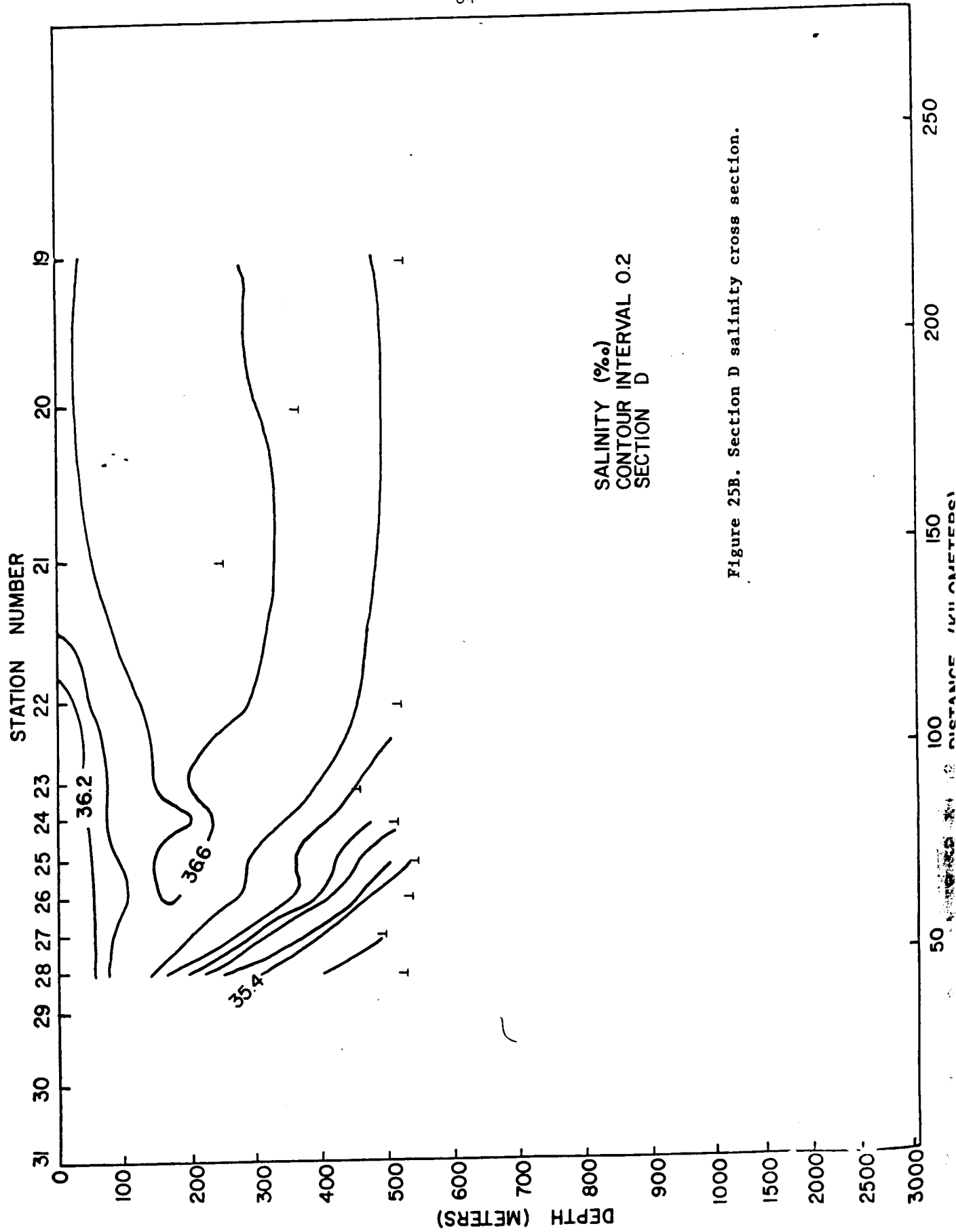
Figure 25B. Section D salinity cross section.

SIGMA-T
CONTOUR INTERVAL 0.2
SECTION D
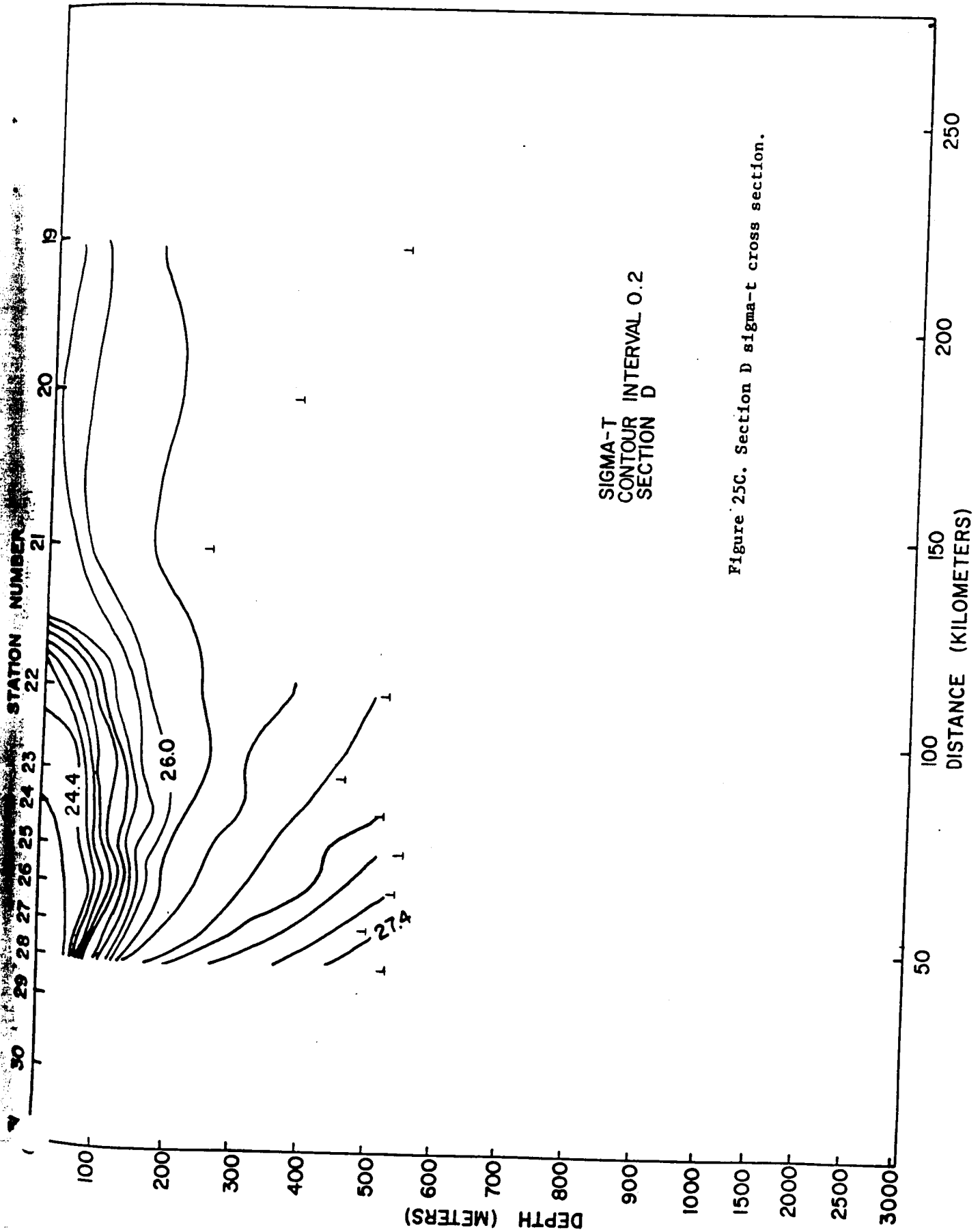
Figure 25C. Section D sigma-t cross section.
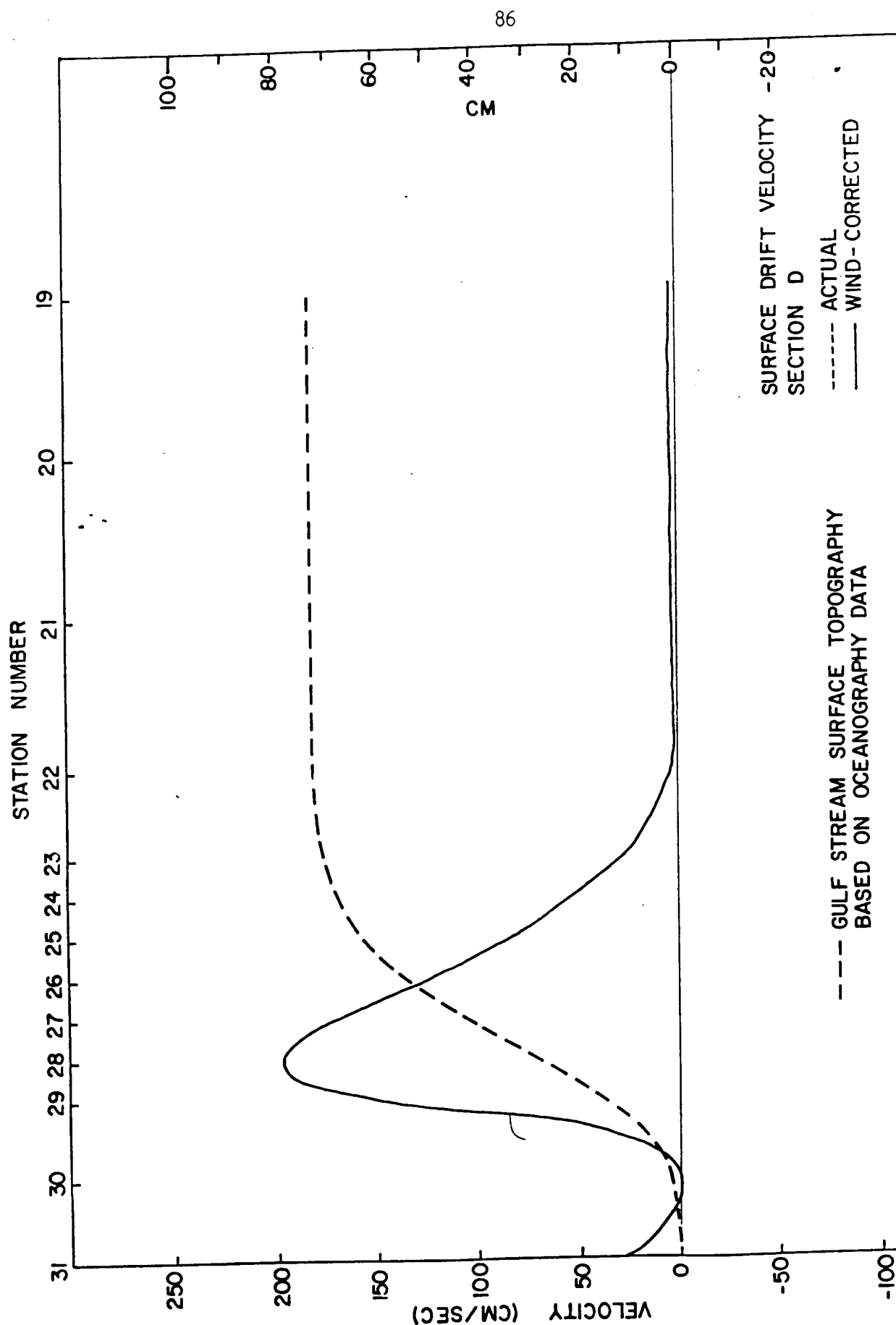
Figure 26.   Section D surface drift velocity and Gulf Stream surface topography.

Figure 27. Section D absolute geostrophic velocity cross section.
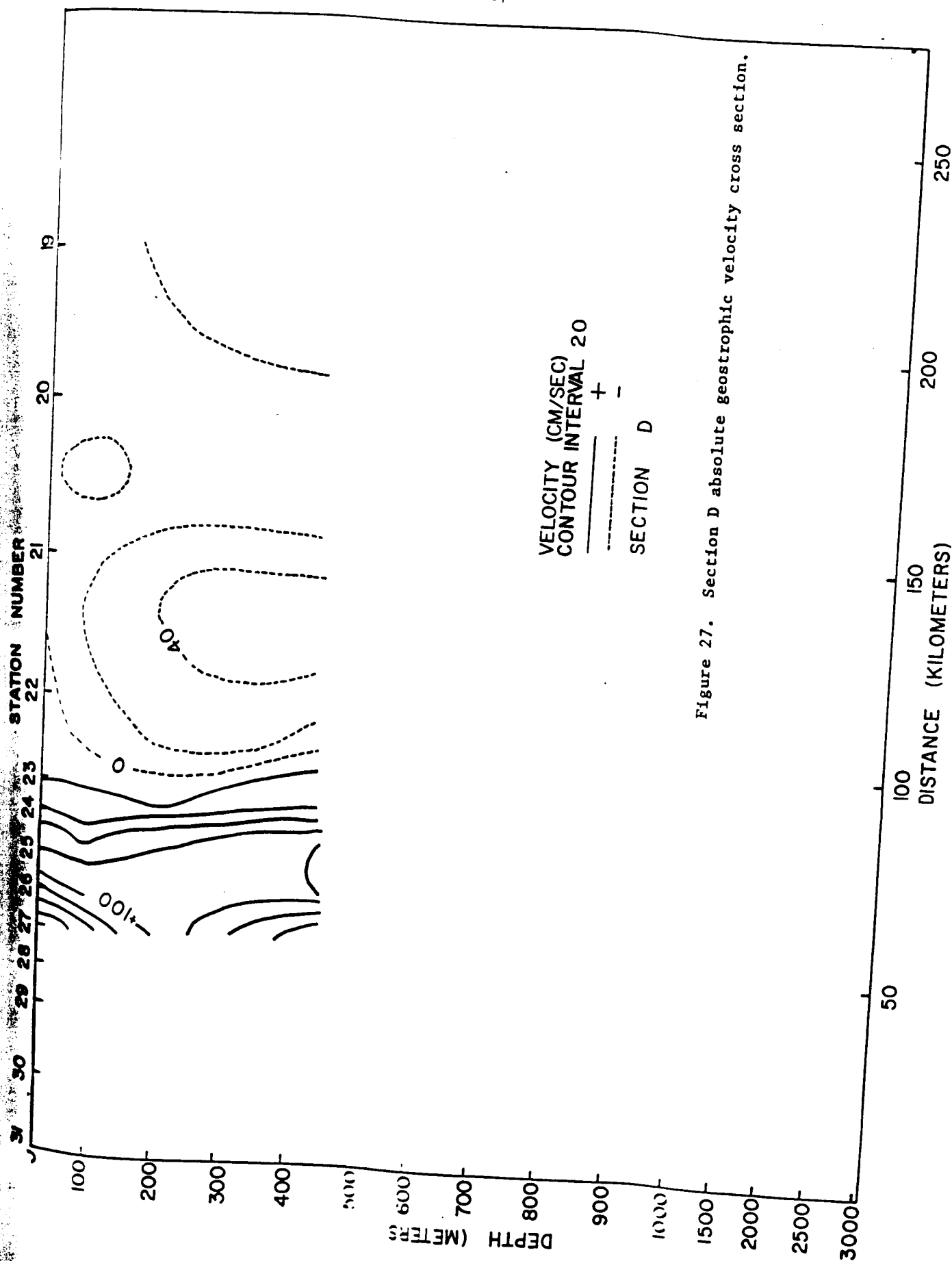
3.5

Section E

Figure 28. Section E station positions and observed wind, swell vectors.

Table 10. Atmospheric and Sea Surface Observations at Section E Stations

STATION NUMBER	WIND		SWELL			ATM PRESSURE	AIR TEMPERATURE		HUMIDITY
	DIR FROM (°T)	SPEED (M/S)	DIR TO (°T)	HT (M)	PER (S)	SURFACE (MB)	DRY (°C)	WET (°C)	RELATIVE (%)
31	340	2.6	203	.6	6	1019.0	13.9	11.2	73
30	340	4.1	225	1.5	6	1021.0	16.7	13.4	70
29	340	6.2	225	1.2	4	1021.0	16.7	16.1	94
28	340	5.1	220	1.8	4	1021.0	21.6	15.5	53
27	340	5.1	220	1.8	6	1020.3	22.1	15.5	50
26	080	5.1	225	1.8	6	1020.3	21.8	16.5	59
25	075	4.1	225	1.5	6	1020.3	22.3	15.8	51
24	075	4.1	202	1.5	6	1020.3	21.2	16.1	59
23	075	4.6	220	1.5	6	1020.3	20.2	15.2	59
22	030	5.1	225	1.8	6	1021.0	22.8	17.8	62
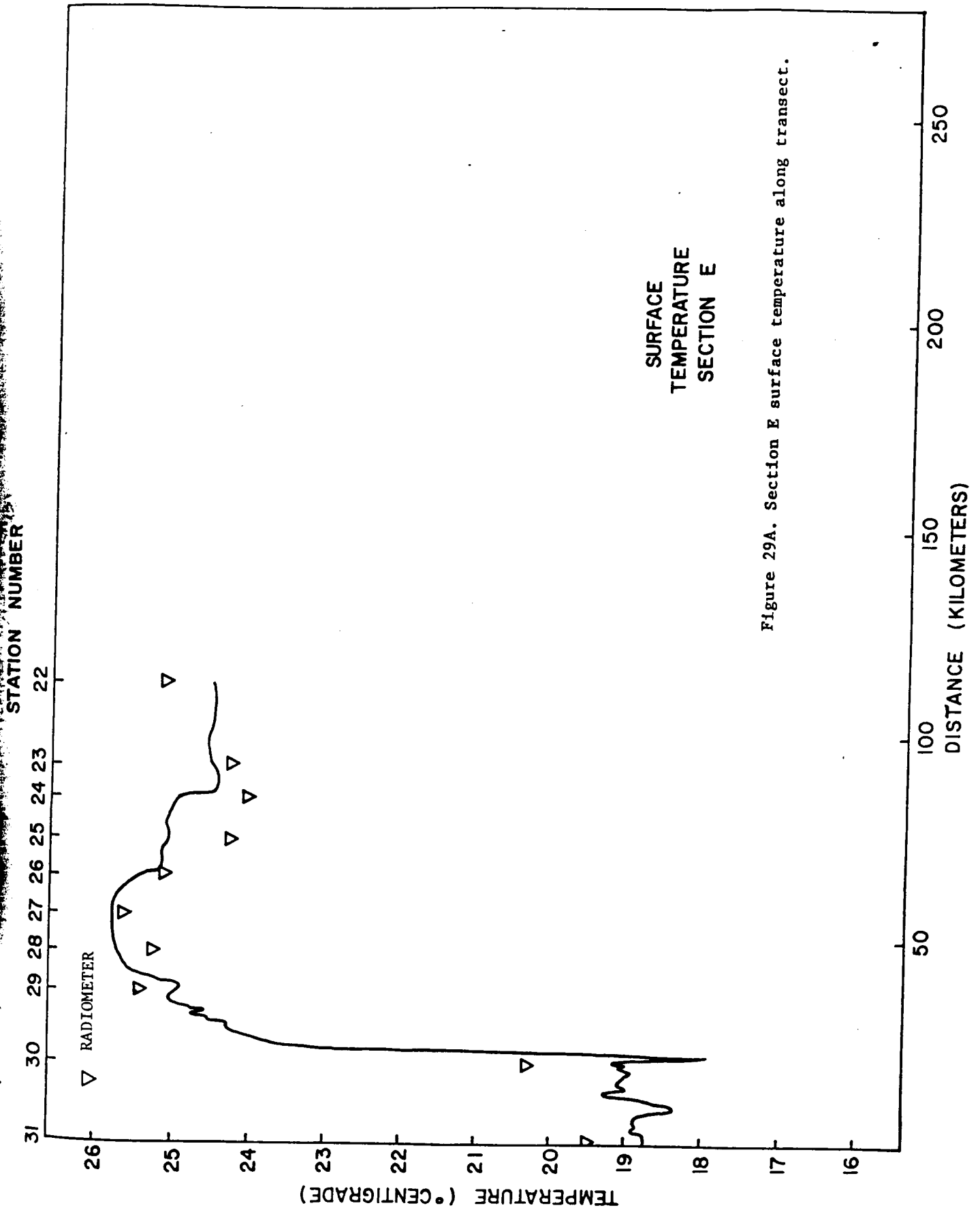
Figure 29A. Section E surface temperature along transect.

Figure 29B. Section E surface salinity along transect.
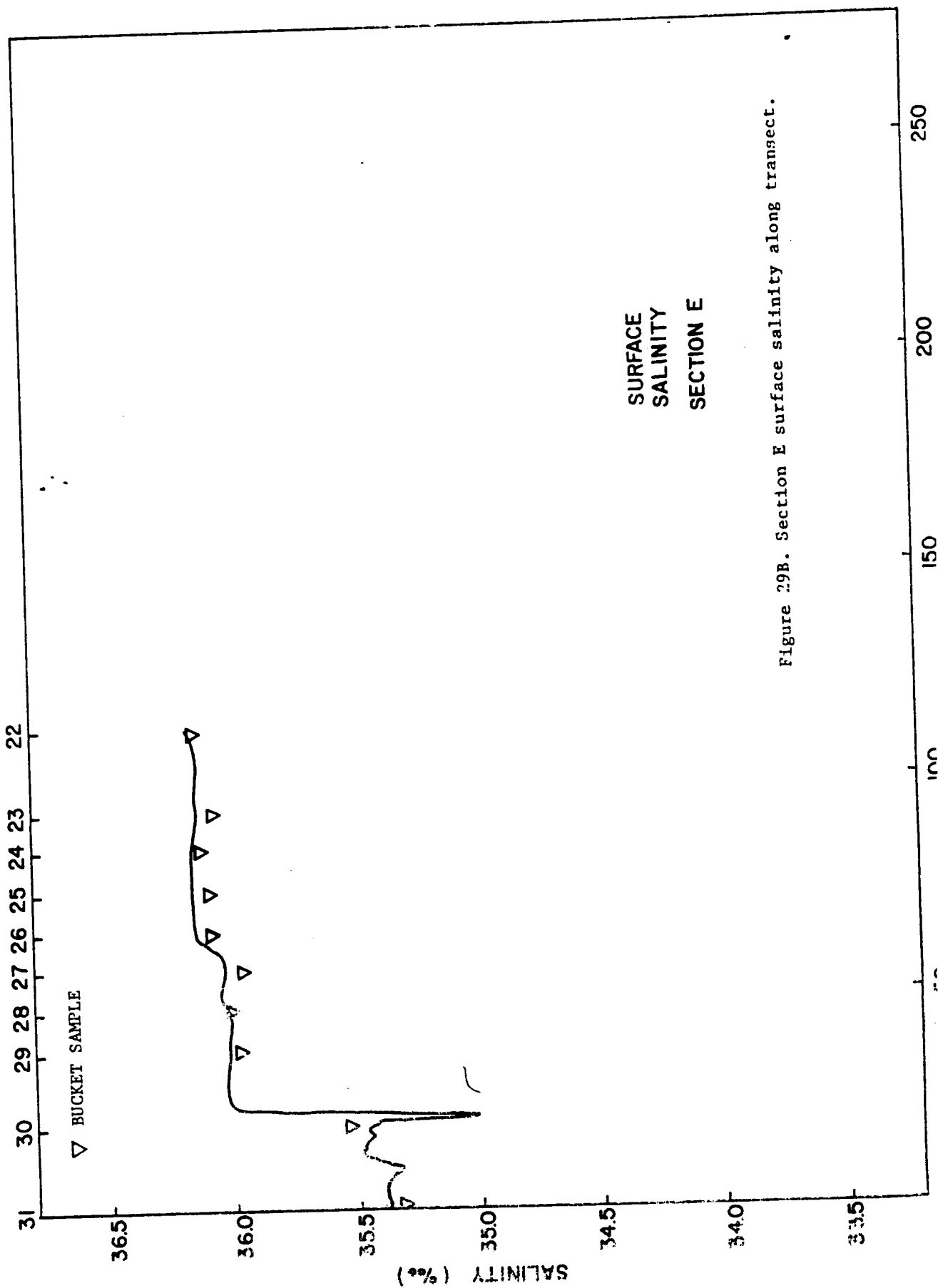
SURFACE
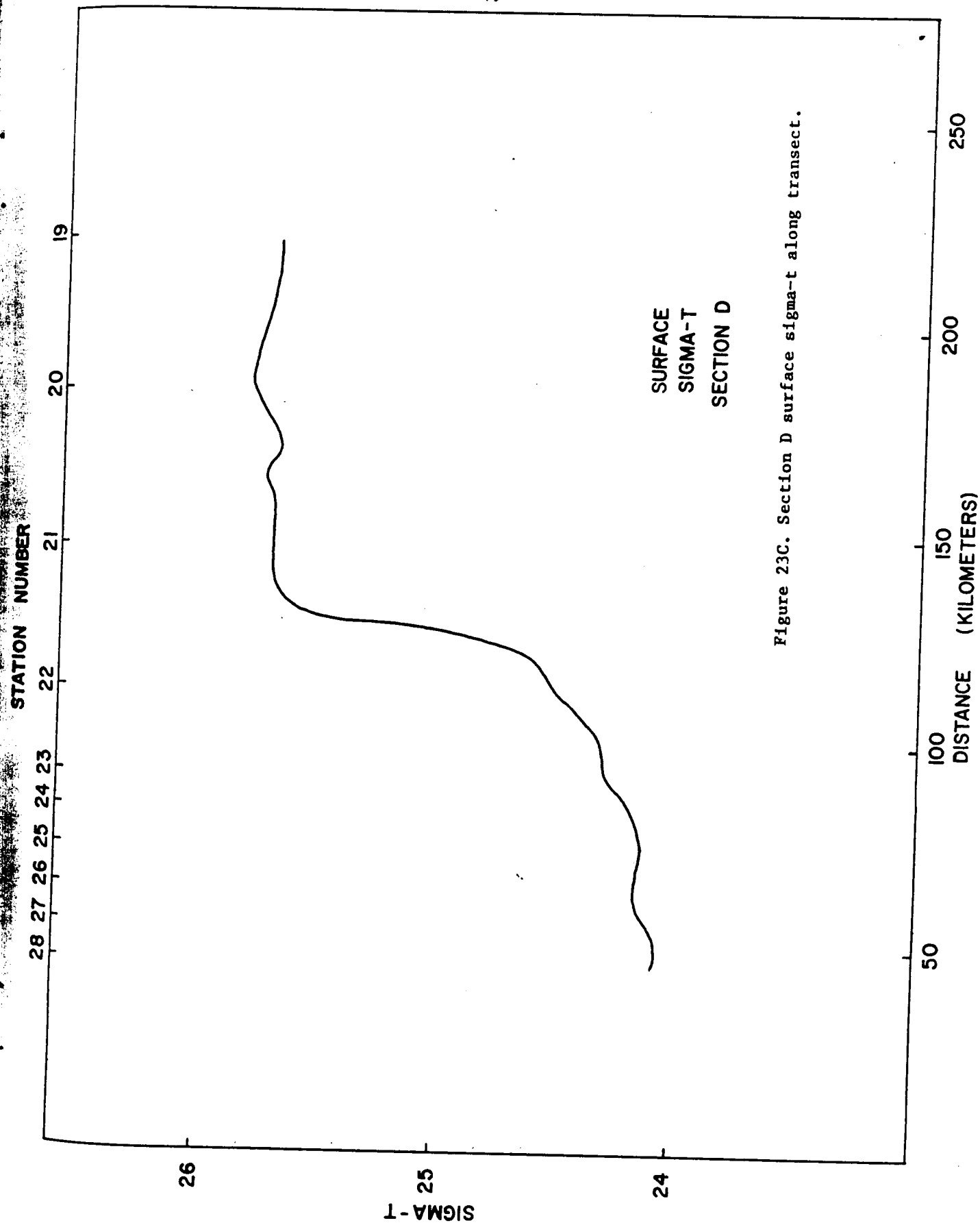SALINITY
SECTION E
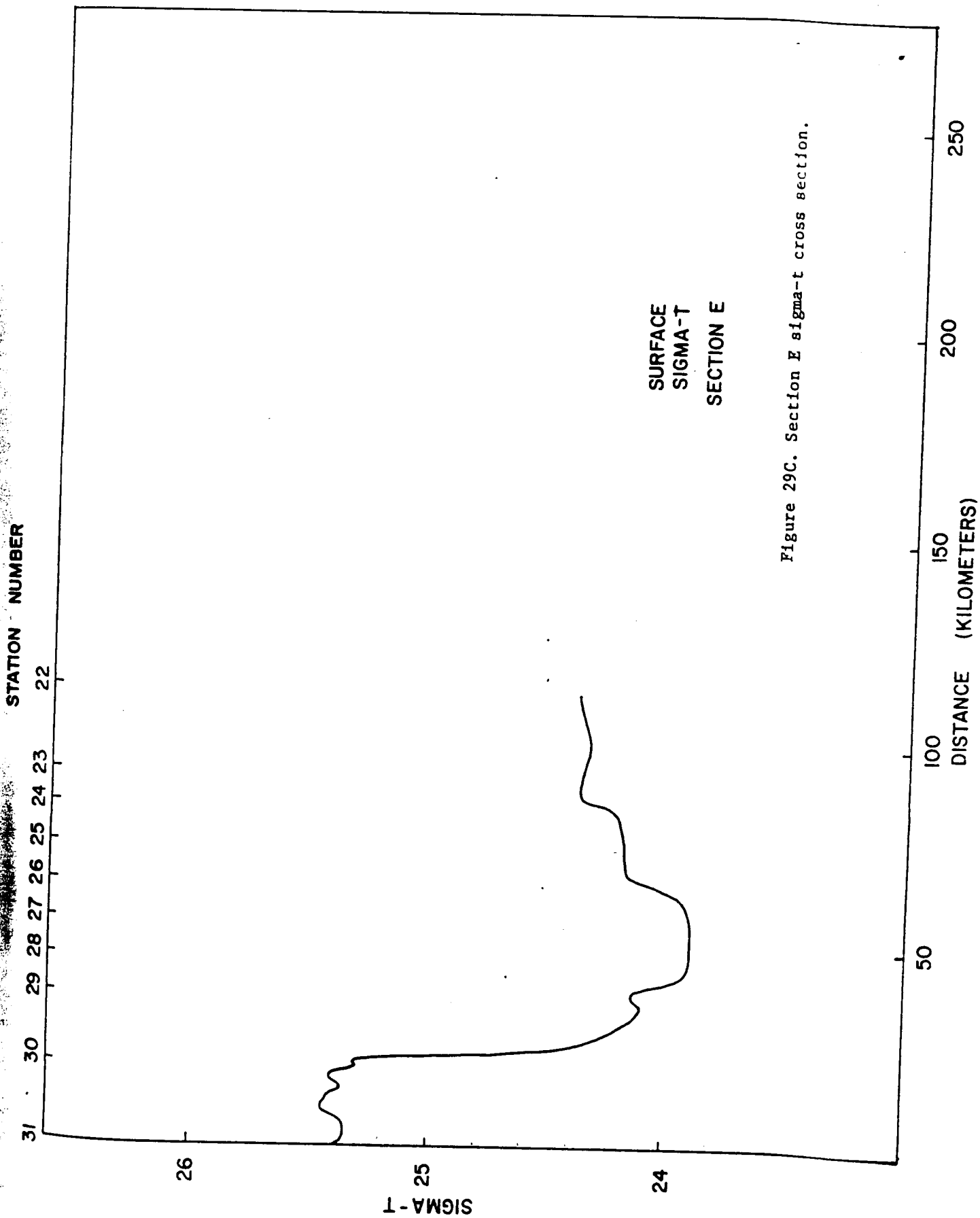
Figure 29C. Section E sigma-t cross section.
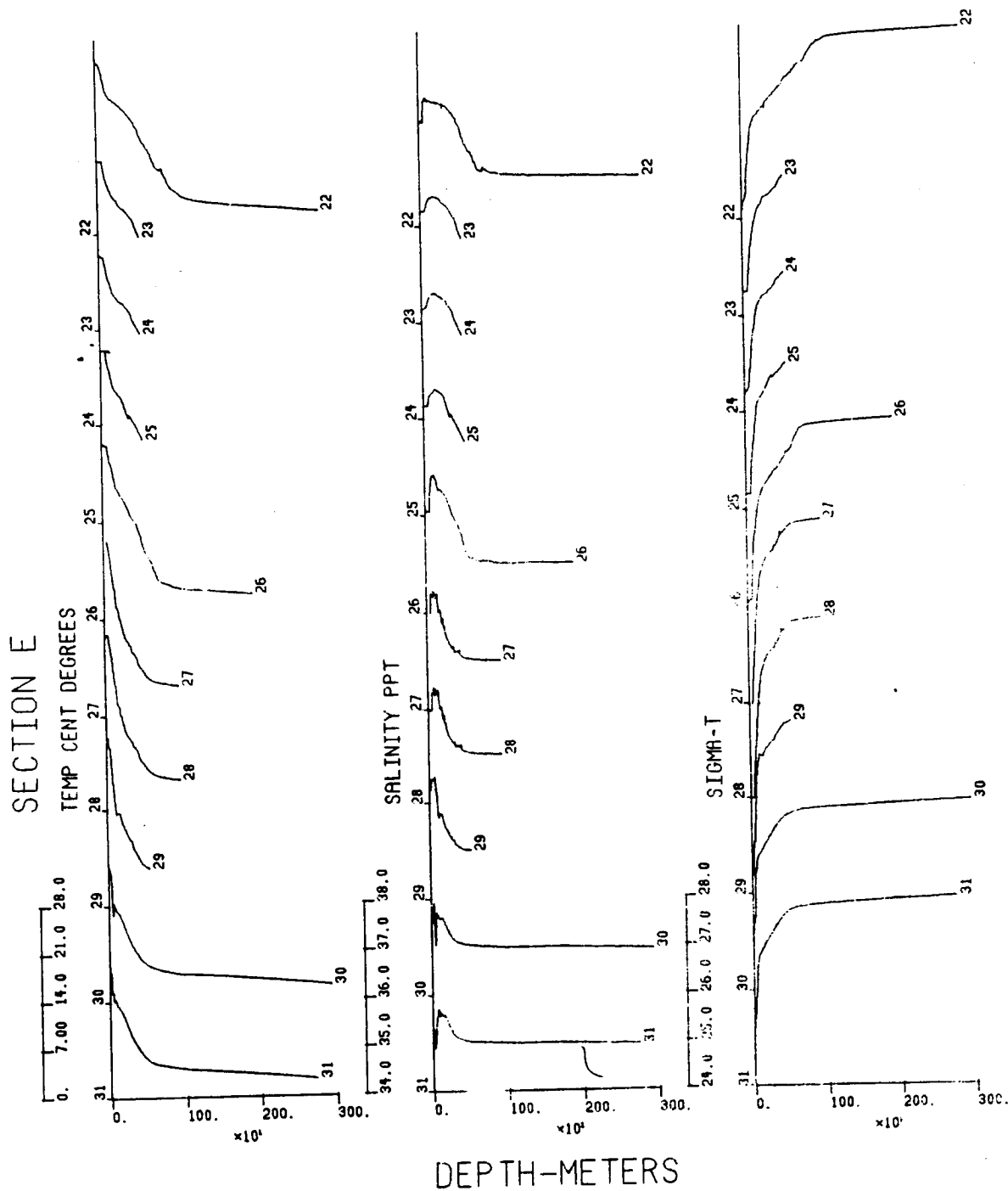
SECTION E

Figure 30. Section E observed and derived station profiles.

SECTION E

SPECIFIC VOLUME

DELD

SOUND VEL M/S

DEPTH-METERS
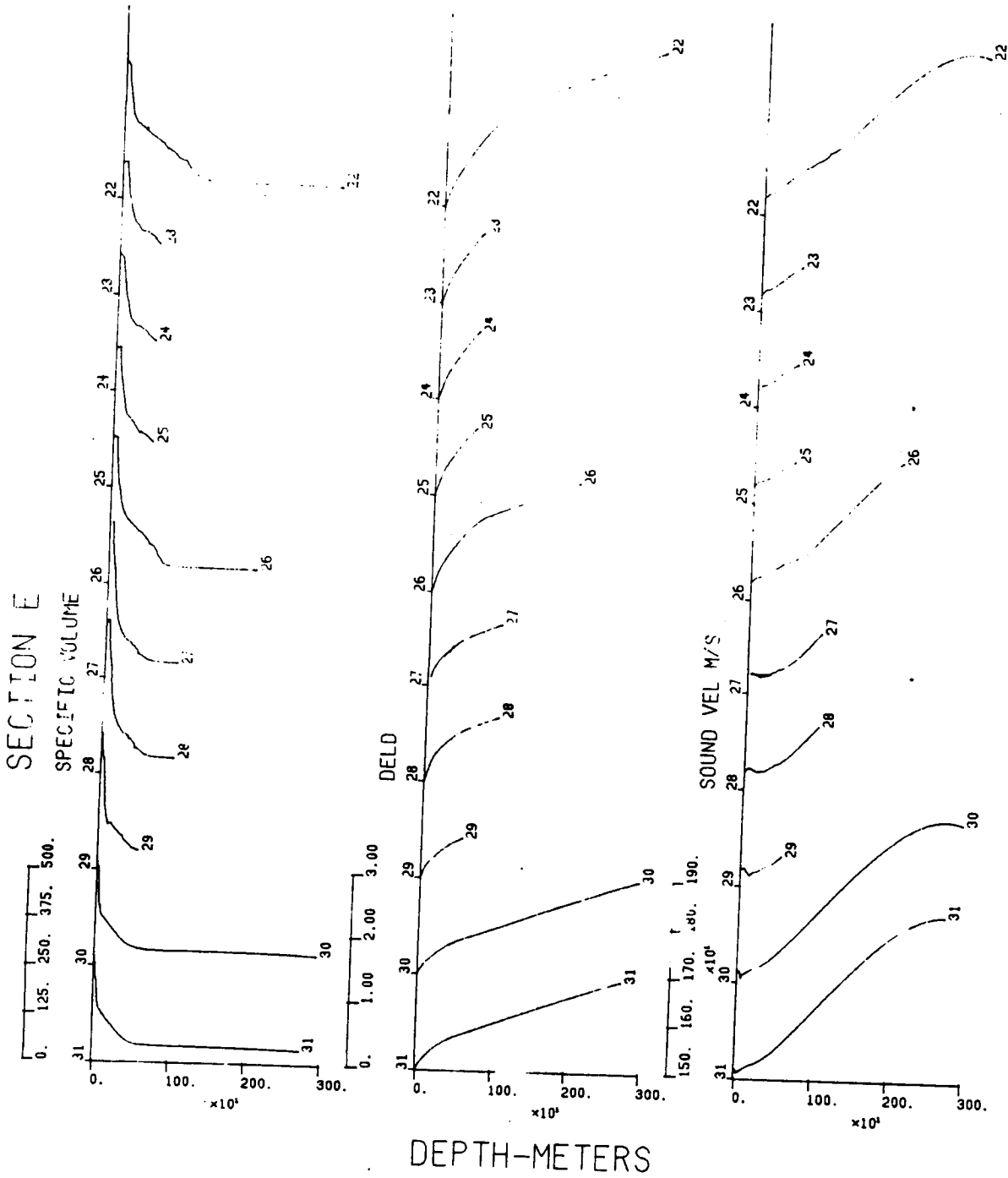
Figure 30. Continued.

Figure 30. Continued.

TEMPERATURE (°C)
CONTOUR INTERVAL 2.0
SECTION E

Figure 31A. Section E temperature cross section.

Figure 31B. Section E salinity cross section.

SIGMA-T
CONTOUR INTERVAL 0.2
SECTION E

Figure 31C. Section E sigma-t cross section.

Figure 32. Section E surface drift velocity and Gulf Stream surface topography.

Figure 33. Section E absolute geostrophic velocity cross section.
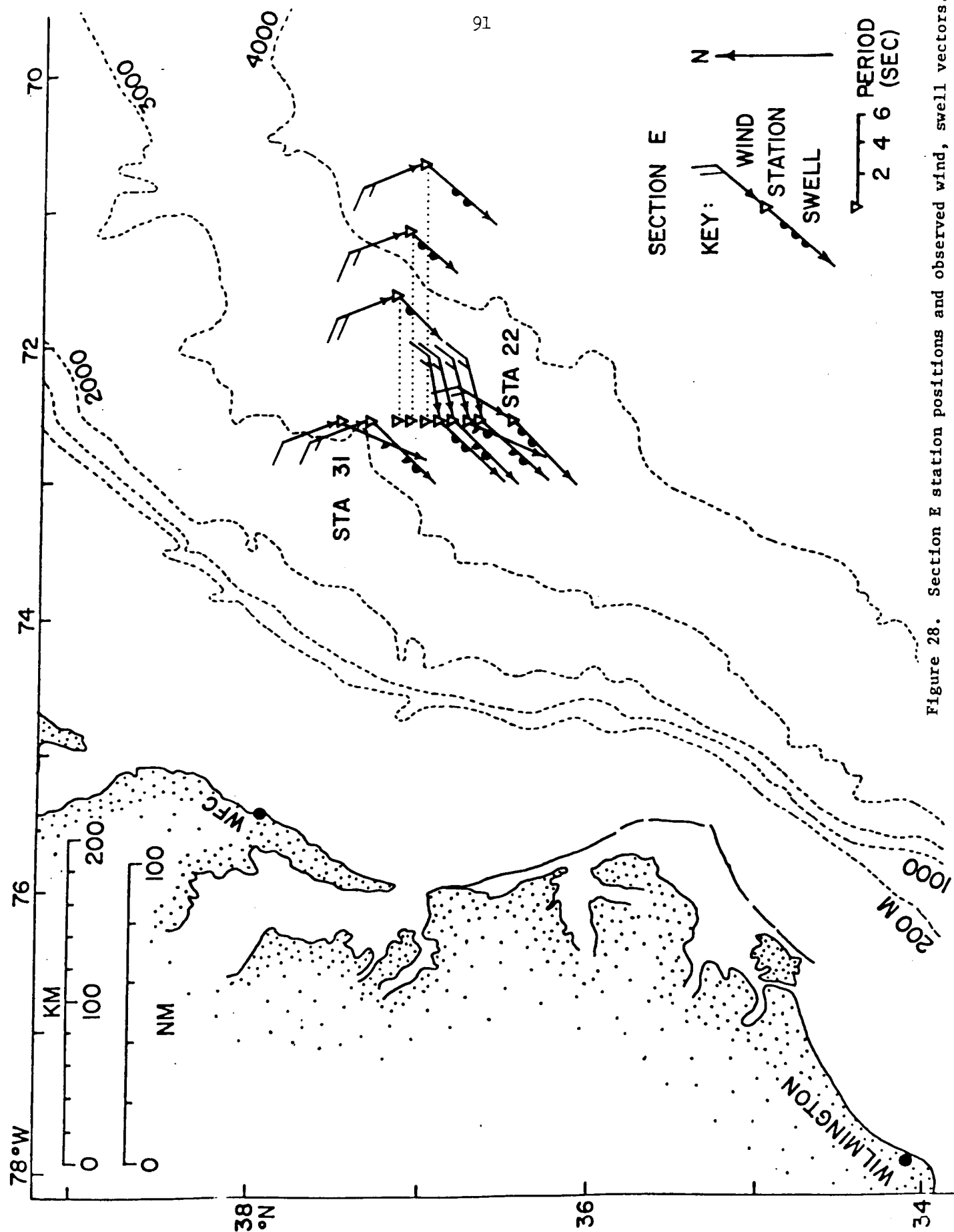
3.6
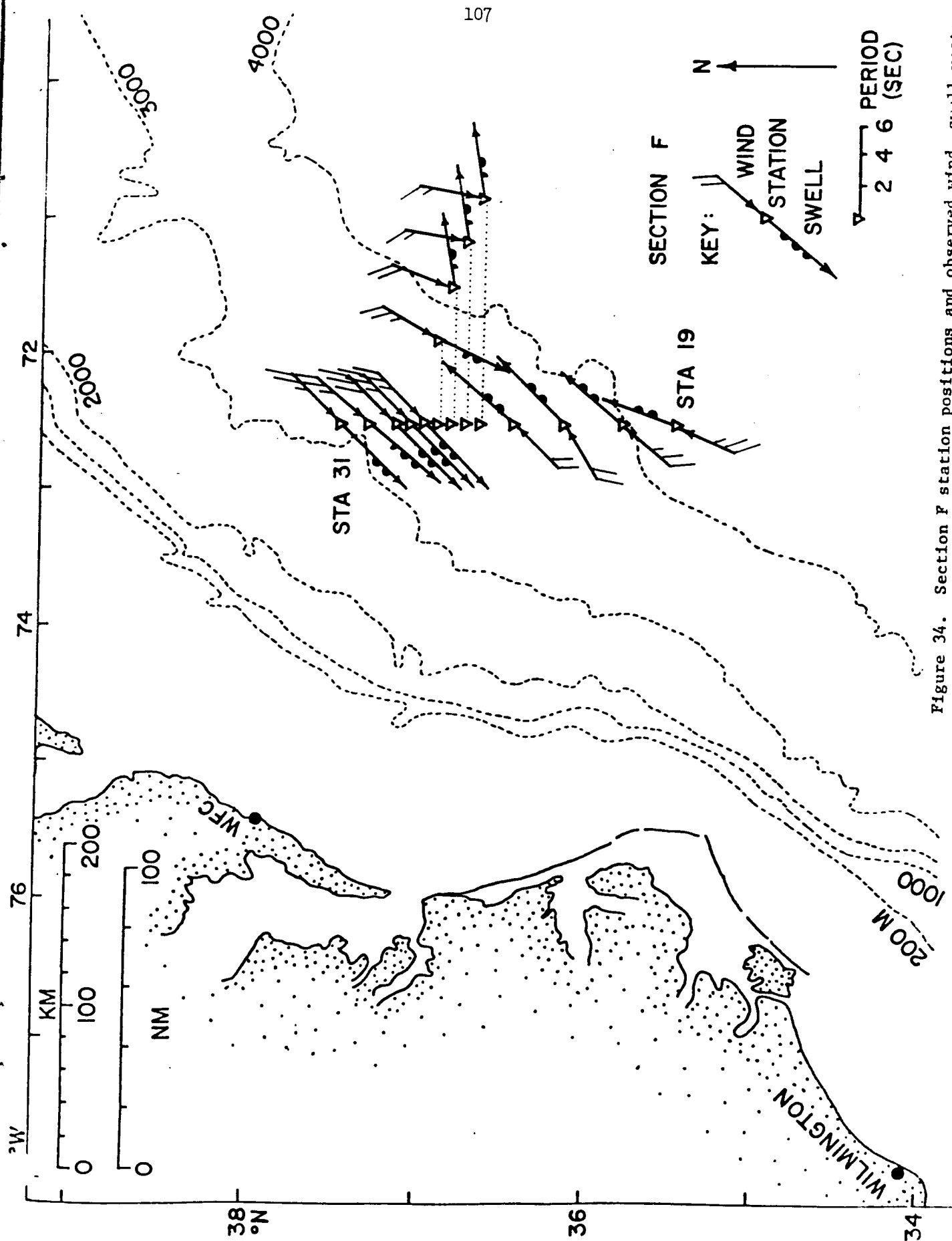
Section F

Figure 34. Section F station positions and observed wind, swell vectors.

Table 11. Atmospheric and Sea Surface Observations at Section F Stations

STATION NUMBER	WIND		SWELL			ATM PRESSURE SURFACE (MB)	AIR TEMPERATURE		HUMIDITY RELATIVE (%)
	DIR FROM (°T)	SPEED (M/S)	DIR TO (°T)	HT (M)	PER (S)		DRY (°C)	WET (°C)	
31	045	10.3	225	2.1	6	1016.3	17.9	16.3	85
30	040	10.3	220	2.4	6	1016.3	17.8	17.2	94
29	045	12.9	225	1.8	6	1014.2	19.7	19.1	95
28	045	9.3	225	1.8	6	1014.2	20.3	19.7	95
27	045	9.3	225	1.8	6	1014.2	21.0	20.0	91
26	030	9.8	205	1.5	5	1014.6	21.3	19.7	86
25	020	6.2	080	1.5	5	1014.6	21.3	20.5	93
24	010	5.1	080	1.5	5	1014.6	21.9	20.7	90
23	010	5.1	080	1.5	5	1013.5	22.2	20.5	86
22	224	6.7	040	2.1	6	1013.5	23.1	20.6	56
21	240	7.2	045	2.1	6	1013.2	24.4	21.6	79
20	220	8.7	040	1.8	5	1013.5	26.9	23.2	73
19	203	8.7	020	1.8	5	1013.5	23.3	22.4	93
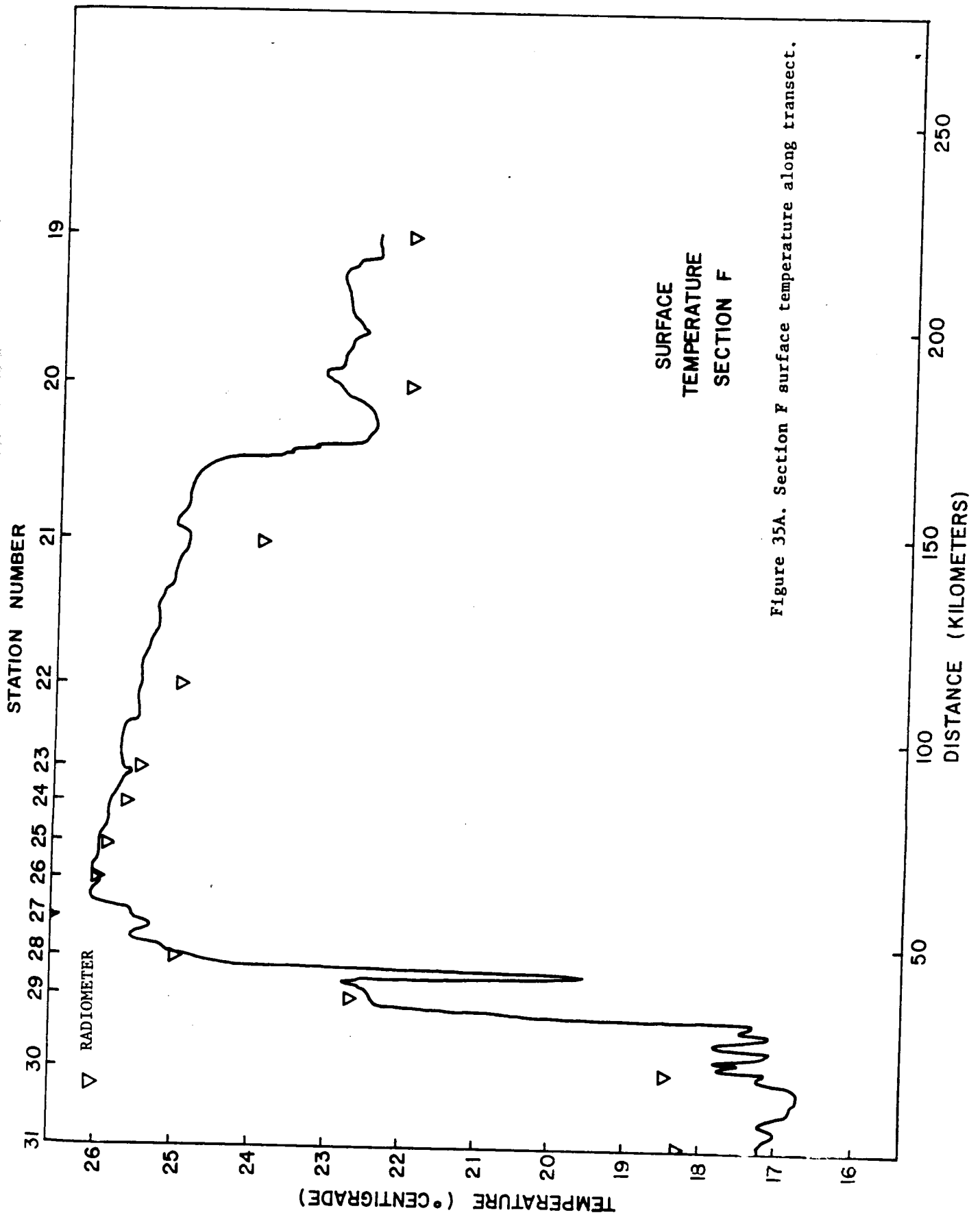
Figure 35A. Section F surface temperature along transect.
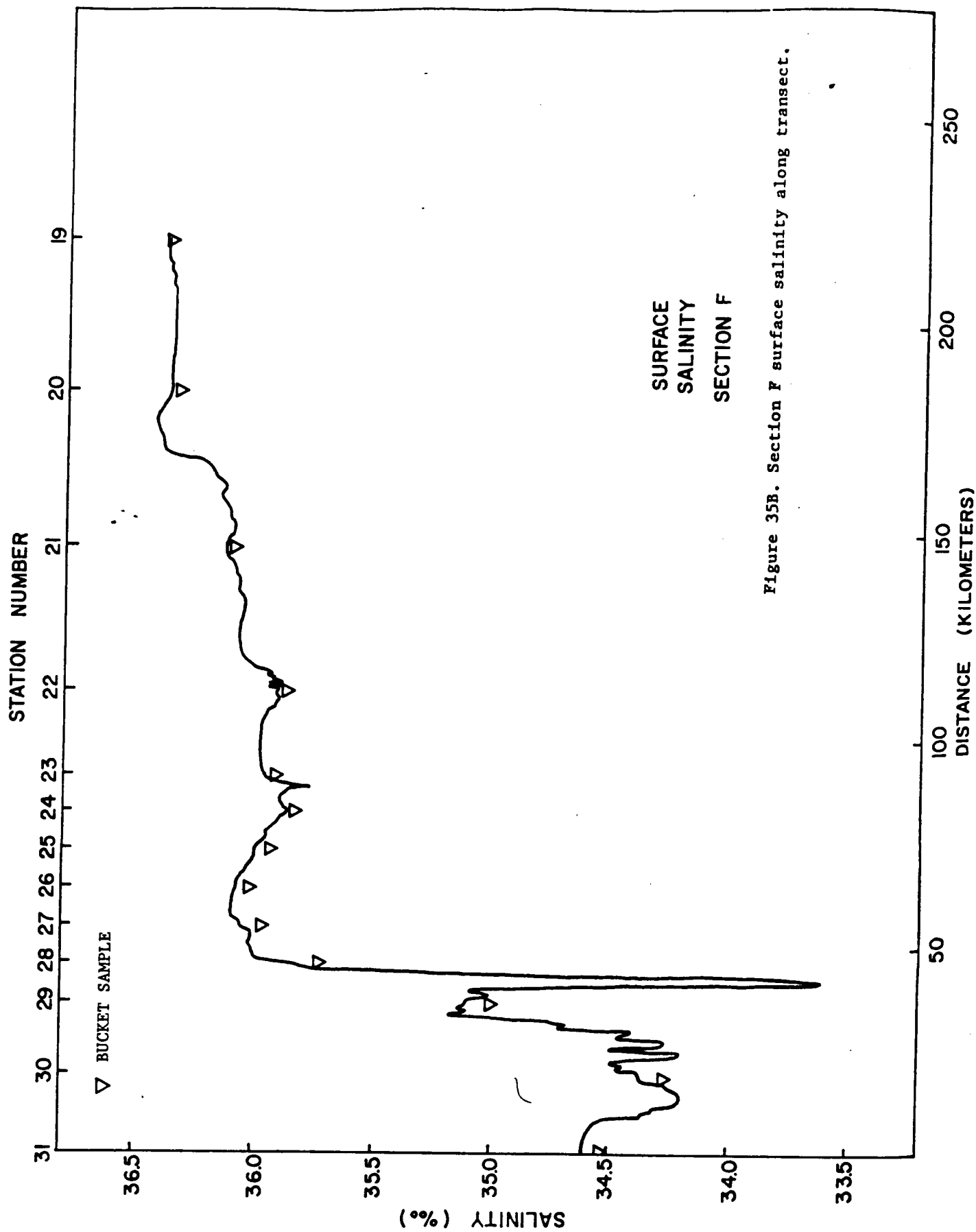
Figure 35B. Section F surface salinity along transect.
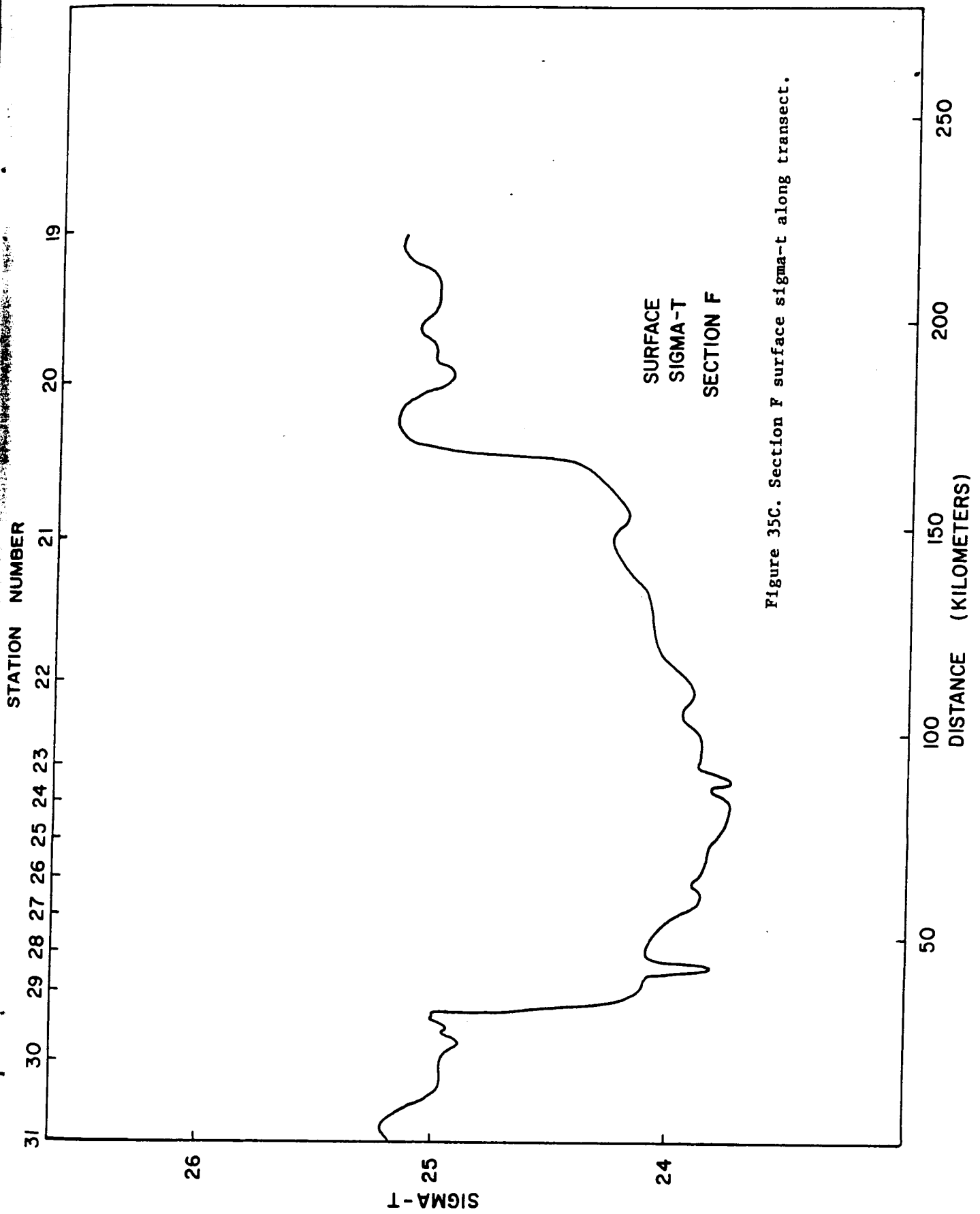
Figure 35C. Section F surface sigma-t along transect.

Figure 36. Section F observed and derived station profiles.
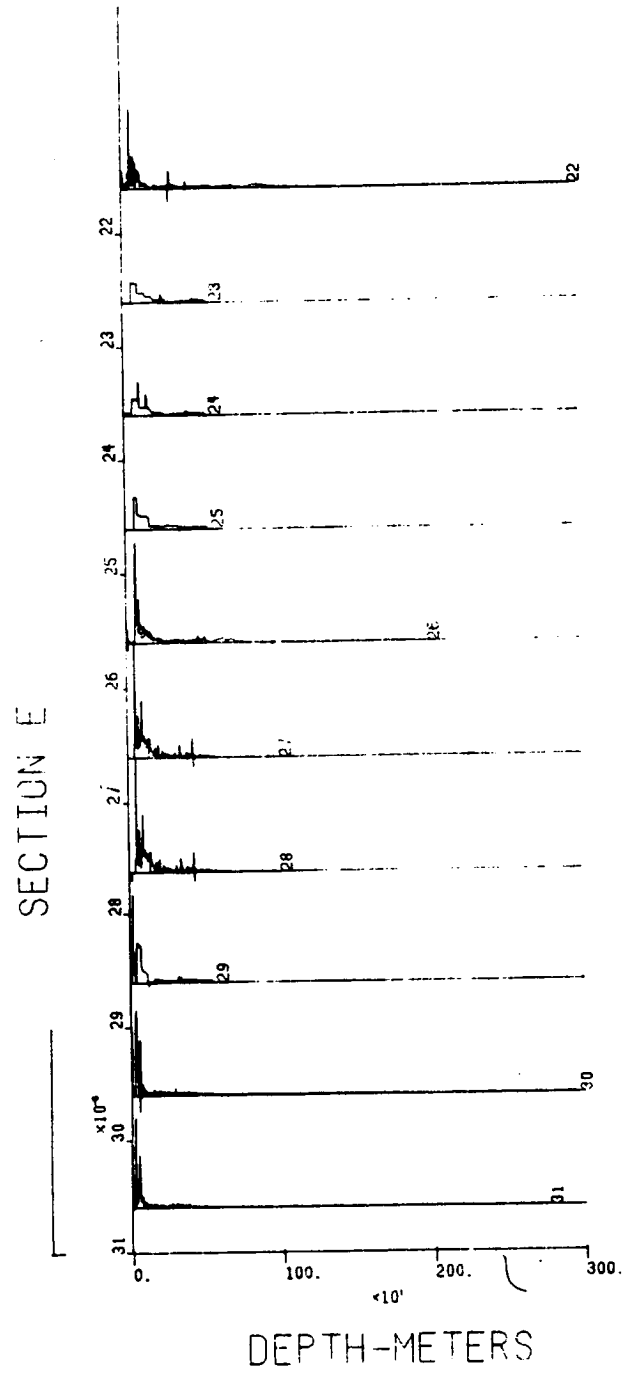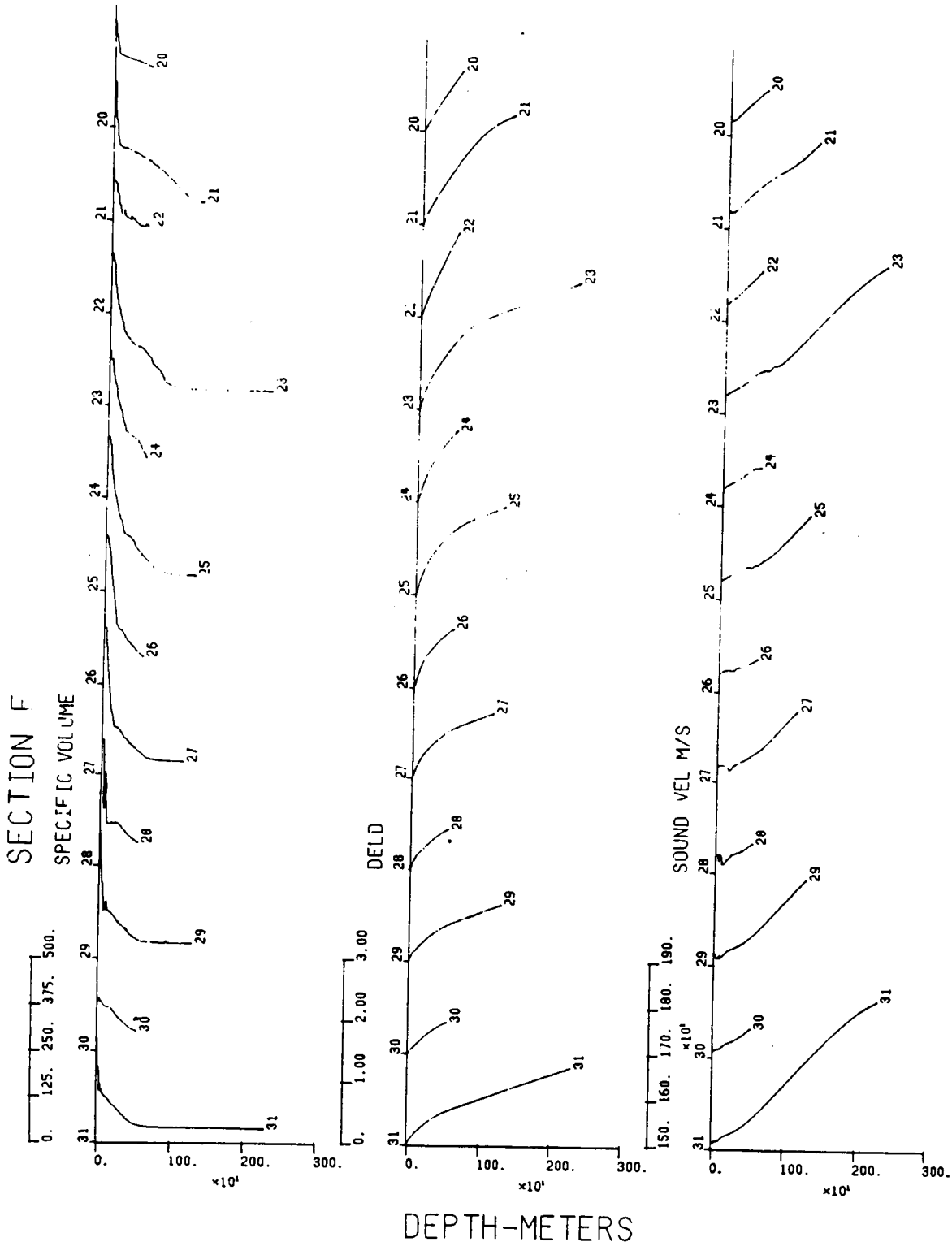
Figure 36. Continued.
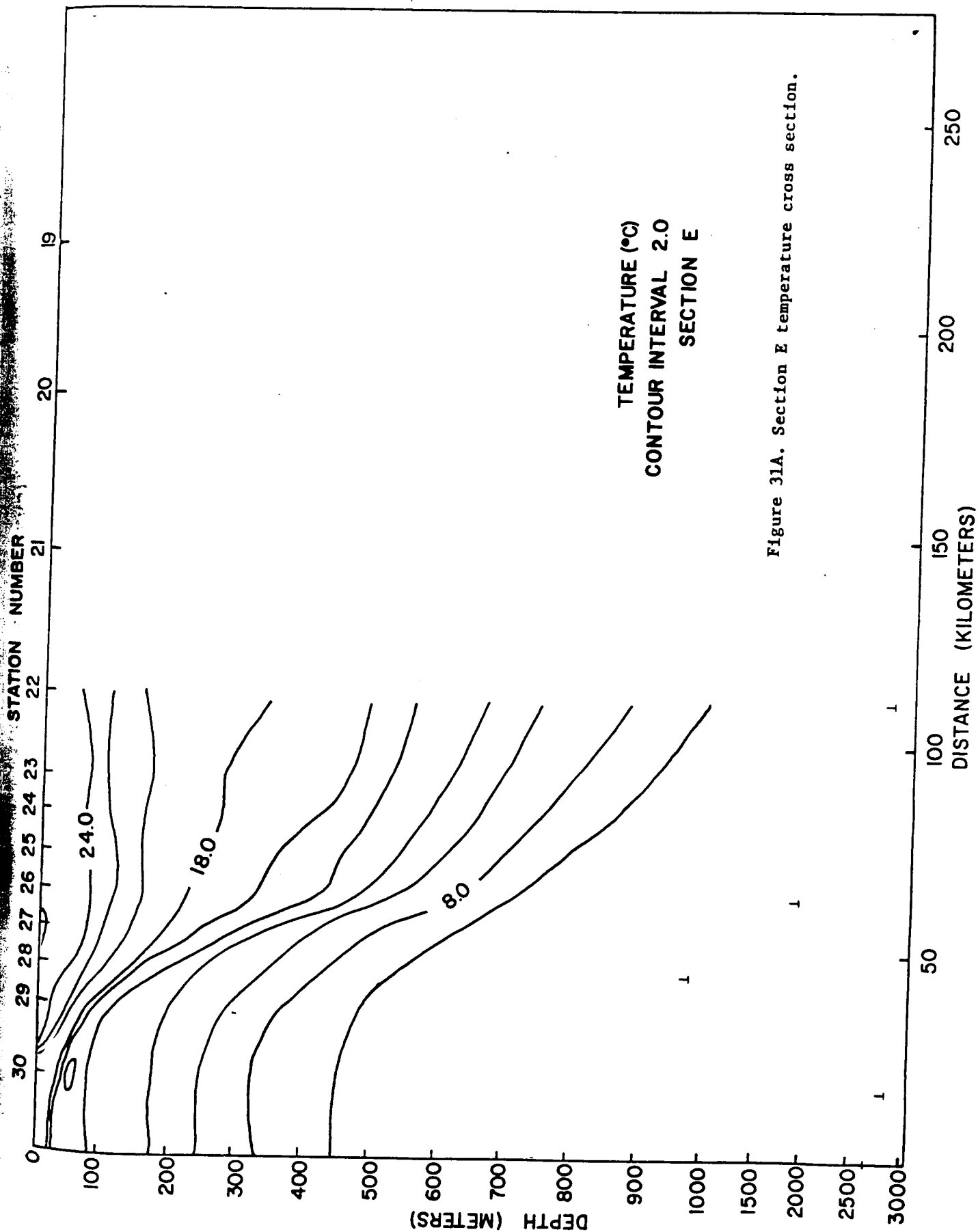
Figure 36. Continued.

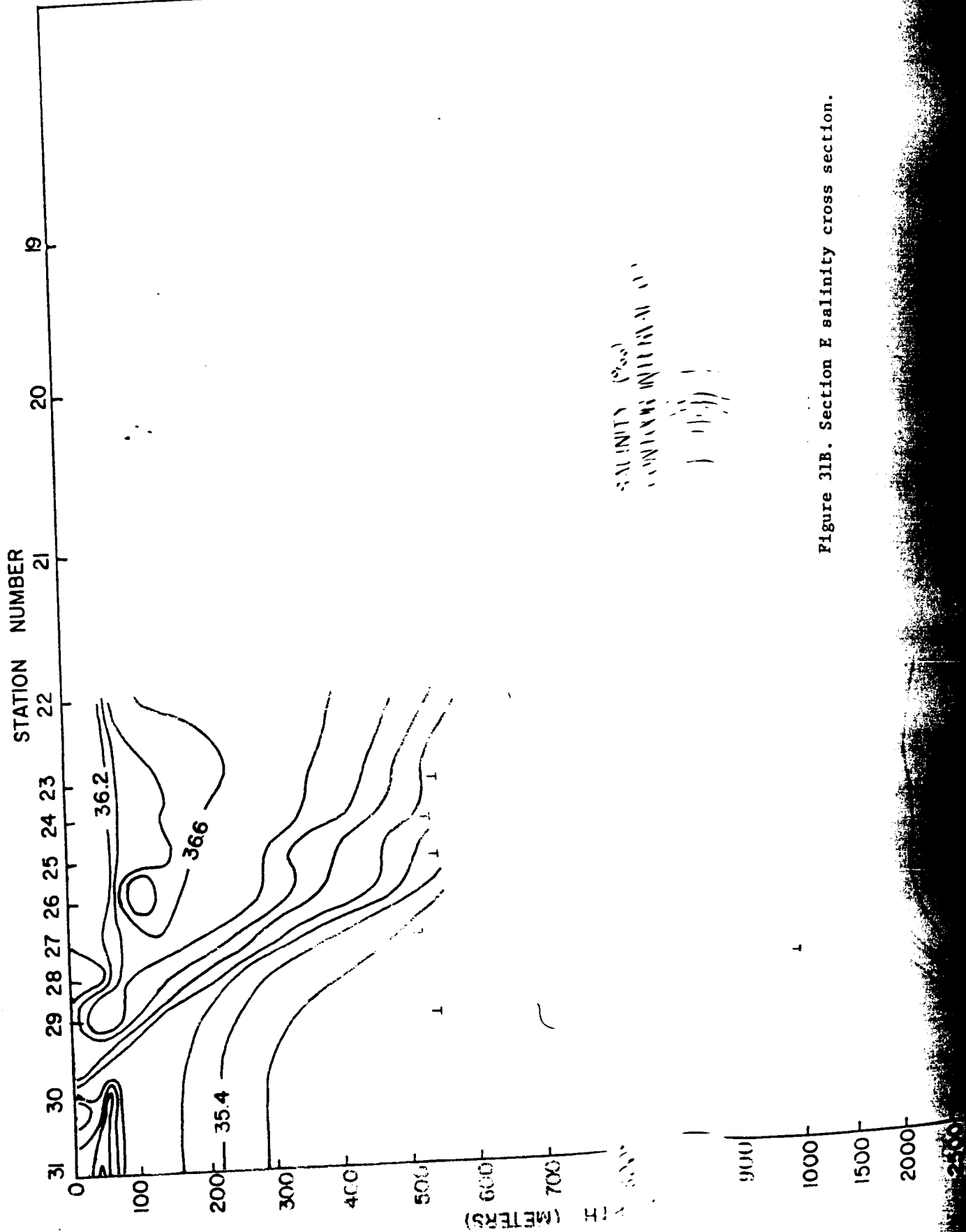Figure 37A. Section F temperature cross section.
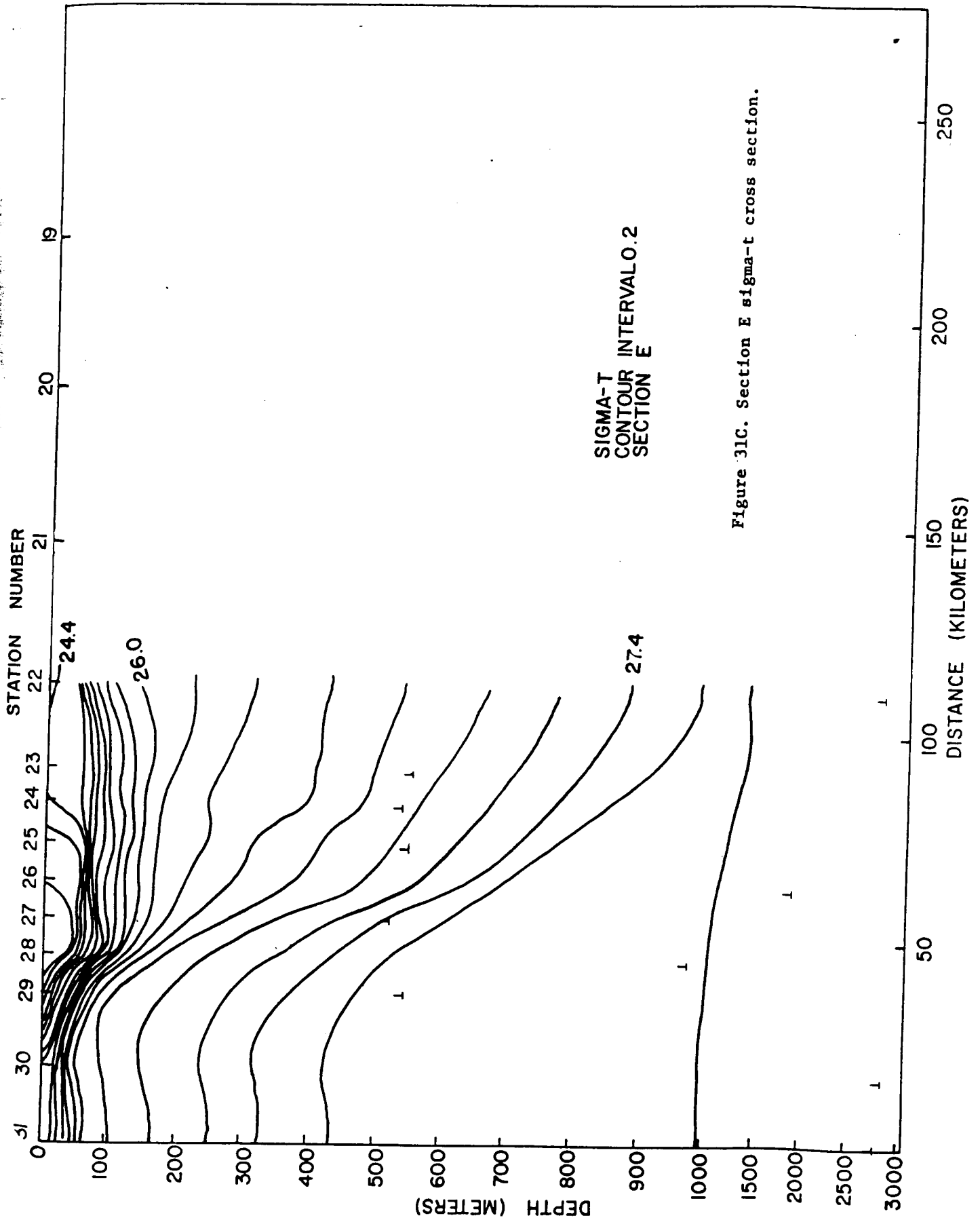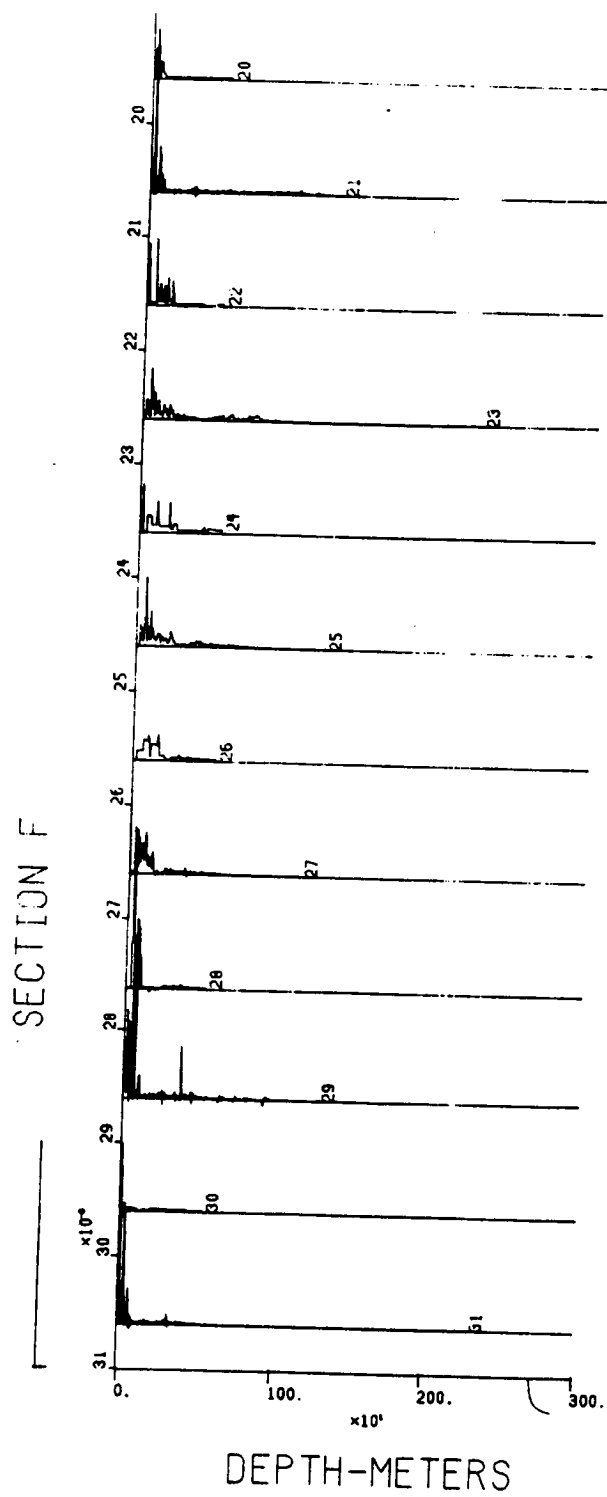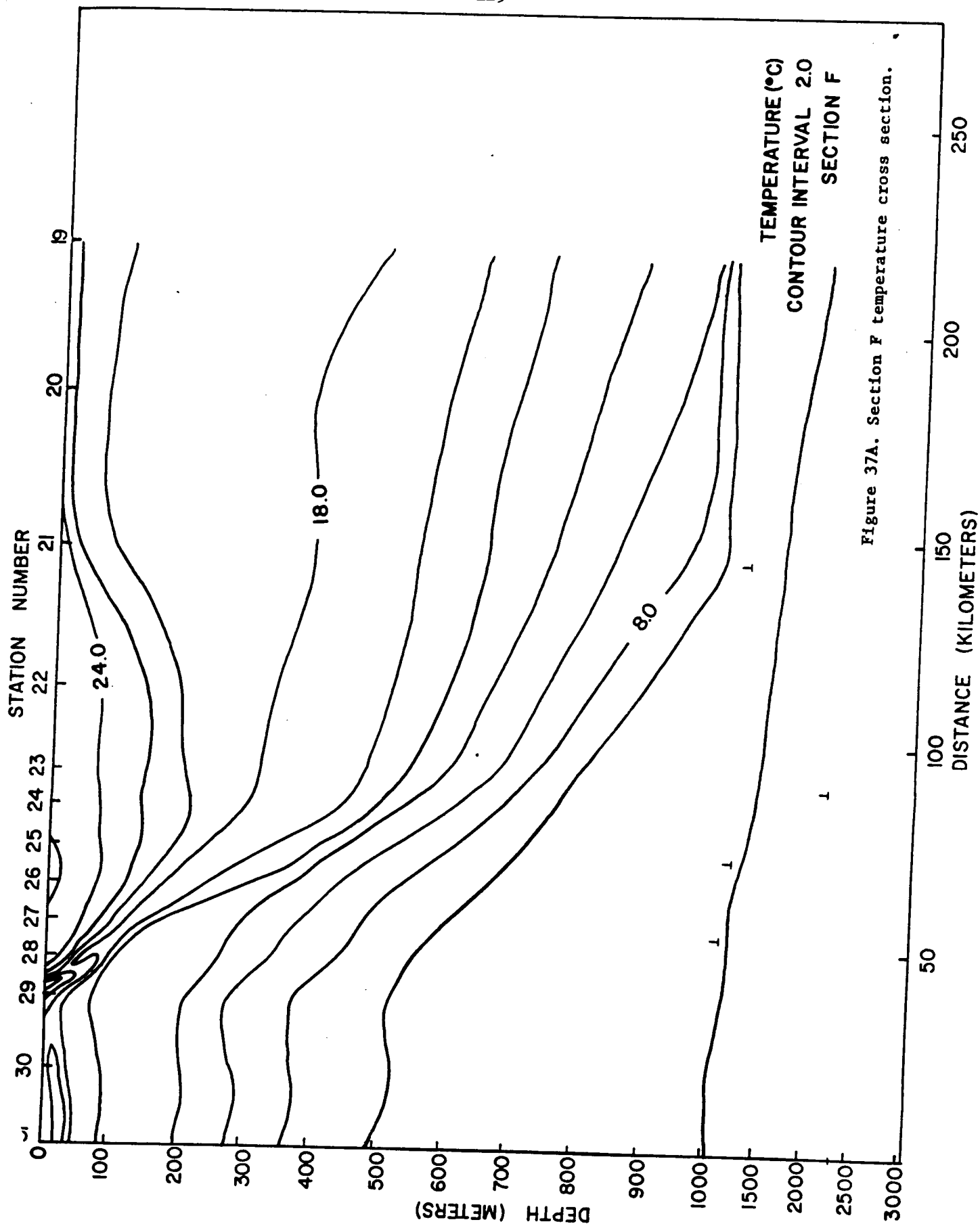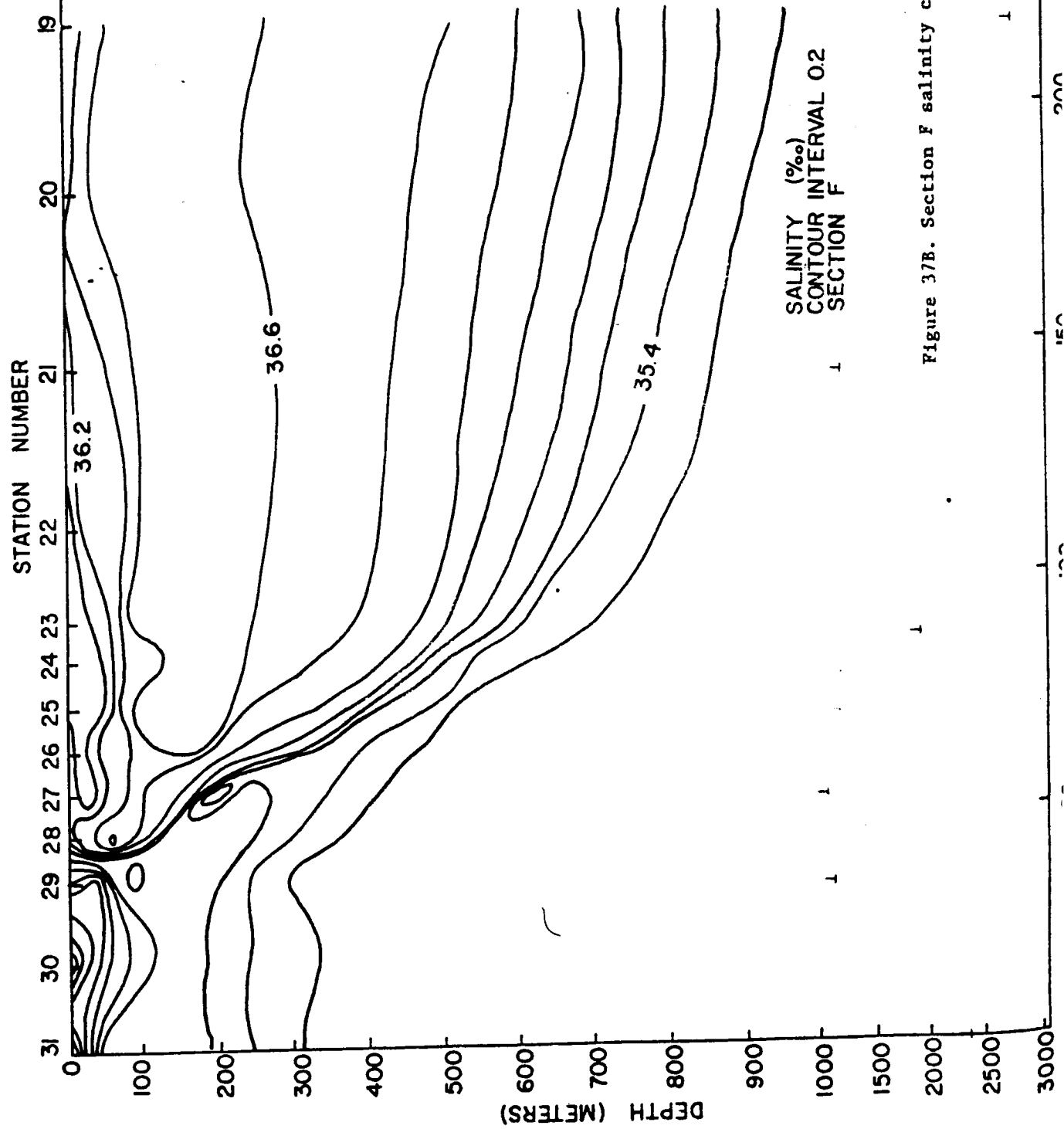
Figure 37B. Section F salinity cross section.
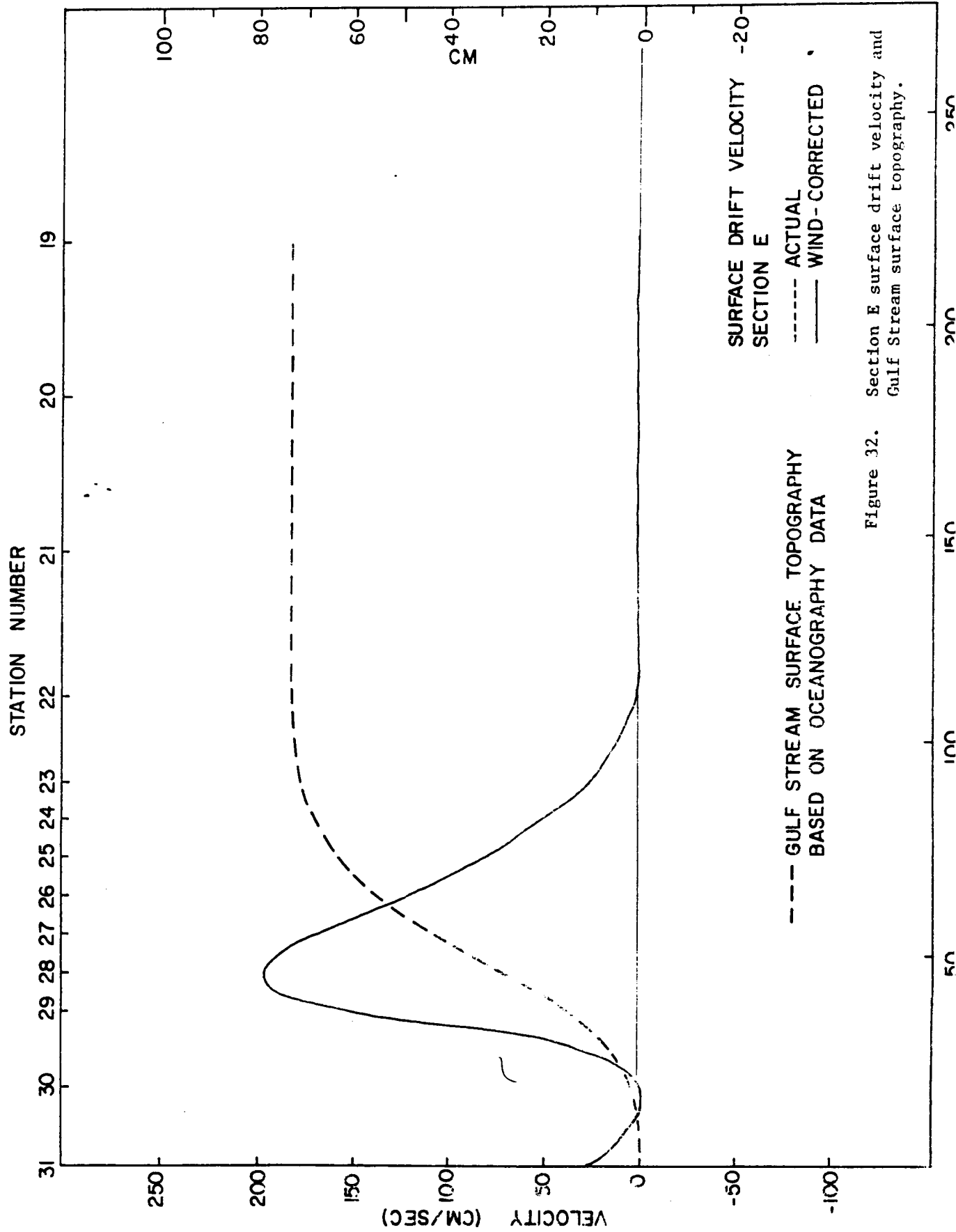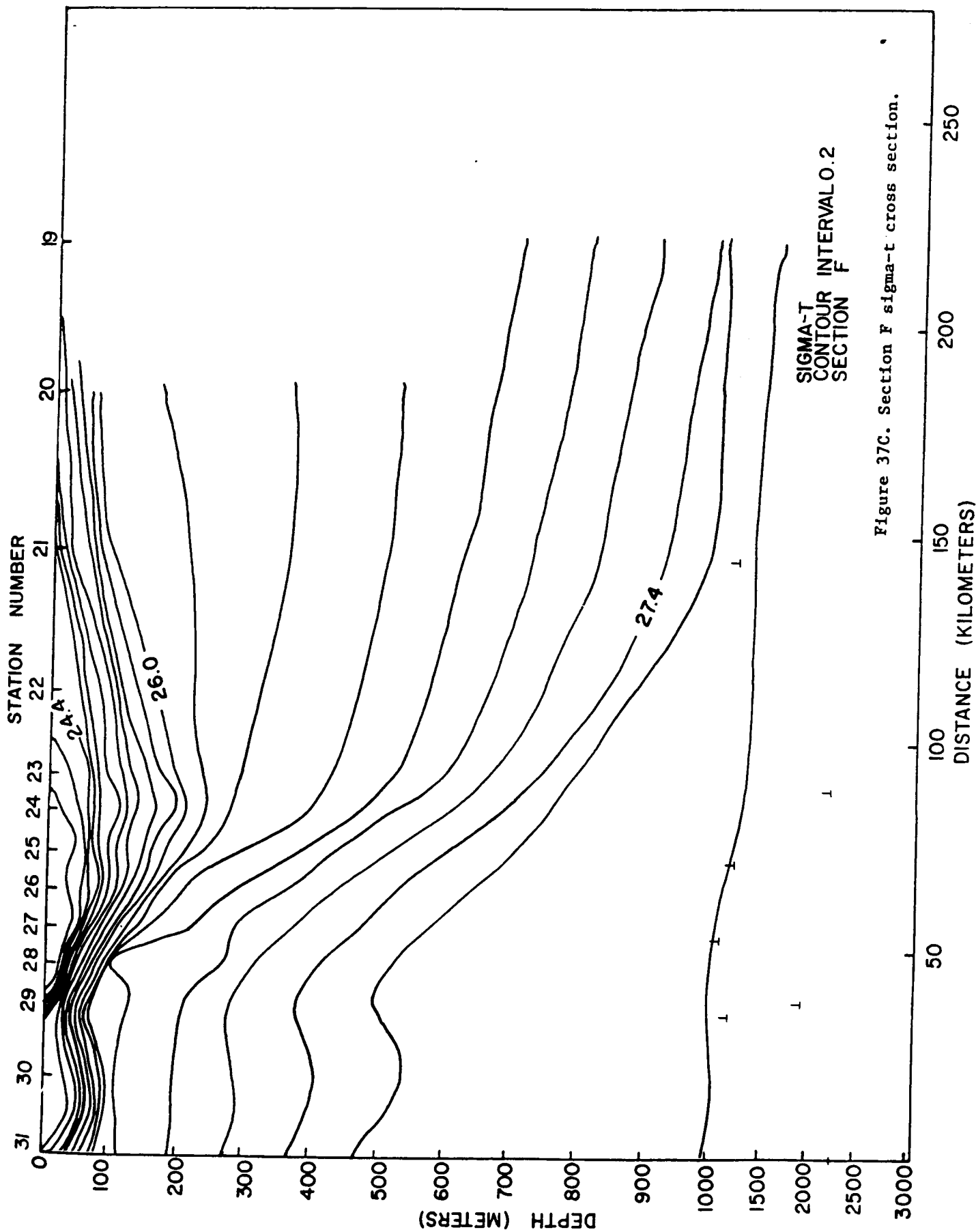
Figure 37C. Section F sigma-t cross section.

SURFACE DRIFT VELOCITY
SECTION F

----- ACTUAL
——— WIND-CORRECTED

--- GULF STREAM SURFACE TOPOGRAPHY
BASED ON OCEANOGRAPHY DATA

Figure 38. Section F surface drift velocity and
Gulf Stream surface topography.

STATION NUMBER

VELOCITY (CM/SEC)

CM
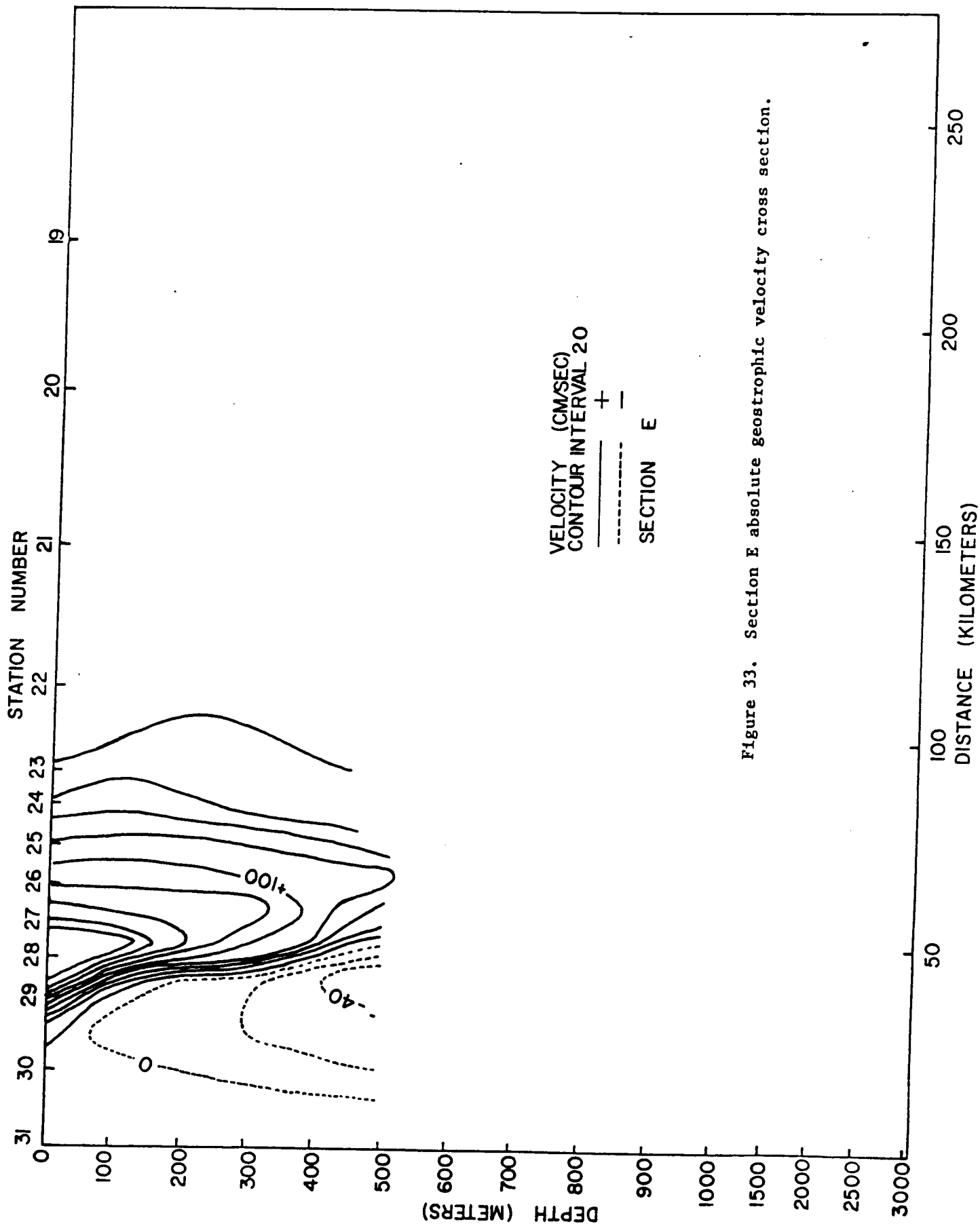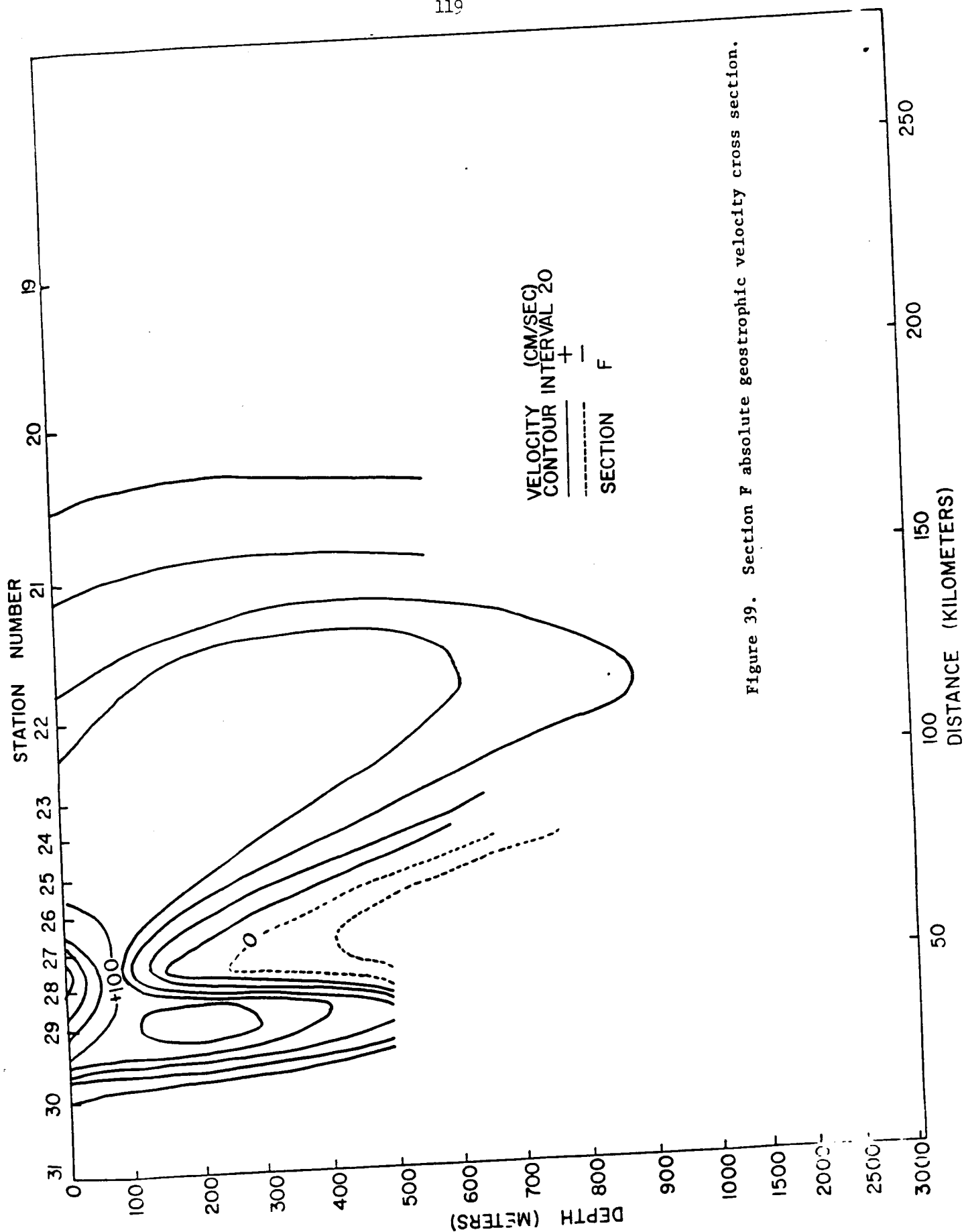
Figure 39. Section F absolute geostrophic velocity cross section.

3.7
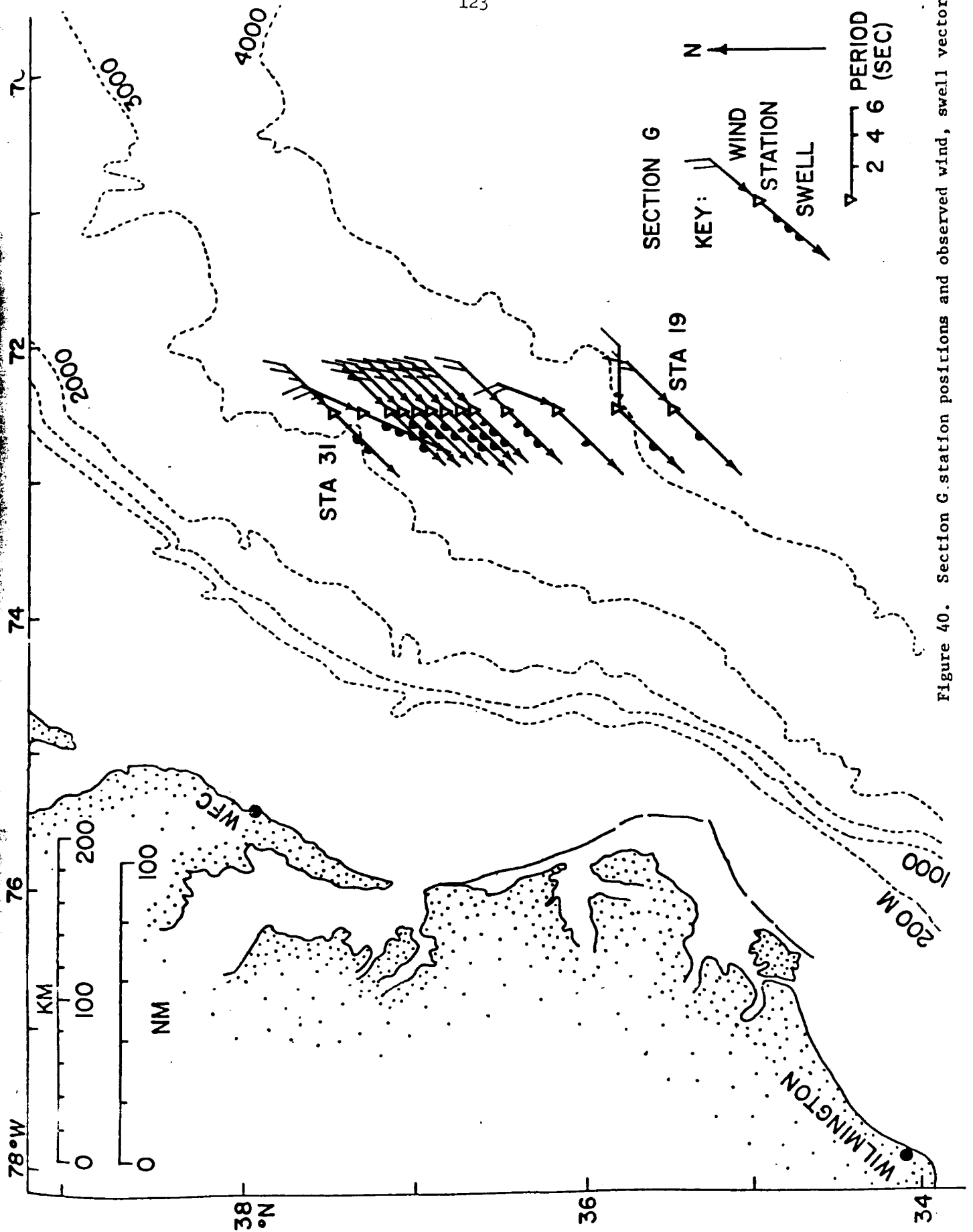
Section G

Figure 40. Section G.station positions and observed wind, swell vectors.

Table 12. Atmospheric and Sea Surface Observations at Section G Stations

| STATION NUMBER	WIND DIR FROM (°T)	WIND SPEED (M/S)	SWELL DIR TO (°T)	SWELL HT (M)	PER (S)	ATM PRESSURE SURFACE (MB)	AIR TEMPERATURE DRY (°C)	AIR TEMPERATURE WET (°C)	HUMIDITY RELATIVE (%)
31	045	10.3	225	2.1	6	1016.3	17.9	16.3	85
30	025	10.3	205	2.1	6	1015.9	18.1	16.8	88
29	045	10.3	225	2.1	5	1015.2	19.9	19.1	93
28	045	11.8	225	2.1	5	1015.2	20.8	20.3	96
27	045	9.3	225	2.1	5	1016.3	22.0	20.5	87
26	045	9.3	225	1.8	5	1016.6	22.4	20.7	86
25	045	10.3	225	2.4	6	1016.9	23.1	20.6	80
24	045	10.3	225	2.7	5	1016.6	21.8	20.7	91
23	045	10.3	225	2.7	5	1016.6	21.7	20.4	89
22	045	8.2	225	2.4	5	1016.6	21.6	20.1	87
21	022	5.1	225	0.6	6	1015.7	23.1	21.4	86
20	090	5.1	225	1.2	6	1015.9	22.5	21.4	91
19	045	5.1	225	1.2	6	1015.9	22.7	21.3	88
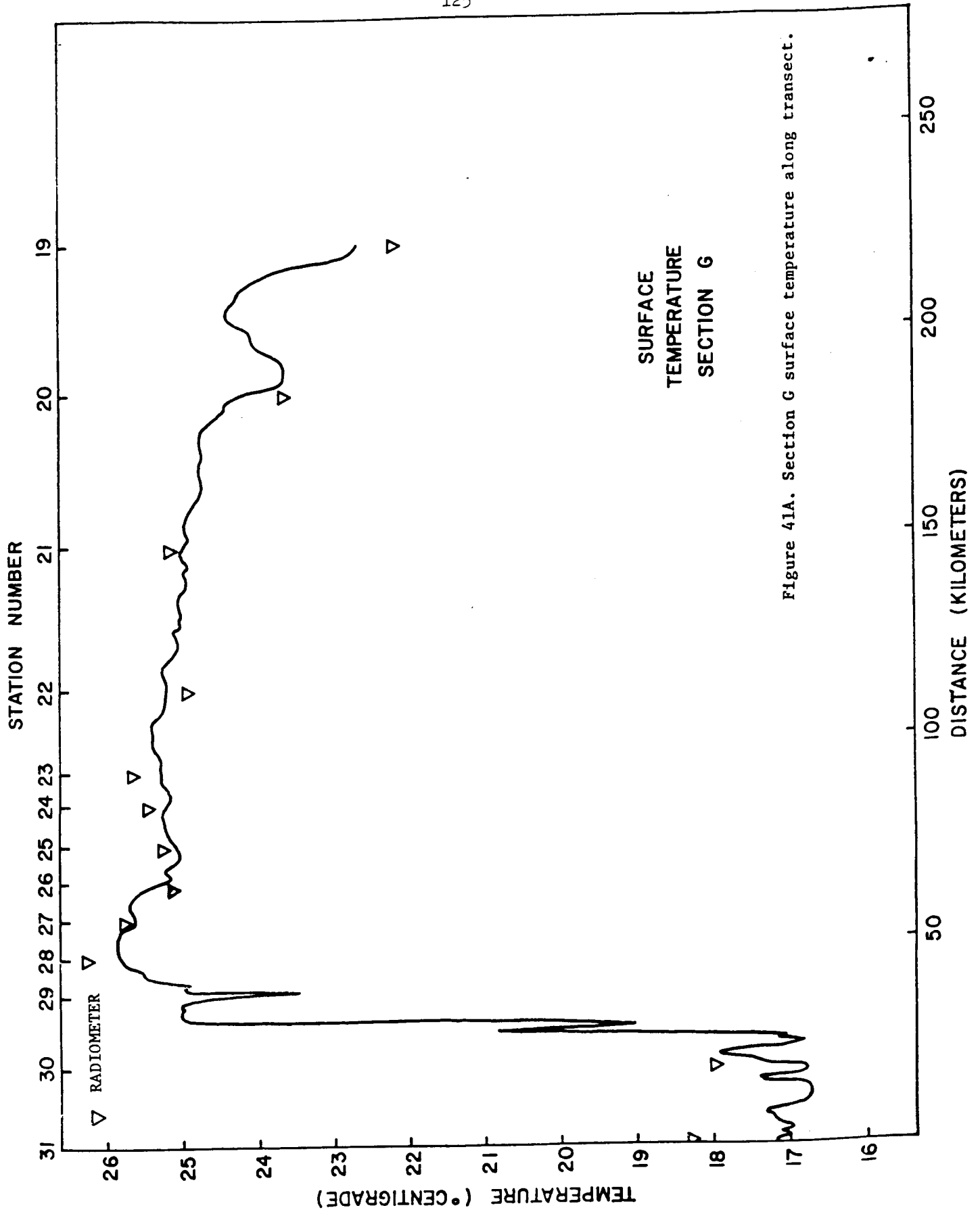
Figure 41A. Section G surface temperature along transect.

Figure 41B. Section G surface salinity along transect.
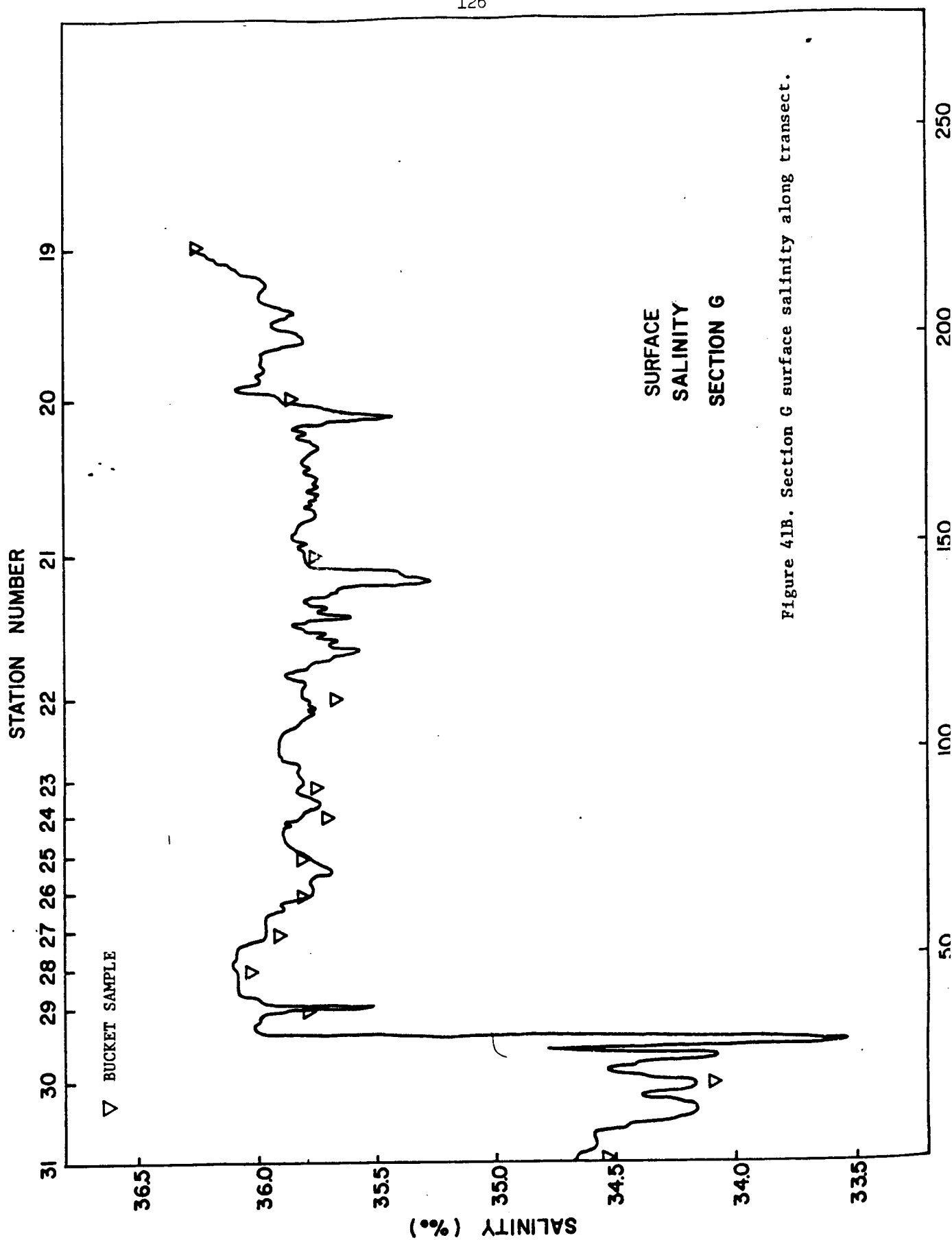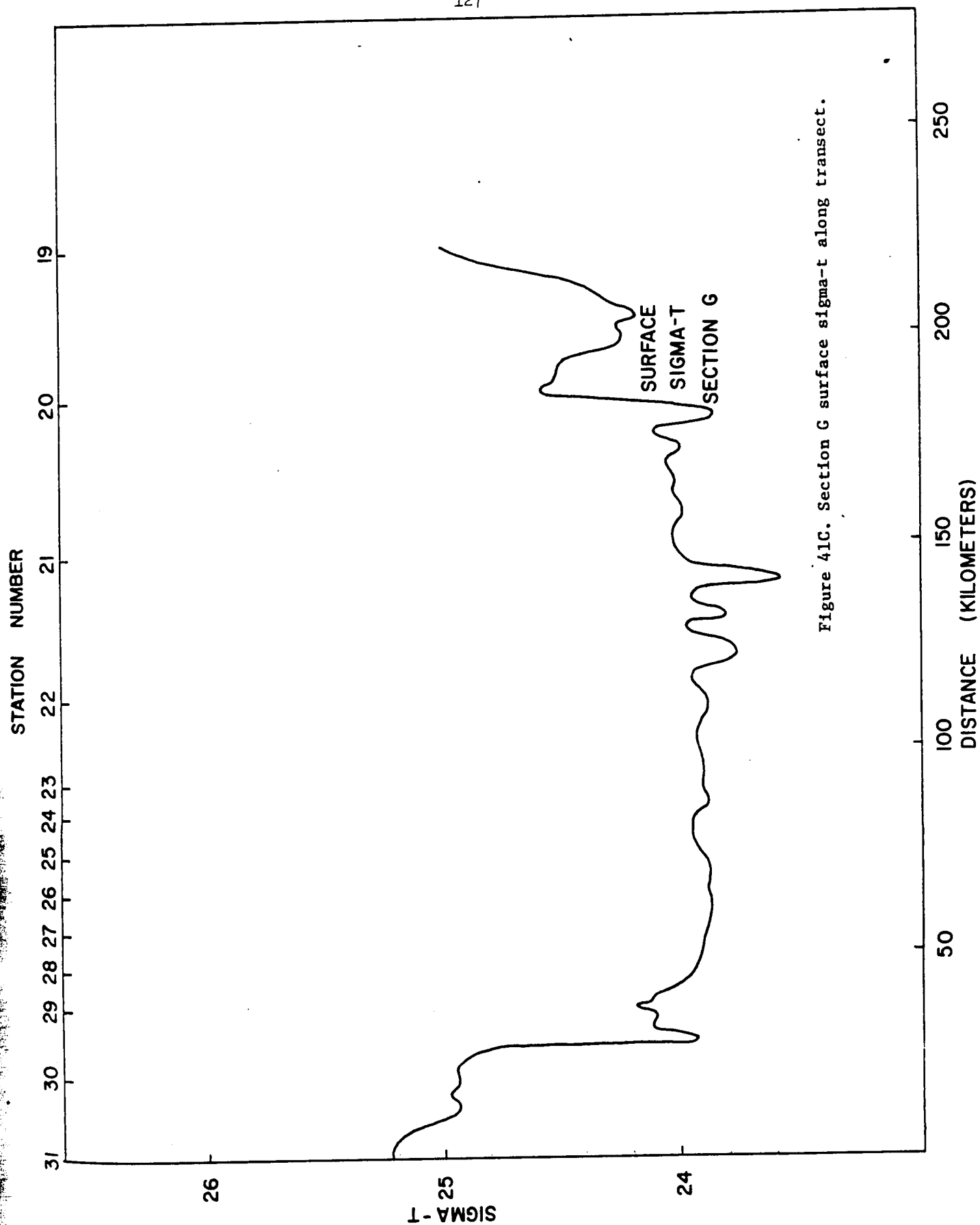
Figure 41C. Section G surface sigma-t along transect.
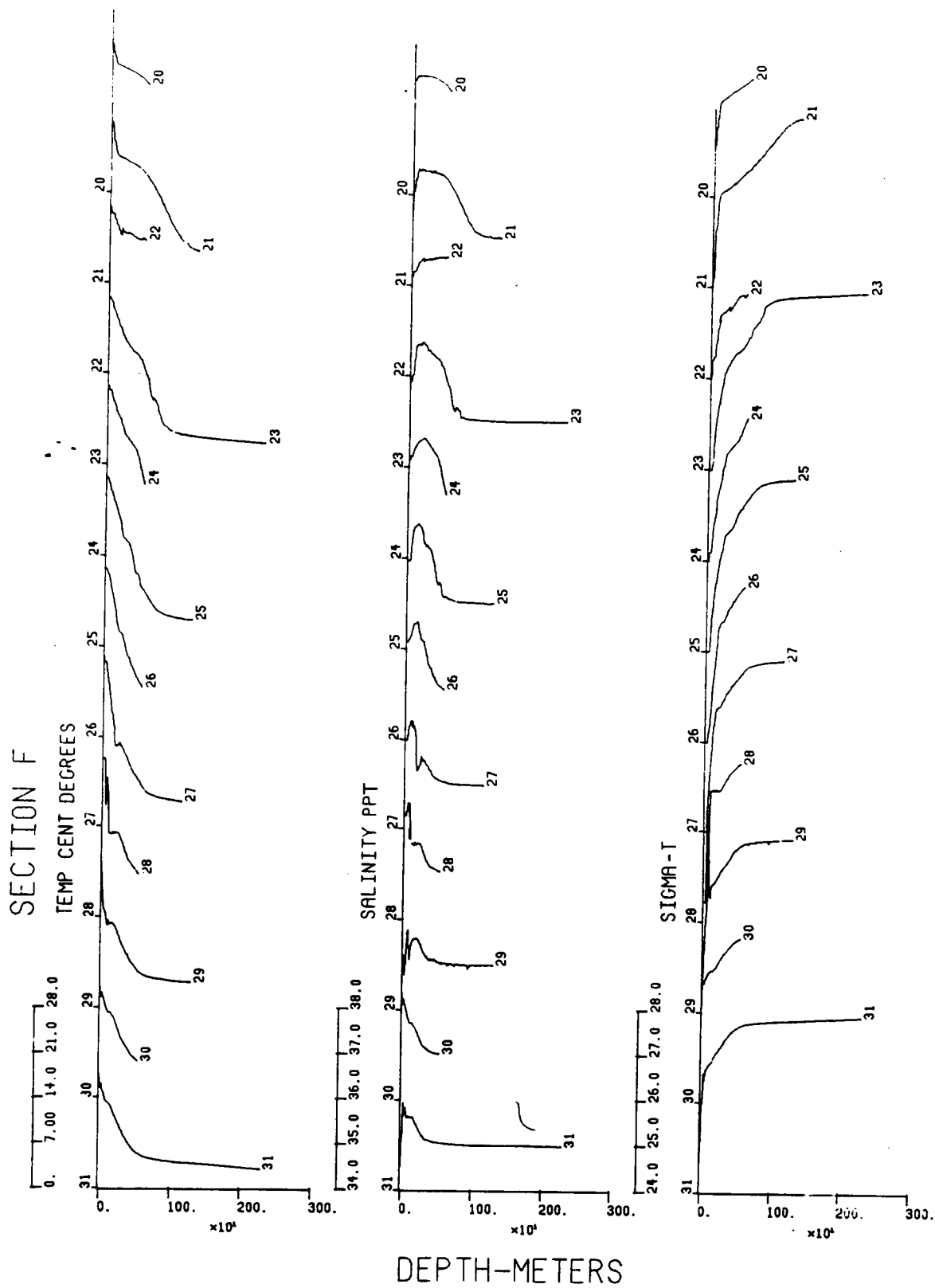
SECTION G

TEMP CENT DEGREES

SALINITY PPT

SIGMA-T

DEPTH-METERS
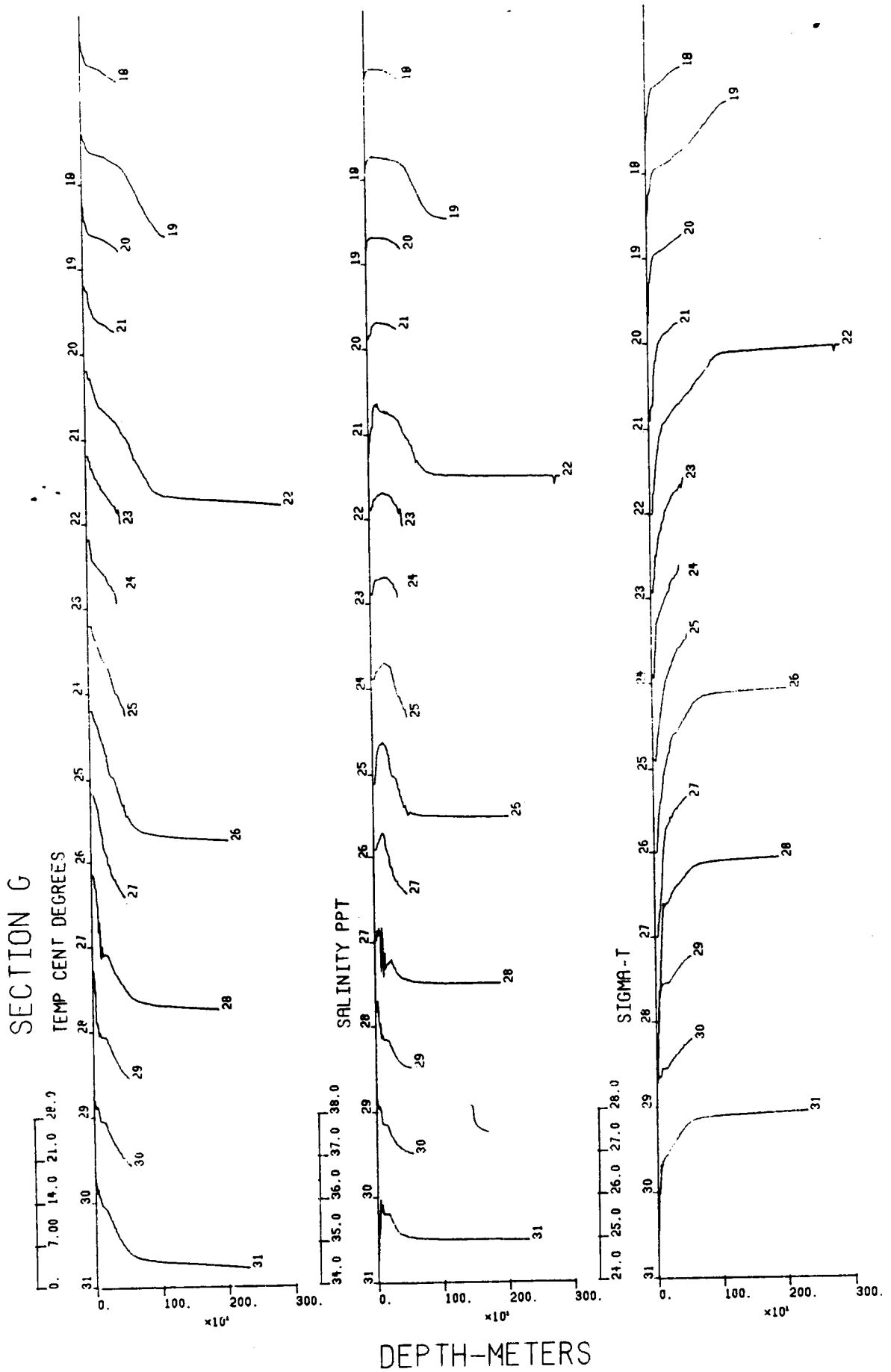
Figure 42. Section G observed and derived station profiles.

SECTION G

SPECIFIC VOLUME

DELD

SOUND VEL M/S

DEPTH-METERS
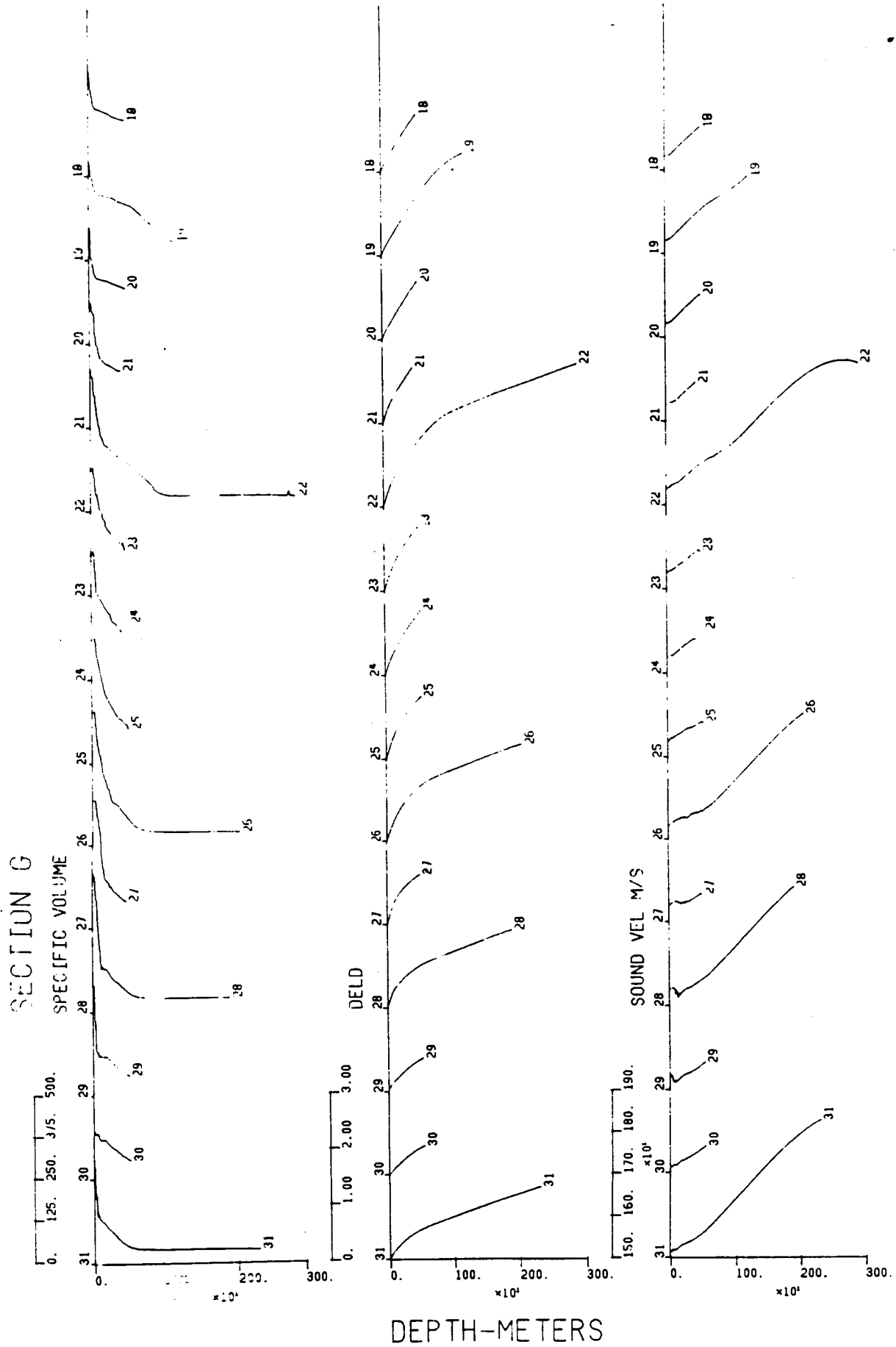
Figure 42. Continued.

Figure 42. Continued.

Figure 43A. Section G temperature cross section.

SALINITY (‰)
CONTOUR INTERVAL 0.2
SECTION G
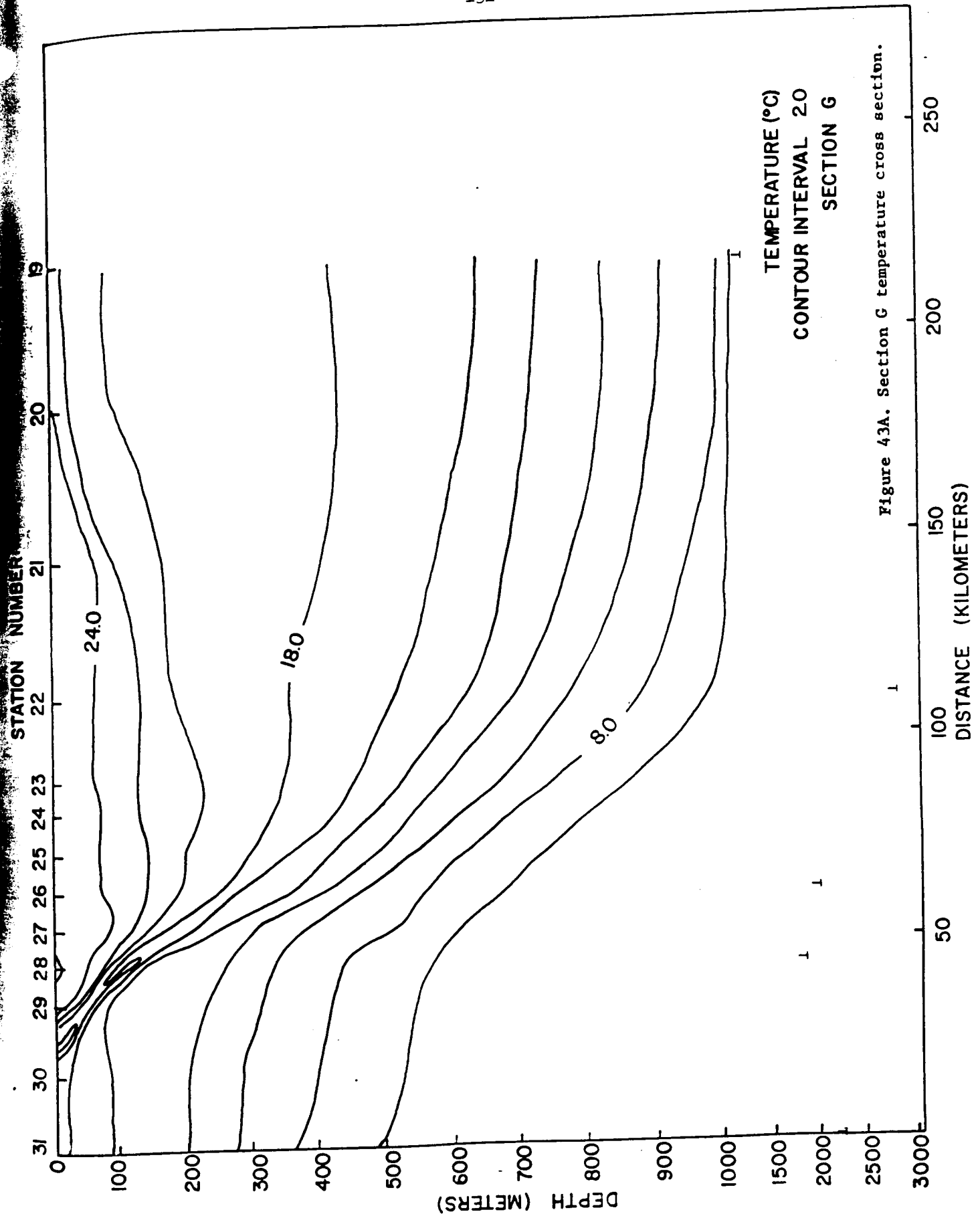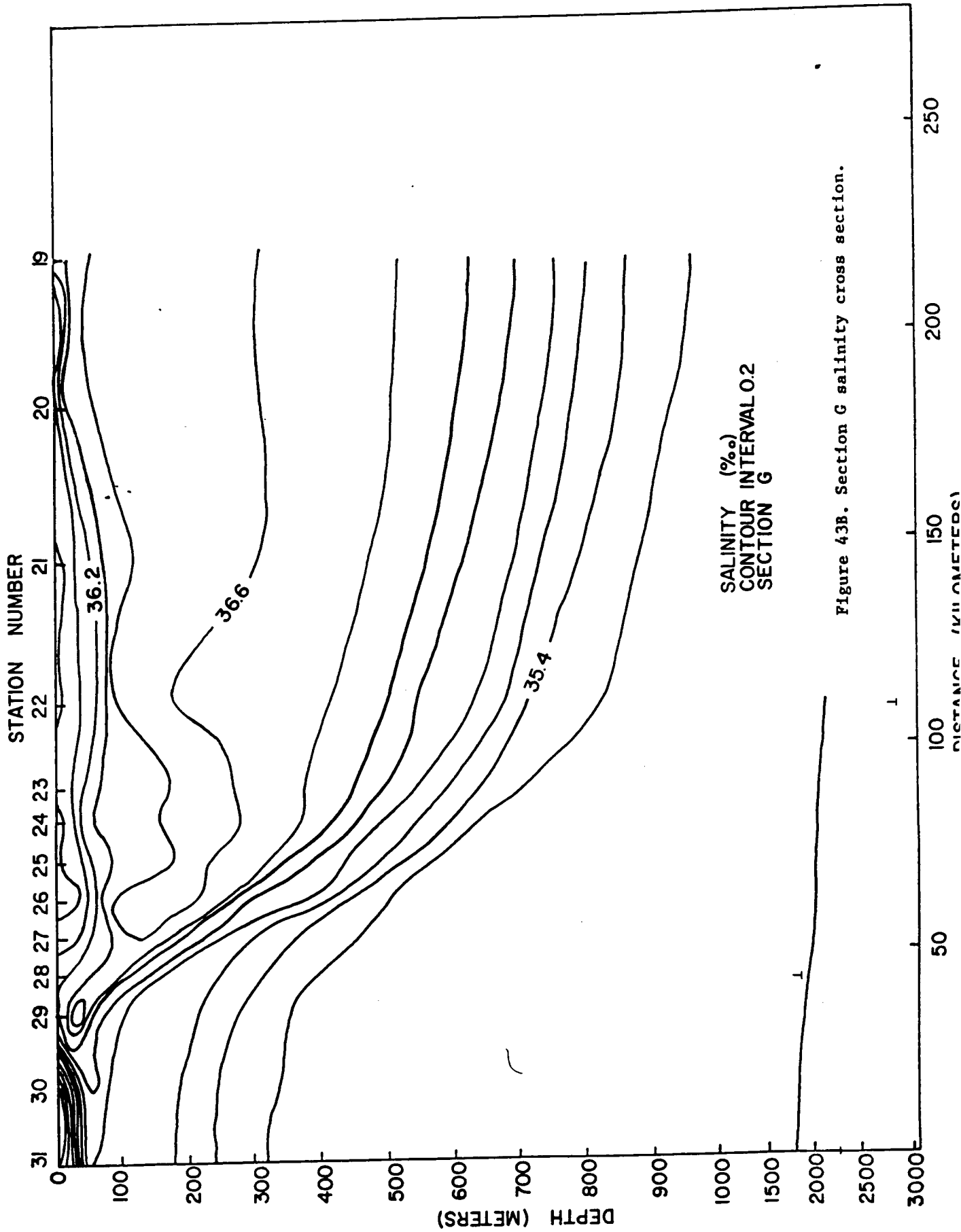
Figure 43B. Section G salinity cross section.

SIGMA-T
CONTOUR INTERVAL 0.2
SECTION G

Figure 43C. Section G sigma-t cross section.
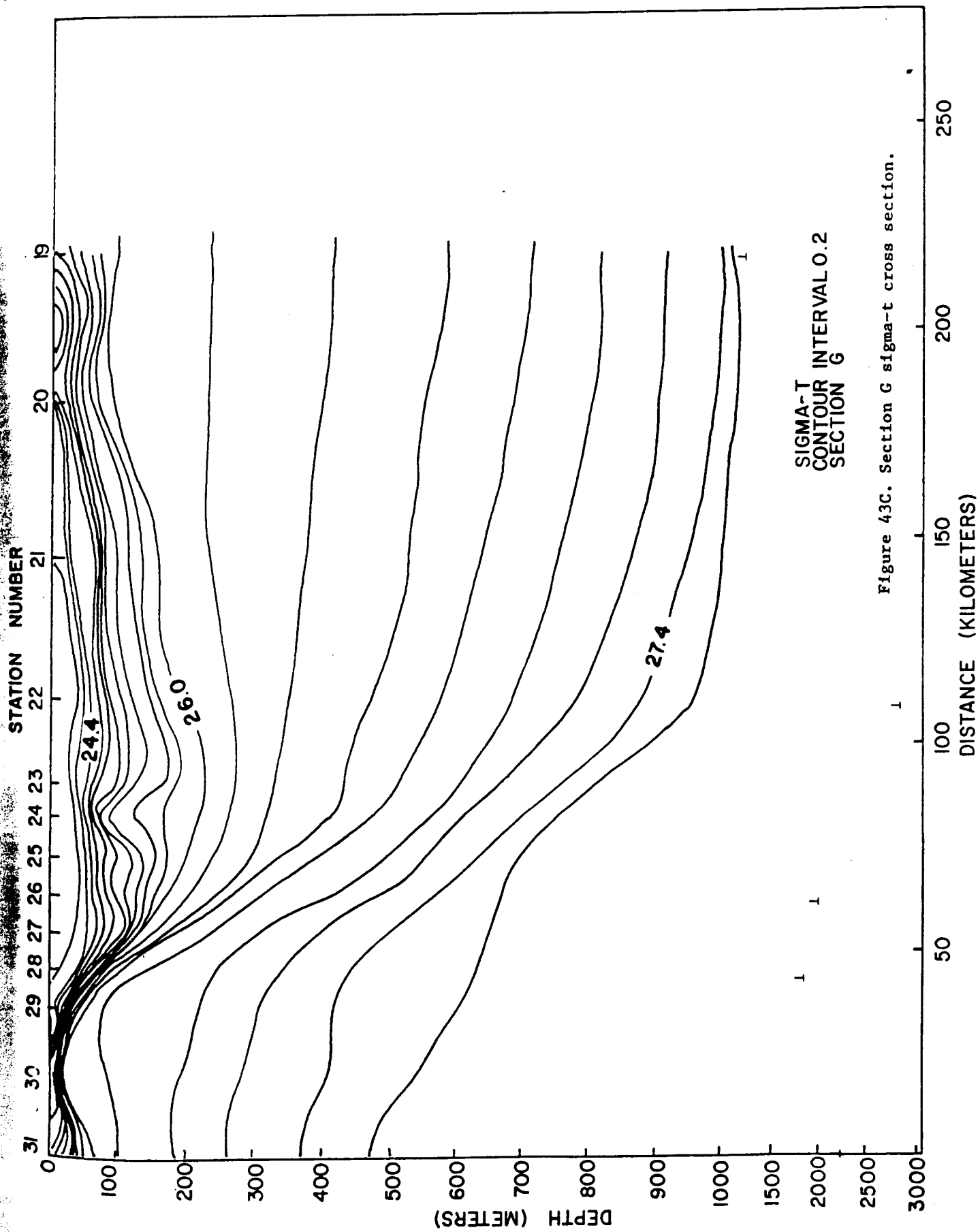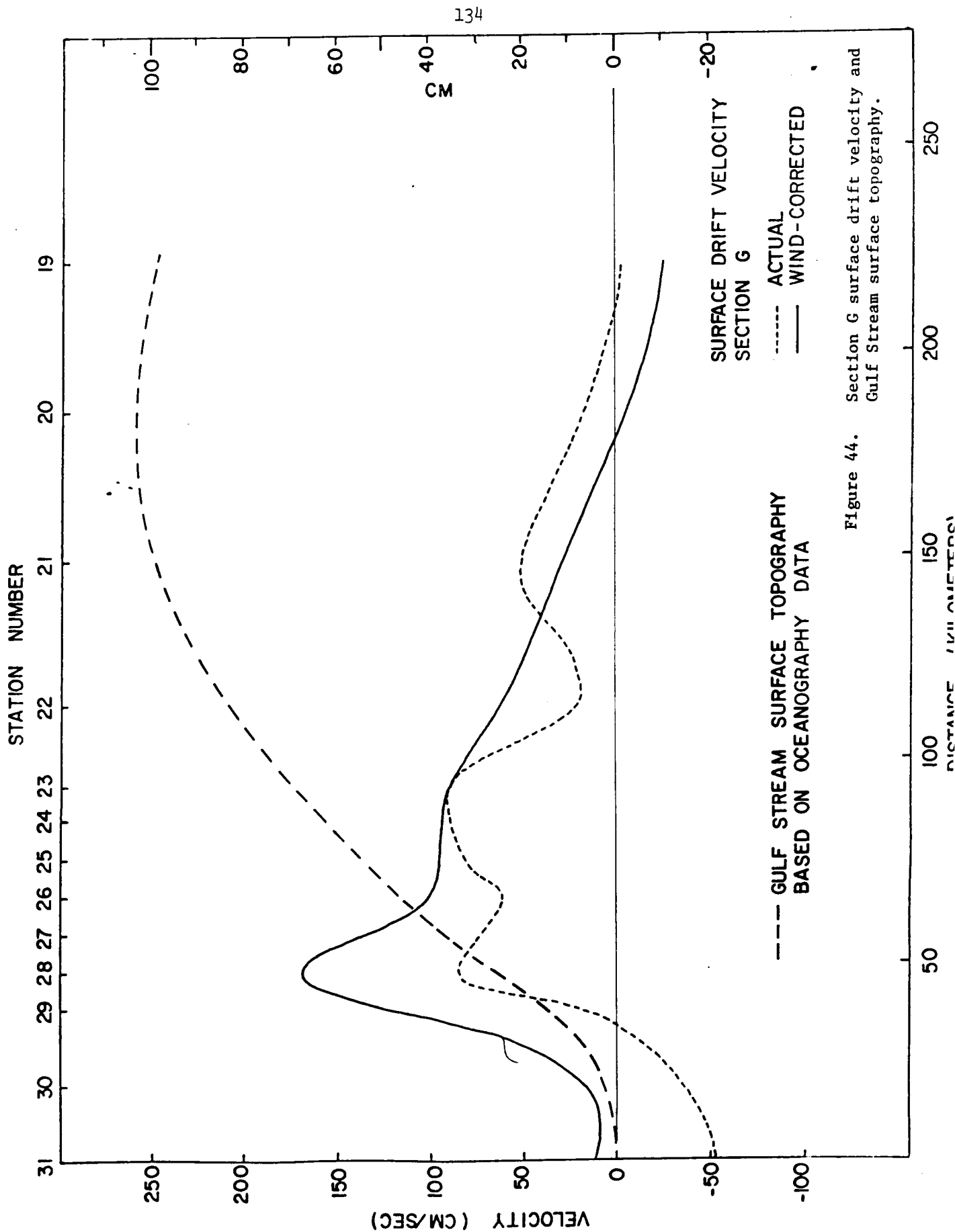
Figure 44. Section G surface drift velocity and
Gulf Stream surface topography.
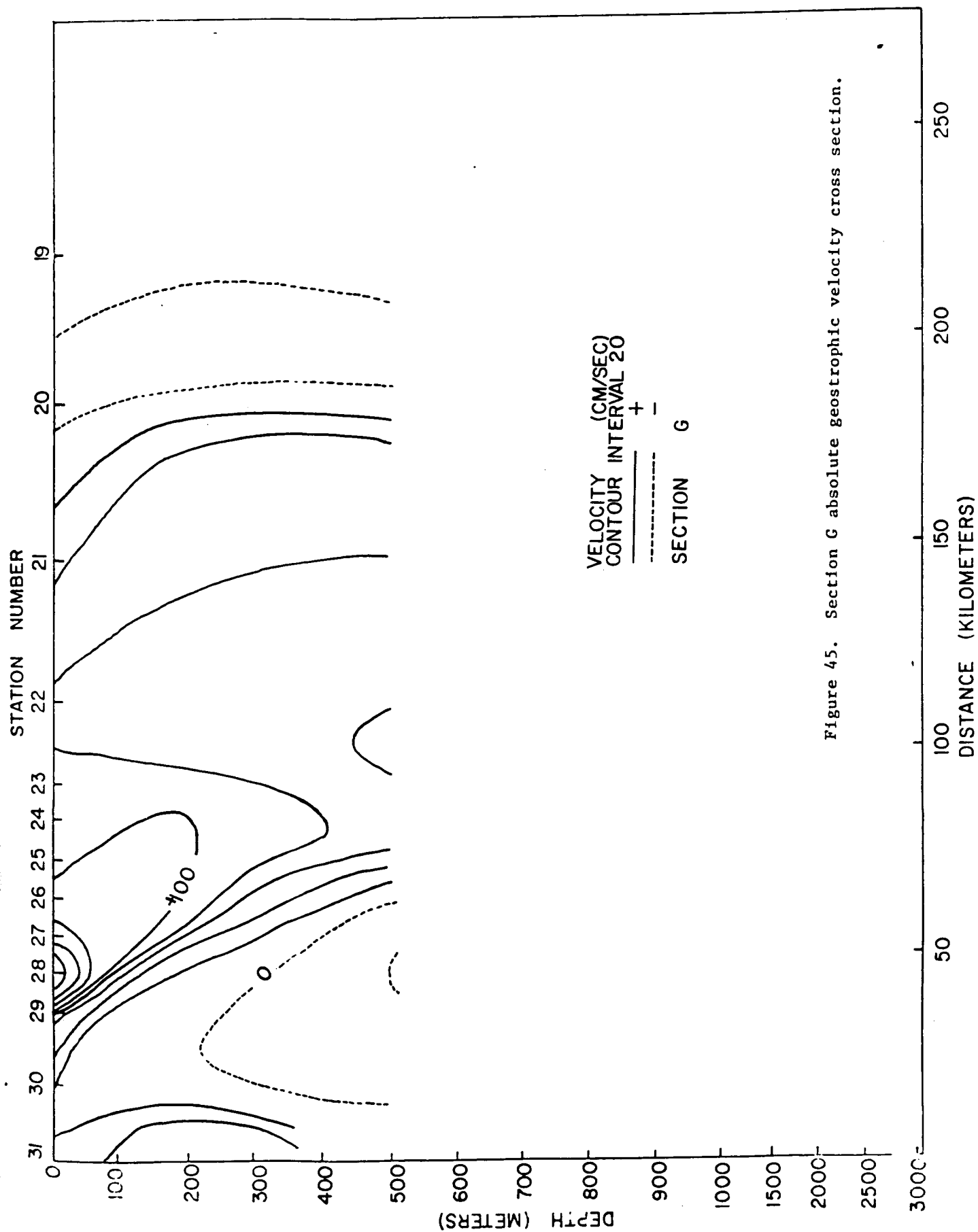
Figure 45. Section G absolute geostrophic velocity cross section.

REFERENCES

Charnell, R. L., J. Apel, W. Manning, and R. Qualset (1974) Utility
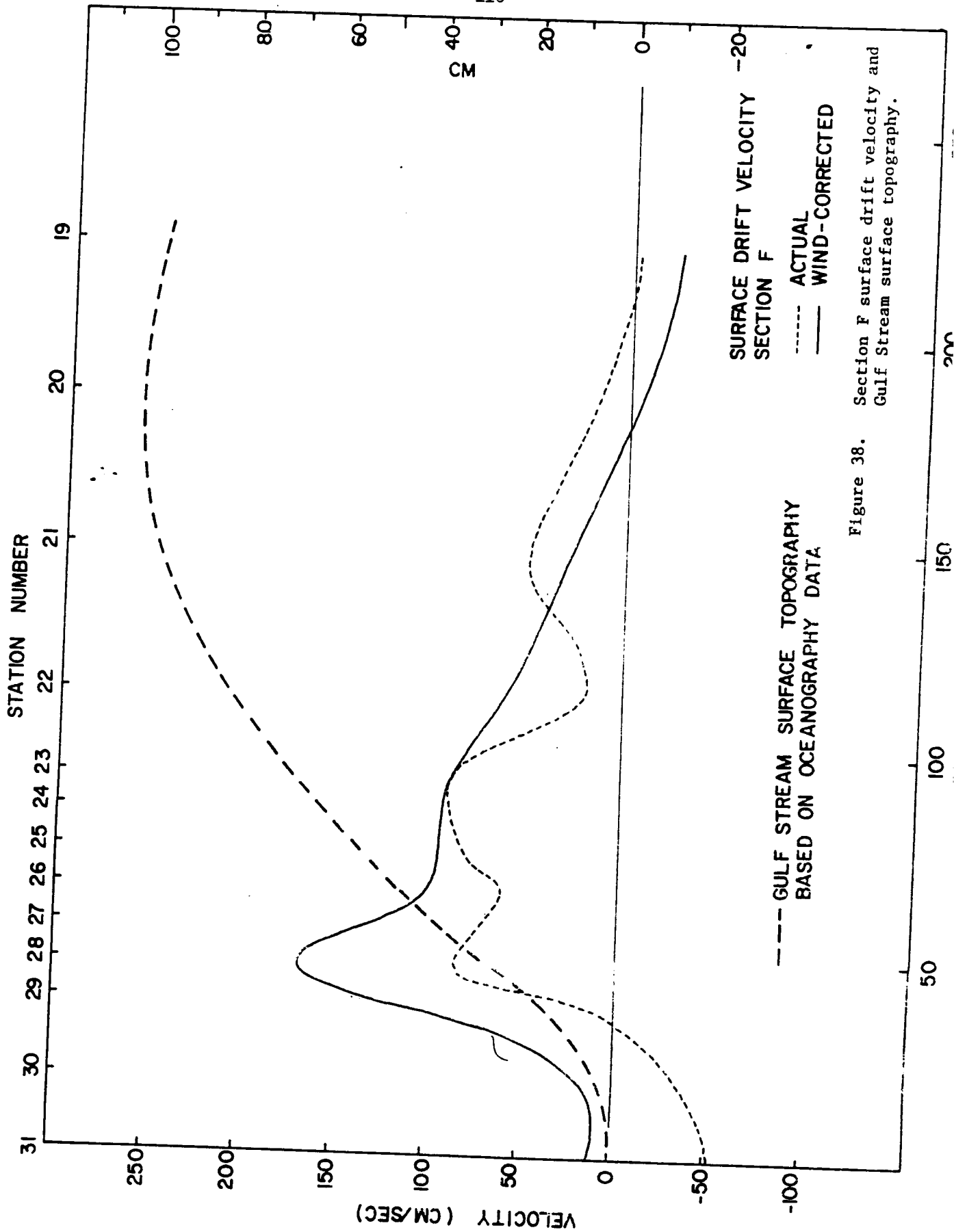   of ERTS-1 for Coastal Ocean Observation: The New York Bight
    Example, Marine Technology Journal, 8(3), 42-47.

Curtin, T. B. and D. Britton (1978) Processing programs and proced-
    ures designed for Guildline CTD data. Tech. Rpt. No. 99, Center
    Mar. Coastal Studies. N.C. State Univ., Raleigh.

DeRycke, R. J. and P. Rao (1973) Eddies Along a Gulf Stream Boundary
    Viewed from a Very High Resolution Radiometer, Journal of
    Physical Oceanography. 3(4), 490-492.

Ekman, V. W. (1908) Die Zusammendruckbarkeit des Meerswassers. Cons.
    Perm. Int. Explor. Mer Publ. Circonstance, 43: 1-47.

Fofonoff, N. P. (1962) Physical Properties of Seawater. The Sea, 1,
    edited by M. N. Hill. Interscience, New York, 3-30.

Fofonoff, N. P. and S. Tabata (1958) Program for Oceanographic Com-
    putations and Data Processing on the Electronic Digital Computer,
    ALWAS III-E. PSW-1 Programs for Properties of Seawater. Manu-
    script Rep., 25, Fish Res. Bd. Canada, Ottawa, Ont., 37 pp.

Knudsen, M. (1901) Hydrographische Tabellen. G. E. C. Gad, Copen-
    hagen, Williams and Northgate, London, 1-63.

Maul, George A. (1975) An Evaluation of the Use of the Earth Res-
    ources Technology Satellite for Observing Ocean Current Boundar-
    ies in The Gulf Stream System. National Oceanic and Atmospheric
    Administration, Boulder, Colorado, January 1975, 125 pp.

Richardson, P. L., A. E. Strong, and J. Knauss (1973) Gulf Stream
    Eddies: Recent Observations in the Western Sargasso Sea, Journal
    of Physical Oceanography, 3(3), 297-301.

Strong, A. E. and R. J. DeRycke (1973) Ocean Current Monitoring Em-
    ploying a New Satellite Sensing Technique, Science, 182 (4111),
    482-484.

Strong, A. E., R. J. DeRycke, and H. G. Stumpf (1974) Extensive Areas
    of Reduced Waves Leeward of the Lesser Antilles, Geophysical
    Research Letters, 1(1), 47-49.

Sturges, Wilton (1972) Comments on Ocean Circulation with Regard to
    Satellite Altimetry, in Sea Surface Topography From Space, ed.
    J. R. Apel, U. S. Dept. of Commerce, NOAA, TR ERL 228-AOML 7&7-2,
    Feb. 1972.

Szekielda, K. H. (1972) Upwelling Studies with Satellites, _International Council for the Exploration of the Sea, Journal du Conseil_, 34(3), 379–388.

Wang, D. P. and F. J. Millero (1973) Precise Representation of the P–V–T Properties of Water and Seawater Determined from Sound Speeds. J. Geophys. Res., _78_(30): 7122–7128.

Warneke, G., L. Allison, L. McMillin, and K. H. Szekielda (1971) Remote Sensing of Ocean Currents and Sea Surface Temperature Changes Derived from the Nimbus II Satellite, _Journal of Physical Oceanography_, 1(1), 45–60.

REMOTE CURRENT SENSING BIBLIOGRAPHY (1973-1976)

Allred, T. C., "New prospects: Sensing oceans from space," Ocean Industry, 9(6): 59-63, June 1974.

Allshouse, J. C., "A summary of the radiometric technology model of the ocean surface in the microwave region," NOAA Tech. Memo. NESS-66, Publication NOAA 7505 2201, 31 pp.

Apel, J. R., "Sea Surface Topography from Space." v. 1 and 2, U.S. Dept. of Commerce, NOAA, TR ERL 228-AOML 7 and 7-2, Feb. 1972.

Apel, J. R. and J. R. Proni, "Scientific results from remote sensing of the oceans," Marine Technology Scoeity Journal 8(1)25-28, Jan. 1974.

Apel, J. R., "Ocean Remote Sensing," S.A.T.A.R., 13(2): P-21, Jan. 23, 1975.

Apel, J. R., "Seasat: A spacecraft views the marine environment with microwave sensors," Remote sensing: energy related studies edited by T. N. Veziroglio; Advanced in Thermal Engineering, Wash., D.C.: Hemisphere Publishing Corp., 1975, pp. 47-60.

Basharinov, "Effect of sea state on brightness temperature," GRA, 73(20): 80, Oct. 25, 1973.

Bolle, H.J., "Ocean pollution and the ocean-atmosphere system," S.A.T.A.R., 2(22): 2685, Nov. 23, 1974. Also in ESRO: 4, 1973, 22 pp., Implic. for Euro Space Progr. of Poss. of Man Missions.

Bruce, J. G., "Comparison of near surface dynamic topography during the two monsoons in the western Indian Ocean," DSR 15, 665-677.

Charnell, R. L., "Utility of ERTS-1 for coastal ocean observation: The New York Bight Example," Marine Tech. Journal 8(3) 42-47, March 1974.

Charnell, R. L., et al., "Oceanic Observation of New York Bight by ERTS-1," Nature, vol. 242, pp. 451-2.

Chen, D. T., "Use of LIDAR systems in measuring certain physical oceanographic parameters," SCIENTIFIC and TECHNICAL AEROSPACE REPORTS, 13(21): 2674, Nov. 8, 1975 (also 2704).

Cogan, J. L., "Measurement of sea surface temperature by the NOAA-2 satellite," Third Symposium on Met. Obs. & Instr. of AMS, Preprints, Boston: AMS (1975) pp. 123-30.

De Rycke, R. J., "Eddies along a Gulf Stream boundary viewed from a very high resolution radiometer, JPO, 3(4): 490-2. Oct. 1973.

Duntley, S. G., et al., "Ocean color analysis," SATAR 12(24) 2945-6.

Emmanuel, C. B., "A feasibility study for the remote measurement of underwater currents using acoustic Doppler techniques," GRA 74(2): 94-95, Jan. 25, 1974. Also in Env. Res. Labs. TR: NOAA-TR-ERL-278 Aug. 1973, 41 pp. and U.S. NOAA. Wave Pr. Lab. Rep. WPL-25.

Flanders, A. F., "NOAA requirements and programs," Scientific and Technical Aerospace Reports, 13(7): 787, Apr. 8, 1975.

Gotthardt, G. A., "Life cycle of a Gulf Stream anticyclonic eddy observed from several oceanographic platforms," J. Phys. Oc., 4(1): 131-34, Jan. 1974.

Greenwood, et al., "Oceanographic applications of radar altimetry from a spacecraft," Remote Sensing of the Environment, 1, 71-80, Elsevier, New York.

Hanson, K., "Remote detection of ocean features in the Lesser Antilles using ERTS-1 data," Govt. Reports Ann. 14(7): 81, Apr. 5, 1974; SATAR 12(6): 659-660, Mar. 23, 1974.

Hendrickson, J. R., "Study of the marine environment of the northern Gulf of California," G.R.A. 74(8): 82, Apr. 19, 1974; SATAR, 12(7) 782, Apr 8, 1974.

"International Symposium on Remote Sensing of Environment," Env. Research - Inst. of Michigan, Willow Run Labs, Report 195600-1-X, Apr. 1973, 2331 pp.

Kaminski, H., "Environmental Satellites and ERTS-1 imagery S.A.T.A.R., 13(5): 548, Mar. 8, 1975. Also in ESRO Euro Earth-Res. Sat. Expts., May 1974, pp. 1-19.

V. Klemas, "Monitoring coastal water properties and circulation from ERTS-1. GRA 74(4): 78, Feb. 22, 1974.

LaFond, E. C., "Sea surface features," Marine Bio. Assoc. of India Journal 14(1): 1-14.

LaViolette, et al., "Nimbus II satellite sea surface temperatures versus historical data in a selected region: A comparative study," DSR, 15: 614-22, 1968.

LaViolette, P. E., "Preliminary Results of Little Window 2: A satellite ocean station experiment in the Gulf of California," Govt. Repts. Ann. 75(4): 51, Feb. 21, 1975. Also in U.S. NAVOCEANO Rept. NOO-SP-261, Apr. 1974, 100 pp.

LaViolette, P. E., "Use of APT satellite infrared data in oceanography survey operations," TRANS, AGU 56 51: 276-282, May 1975.

LeGeckis, R. V., "Application of NOAA's synchronous meteorological satellite to the study of time dependent ocean circulation," TRANS, AGU 56(6): 378, June 1975.

Maul, G. A., "Remote sensing of ocean current boundary layer," Govt. Repts. Ann. 74(7): 73, April 5, 1974.

Maul, G. A., "Remote sensing of ocean currents," GRA 74(9): 81, May 3, 1974; 74(3): 25, Feb. 8, 1974, 73(15): 80, Aug. 10, 1973.

Moravek, D., "Gulf Stream Wall Bulletin," Mariners Weather Log, 19(1): 19-21 January 1975.

Otterman, J., "Oceanic Eddy in the Gulf of Suez," DSR 21(2): 4 pp., Feb. 1974.

Paul, C. K., "Microwave remote sensing of the oceans from space," OTC Seventh Annual Proc. Vol. III, 1975, pp. 795-804.

Pearcy, W., "Multispectral scanner studies of the ocean off the Oregon coast," GRA, 73 (17): 74, Sept. 10, 1973.

Pearcy, W. G., "Remote sensing of water color and sea surface temperatures off the Oregon coast," Limnology and Oceanography, 19(4): 573-583, July, 1974.

Pierson, W. J. Jr., "Ocean dynamics remote sensing study," GRA, 73(15): 79, Aug. 10, 1973. Also in NYU Dept. of MY. and Oc. TR-73-3, Jan. 1973, 30 pp.

Pilon, R. O., "Determination of ocean surface descriptors using sea photo analysis techniques," GRA 73(19): 75, Oct. 10, 1973.

Pirie, D. M., "California coast nearshore processes study," GRA 73(17): 68, Sept. 10, 1973.

Pouquet, J., "Earth Sciences in the Age of the Satellite," Boston: D. Reidel Pub. Co., 1974, 176 pp.

Richardson, P. L., "Gulf Stream eddies: Recent observations in the western Sargasso Sea," JPO, 3(3): 297-301, July, 1973.

Sabatini, R. R., "The application of the NIMBUS 5 ESMR to sea surface wind determination." Third Symposium on Met. Obs. & Instr. of AMS, Preprints, Boston: AMS (1975), pp. 131-136.

Sharma, G. D., "Sea ice and surface water circulation, Alaska Continental Shelf," GRA 74(5): 72, Mar. 8, 1974.

Shenk, W. E., "Satellite ocean temperature analysis of the Indian Ocean," Marine Bio. Assoc. of India Journal 14(1): 102-108, June 1972.

Sherman, J. W. III, "Aerospace remote sensing oceanography," U.S. Enviro. Data Service: 3-12, Sept. 1973.

Strong, A. E., et al., "Ocean current monitoring employing a new satellite sensing technique," Science, 182 (4111), 482-4, Nov. 2, 1973.

Strong, A. E., "Extensive areas of reduced waves leeward of the Lesser Antilles," Geophys. Research Letters, 1(1): 47-49, May 1974.

Struebing, K., "Oceanography, fishery," SATAR, 12(22): 2685, N 23, 1974.

Sturges, W., "Comments on Ocean Circulation with Regard to Sattelite Altimetry," U.S. Dept. of Commerce, NOAA, TR ERL 228-AOML 7 and 7-2, part 24, Feb. 1972.

Szekielda, K.-H., "Upwelling studies with satellites," Int. Council for the Exploration of the Sea, Journal du Conseil, 34 (3): 379-388, Oct. 1972.

U.S. Naval Oceanographic Office, "Microwave Observations of the Ocean Surface," SP 152 (June 1969).

Vonder Haar, J. H., "New estimate of annual poleward energy transport by northern hemisphere oceans," JPO 3(2): 169-172, April 1973.

Warnecke, G., et al., "Remote sensing of ocean currents and sea surface temperature changes derived from the Nimbus II satellite," J. Phys. Oc. 1:45-60.

Wilkerson, "The Gulf Stream from space," Oceanus, 13, 2-3, 1-8, 1967.

Wright, F. F., "Sea-surface circulation, sediment transport and marine mammal distribution, Alaska Continental Shelf," GRA, 73(10): 76-77, May 25, 1973. NASA CR-131011, Feb. 20, 1973.

Anon., "The Gulf Stream," Gulf Stream, U.S. Naval Oc. Off., 8(11): 6 pp., Nov. 1973; 9(2): 6 pp., Feb. 1974.

Anon., Wave measurements during the Joint North Sea Wave Project (Jonswap 2) Wormley, Eng. Inst. Oc. Sci. Cruise Report 7, June, 1974, 12 pp.

Appendix A

Numerical Data Listings

These data listings are omitted in this edition of Oceanographic Observations Across the Northern Gulf Stream. Editions of this report containing these listings are available on request by those in need.

PUBLICATIONS PUBLISHED BY THE
DEPARTMENT OF MARINE SCIENCE AND ENGINEERING
(PREVIOUSLY THE CENTER FOR MARINE AND COASTAL STUDIES)

Wave-Current Force Spectra, C. C. Tung and N. E. Huang, Report No. 72-2, December, 1972.

A Survey of North Carolina Beach Erosion by Air Photo Methods, H. E. Wahls, Report No. 73-1, May, 1973.

Sediment Movement in Tubbs Inlet, North Carolina, Robert P. Masterson, Jr., Jerry L. Machemehl and Victor V. Cavaroc, Jr., Report No. 73-2, June, 1973.

Influence of Current On Some Statistical Properties of Waves, C. C. Tung and N. E. Huang, Report No. 73-3, December, 1973.

CTD Sensors, Specific Conductance and the Determination of Salinity, C. E. Knowles, Report No. 73-3, August, 1973.

Planning for North Carolina's Coastal Inlets - An Analysis of the Present Process and Recommendations for the Future, William S. Tilley, Report No. 73-4, September, 1973.

A Preliminary Study of Storm-Induced Beach Erosion for North Carolina, C. E. Knowles and Jay Langfelder and Richard McDonald, Report No. 73-5, October, 1973.

A Historical Review of Some of North Carolina's Coastal Inlets, Jay Langfelder, Tom French, Richard McDonald and Richard Ledbetter, Report No. 74-1, January, 1974.

Statistical Properties of Kinematics and Dynamics of a Random Gravity Wave Field, C. C. Tung, Report No. 74-2, June, 1974.

A New Technique of Beach Erosion Control, Tom French, Jerry L. Machemehl and N. E. Huang, Report No. 74-3, June, 1974.

Citizen Participation in North Carolina's Coastal Area Management Program, Steve Tilley, Report No. 74-4, June, 1974.

An Experimental Study of Scour Around Marine Foundations Due to Oscillatory Waves and Undirectional Currents, Greg N. Abad and Jerry L. Machemehl, Report No. 74-5, September, 1974.

Proceedings of A Conference on Coastal Management, Report No. 74-6, September, 1974.

Statistical Properties of Fluid Motion and Fluid Force in A Random Wave Field, Keikhosrow Pajouhi and C. C. Tung, Report No. 75-1, May, 1975.

A Numerical Method for Solutions of Systems of Non-Linear Algebraic Equations, John M. Klinck and Leonard J. Pietrafesa, Report No. 75-2, July, 1975.

Wave-Current Interactions in Water of Variable Depths, A. M. Radwan, C. C. Tung and N. E. Huang, Report No. 75-3, August, 1975.

Conference Proceedings Energy From The Oceans Fact or Fantasy?, Jerome Kohl, Report No. 76-1, UNC-SG-76-04, January, 1976.

Long Waves Trapped by the Cape Fear Continental Shelf Topography: A Model Study of Their Propagation Characteristics and Circulation Patterns, David A. Brooks, Report No. 76-2, July, 1976.

A Comparative Study of Three Methods of Inhibiting Scour Around A Vertical Circular Cylinder, David M. Rooney and Jerry L. Machemehl, Report No. 76-3, September, 1976.

A Flow Study of Drum Inlet, North Carolina, Paul R. Blankinship, Report No. 76-4, UNC-SG-76-13, November, 1976.

Dune Stabilization With Panicum amarum Along the North Carolina Coast, E. D. Seneca, W. W. Woodhouse, Jr., and S. W. Broome, Report. 77-1, UNC-SG-77-03, February, 1977.

A Mathematical Model of Nutrient Distribution In Coastal Waters, Eileen E. Hofmann, Leonard J. Pietrafesa, Larry P. Atkinson, Gustav-A. Paffenhöfer and William M. Dunstan, Report No. 77-2, February, 1977.

An Experimental Investigation of Some Combined Flow Sediment Transport Phenomena, Larry Bliven, Norden E. Huang and Gerald S. Janowitz, Report No. 77-3, UNC-SG-77-04, February, 1977.

Thermal Effluent Transport Pathways In Coastal Waters Near The Mouth Of The Cape Fear River Estuary, Leonard J. Pietrafesa, Paul Blankinship and Richard D'Amato, Report No. 77-4, CP&L No. 77-04, March, 1977.

Onslow Bay Physical/Dynamical Experiments Summer-Fall, 1975 Data Report, L. J. Pietrafesa, D. A. Brooks, R. D'Amato and L. P. Atkinson, Report No. 77-5, ERDA Contract No. E(38-1)-902, UNC-SG-77-07, March, 1977.

Sea Level Fluctuations Off The Carolina Coasts And Their Relation To Atmospheric Forcing, David A. Brooks, Report No. 77-6, May, 1977.

An Experimental Study Of A Nearshore Erosion Control Structure, Herschel R. Ouzts and Jerry L. Machemehl, Report No. 77-7, May, 1977.

Publications Published Cont'd.

Application of a Radiation - Type Boundary Condition to the Wave - Porous Bed Problem, Charles McClain, Norden Huang and Leonard J. Pietrafesa, UNC-SG-77-10, Report No. 77-8, May, 1977.

An Analysis of Beach Overwash Along North Carolina's Coast, Stanley J. Boc and Jay Langfelder, Report No. 77-9, June, 1977.

Flow Dynamics and Sediment Movement In Lockwoods Folly Inlet, N. C., Jerry L. Machemehl, Mike Chambers and Neale Bird, UNC-SG-77-11, Report No. 77-10, June, 1977.

Numerical Flow Model for an Atlantic Coast Barrier Island Tidal Inlet, T. C. Gopalakrishnan and Jerry L. Machemehl, UNC-SG-78-02, Report No. 78-1, February, 1978.

Continental Margin Atmospheric Climatology and Sea Level, (Historical Setting, 1974, 1975) L. J. Pietrafesa, Rich D'Amato, C. Gabriel, R. J. Sawyer, Jr., UNC-SG-78-09, Report No. 78-2.

Oceanographic Observations Across the Northern Gulf Stream, Thomas B. Curtin, Leonard J. Pietrafesa, NASA Contract No. 62617, Report No. 78-3.

Concurrent Satellite and Ship Observations Across the Gulf Stream North of Cape Hatteras, Thomas B. Curtin, Leonard J. Pietrafesa and Norden E. Huang, NASA Contract No. 62617, Report No. 78-4.